ER-4502

EVALUATION OF SHALLOW GEOCHEMICAL AND LITHOLOGIC PROPERTIES IN AN AREA NORTH OF ROCKY MOUNTAIN ARSENAL, DENVER, COLORADO, USING ELECTROMAGNETIC CONDUCTIVITY PROFILING

By

Keirnan L. Conner

ER-4502

A thesis submitted to the Faculty and Board of Trustees of the Colorado School of Mines in partial fulfillment of the requirements for the degree of Master of Engineering (Geological Engineer).

Golden, Colorado

Date 11/12/93

Signed: Keirnan L. Conner

Keirnan L. Conner

Approved: Kenneth E. Kolm

Dr. Kenneth E. Kolm
Thesis Advisor

Golden, Colorado

Date 11/12/93

Dr. Roger M. Slatt
Professor and Head,
Department of Geology and
Geological Engineering

ABSTRACT

This study evaluates shallow subsurface lithologic and geochemical properties of the unconsolidated aquifer using electromagnetic conductivity profiling, ground-water quality, and subsurface lithologic data at a site immediately north of Rocky Mountain Arsenal, Denver, Colorado. The objectives of the study are to evaluate (1) the dependence of the conductivity response on variations in bedrock depth, ground-water quality, water table depth, and instrument coil spacing and (2) potential ground-water contaminant transport pathways within the study area.

The study evaluates the use of the electromagnetic conductivity profiling method for predicting shallow subsurface lithologic and geochemical properties in an area with a shallow, unconfined ground-water system. An area of about 2.5 square miles was investigated using electromagnetic conductivity profiling, induction logging of existing monitoring wells, borehole drilling, monitoring well installation, and ground-water quality sampling and analysis. A hydrogeologic framework of the study area, based on previous work by other investigators, was used. A conceptual geophysical model was developed and evaluated using the soil conductivity data and a combination of subsurface lithologic, geophysical, water quality, and potentiometric data.

Data analysis included regression analyses of apparent conductivity, bedrock depth, total dissolved solids concentration and ground-water electrical conductivity data, and computer modeling of electromagnetic conductivity data. The profile lines were forward modeled using bedrock depths based on borehole data and estimated conductivities based on borehole induction logs and vertical electrical soundings.

Model-generated synthetic data were subtracted from actual field data, the resulting residuals were posted on a map and contoured, and anomalies were evaluated. A qualitative evaluation of conductivity variation with unconsolidated and bedrock lithology was also made. A best fit conceptual model was derived in a test area and refined in a confirmation area. The resulting model was applied to areas of sparse subsurface control to extend the understanding of the study area in terms of the hydrogeologic framework.

The conclusions of this study are that (1) the electrical conductivity of the shallow ground water is proportional to the total dissolved solids concentration, (2) the apparent conductivity response measured at the ground surface is significantly dependent on the concentration of total dissolved solids within ground water, the depth to bedrock, and the depth to the water table, and (3) the residual conductivity data generated during the study are indications of the combined effects of ground-water ionic concentration and possible inaccuracies in depth-to-bedrock estimates.

TABLE OF CONTENTS

TABLE OF CONTENTS
(continued)

LIST OF FIGURES

LIST OF FIGURES (continued)

LIST OF FIGURES (continued)

LIST OF TABLES

LIST OF PLATES

ACKNOWLEDGEMENTS

The author wishes to thank the following people and organizations for their help in compiling and finalizing this report:

Dr. Kenneth E. Kolm, Dr. Norman A. Harthill, and Dr. A. Keith Turner of the Colorado School of Mines (CSM) for their continued support and guidance throughout this study;

Dr. Catherine Skokan of the CSM Geophysics Department for her help with geophysical modeling using the computer program EMIX34P;

Dr. Charles Stoyer of Interpex, Limited, Golden, Colorado, for his help with EMIX34P and his revision of the program to meet my objectives;

Ms. Kathryn Cain of the Program Manager for Rocky Mountain Arsenal, for helping me obtain permission to use the data presented in this report;

Mr. Thor Gjelsteen of Harding Lawson Associates, for providing access to the data base and maps used in this study;

Ms. Charlene Ash for her help in producing this report; and

Geonics Limited of Ontario, Canada, for furnishing technical information on the electromagnetic method, its uses, and their instruments.

The use of trade names in this report does not constitute an endorsement of such commercial products.

Chapter 1
INTRODUCTION

1.1 Purpose and Objectives

The first objective of this study was to evaluate the dependence of apparent electrical conductivity, measured using an electromagnetic geophysical instrument at the ground surface, on variations in bedrock depth, ground-water quality, water-table depth, unconsolidated and bedrock lithology, and electromagnetic coil spacing. The second objective was to evaluate the bedrock topography and ionic concentration distribution within the study area in relation to contaminant transport in ground water.

1.2 General Approach

This study used electrical conductivity and resistivity data, borehole lithologic information, and ground-water analytical data to perform the following tasks:

(1) The degree to which bedrock depth, ground-water quality, water table depth, and unconsolidated and bedrock lithology influence apparent conductivity values, and the degree to which apparent conductivity data can be used to predict variations in these parameters were evaluated using existing data in a known paleochannel with known dimensions and properties;

(2) The reliability of the model was tested using data in a second known paleochannel with known dimensions and properties; and

(3) The results of the model calibration were used to refine the knowledge of the hydrogeologic framework in parts of the study area outside of the areas of abundant borehole and monitoring well data.

The geologic and hydrogeologic frameworks for the study were derived from previous work in the study area. Data analysis was conducted to evaluate the dependence of the conductivity data on the various parameters, and included regression analysis and forward computer modeling of a geophysical model to compare results with actual apparent conductivity data from the study area. Variables in the data analysis included soil electrical conductivity, bedrock depth, ground-water quality (i.e., total ionic concentration), depth to water table, and instrument coil spacing. A qualitative evaluation of the dependence of conductivity on lithology (both unconsolidated and bedrock) was made. Specifically, the following relations were examined:

(1) Apparent conductivity variation with depth to bedrock (assumed to be an inverse relation) was examined by comparing borehole data to conductivity data in areas where the data types coincide;

(2) Apparent conductivity variation with water table conditions was examined where depth to water table is known; the effect of nonsaturated alluvial conditions was also examined;

(3) Apparent conductivity variation and ground-water conductivity variation with ground-water quality were examined using analytical data including concentration of total ionic constituents (total dissolved solids [TDS]); and

(4) Apparent conductivity variation with bedrock and unconsolidated material lithologies was assessed qualitatively where bedrock lithology types are known.

The uncertainties associated with each parameter or factor were examined, including an assessment of whether the effects from different factors can be effectively distinguished or separated.

A geophysical model was developed, and an assessment of the model's reliability was made in areas of abundant data. The model was then applied to areas of more sparse control to evaluate subsurface properties in these areas. Actual and synthetic apparent conductivity profiles, a contour map of residual apparent conductivity values, and a map showing interpreted areas of inaccuracies in bedrock elevation estimates and interpreted boundaries of high ionic concentrations in ground water were produced. The geometry of the two known flow pathways was refined, and the

presence of other potential flow pathways was assessed. The results of the study were used to estimate the lateral boundaries of high-TDS areas within identified paleochannels and to evaluate which parameters are the primary factors influencing apparent conductivity. Some uses for and limitations of the conductivity profiling method for site characterization, within the study area and at other similar sites, were assessed on the basis of the study.

Chapter 2
BACKGROUND

2.1 Description of Study Area

The study area, shown in Figure 2.1, is approximately 2.5 square miles in total area and is located in Sections 11, 12, 13, and 14, Township 2 South, Range 67 West. The area is immediately north of Rocky Mountain Arsenal, Denver, Colorado, and was investigated previously for the evaluation of shallow ground-water contamination using a combination of methods that are discussed in the following sections.

2.2 Description of Previous Work

The study area was investigated previously by Robson and Romero (1981), Konikow (1977), Lindvall (1980 and 1983), Environmental Science and Engineering (ESE) (1988), and Harding Lawson Associates (HLA) (1992). Robson and Romero (1981) conducted a study of the unconsolidated and bedrock geologic units within the Denver Basin. Konikow (1977) conducted a regional ground-water flow study of the area including and surrounding Rocky Mountain Arsenal using chloride concentration data. Lindvall (1980 and 1983) described and mapped the surface geology in the vicinity of the study area.

In an effort to evaluate the hydrogeologic framework and flow system, ESE (1988) drilled borings, installed monitoring wells, and sampled and analyzed ground water as part of a remedial investigation and feasibility study (RI/FS). HLA (1992) continued investigation efforts under the RI/FS by installing additional monitoring wells and conducting additional ground-water quality sampling and analysis. HLA also collected design data for a ground-water intercept and treatment system by performing soil conductivity or electromagnetic (EM) profiling, induction logging of existing monitoring wells, and borehole drilling (HLA, 1990).

During the construction of the intercept and treatment system, HLA collected further geophysical and borehole data to design a well network to monitor the effectiveness of the system (HLA, personal communication). The EM data were used

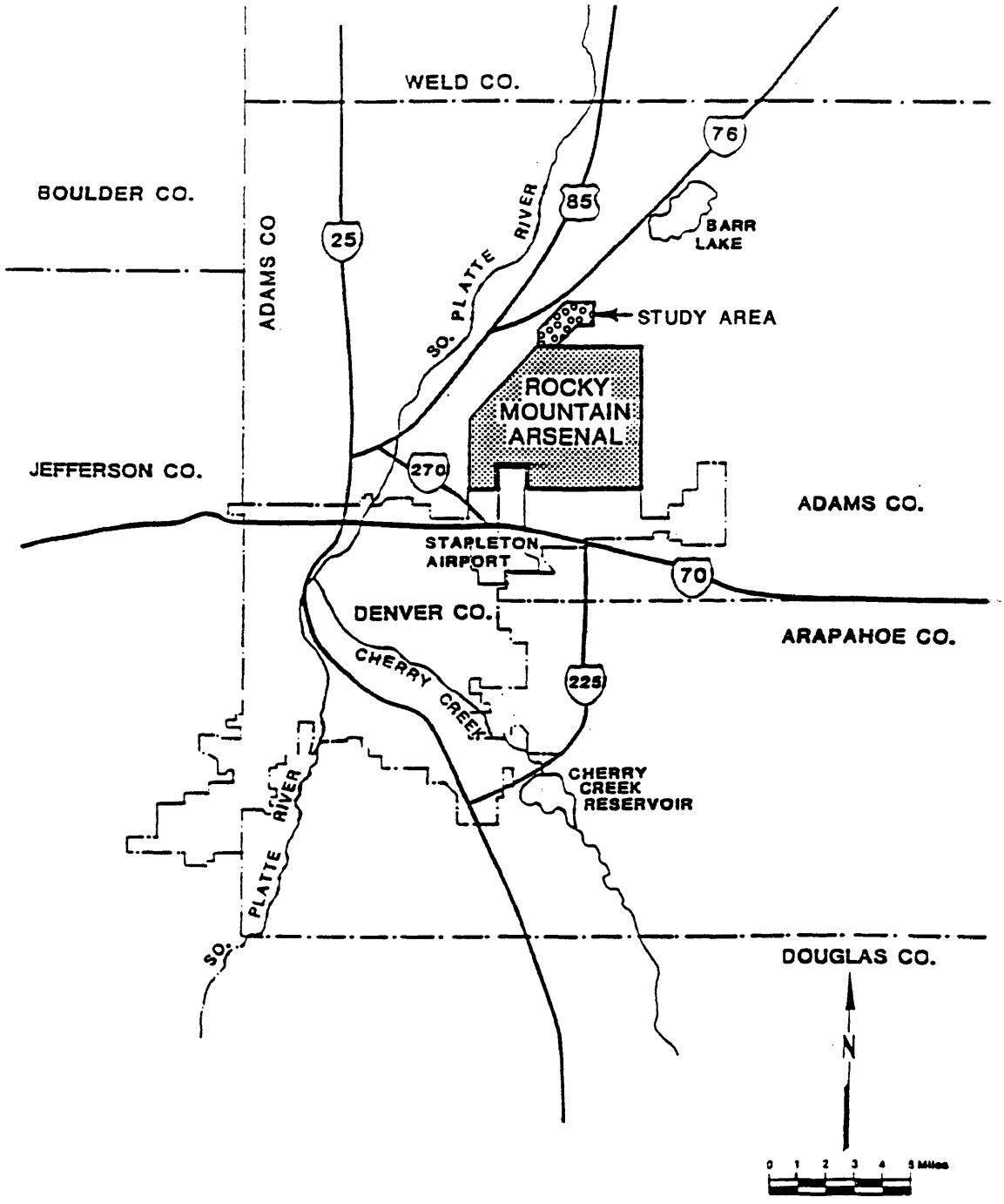

Figure 2.1 Location of Study Area (Modified from ESE, 1988)

as a qualitative tool to evaluate bedrock configuration and guide drilling efforts. Extensive interpretations of the soil conductivity data and induction logging data within the study area and their relationship to lithologic and geochemical parameters were not performed.

In an unrelated study, Mills and others (1988) successfully used time-domain EM soundings to map seawater intrusion in Monterey County, California. Other unpublished studies have been performed at Rocky Mountain Arsenal locations, to assess the configuration of paleochannels incised into the Denver Formation and filled by unconsolidated materials.

2.3 Geologic Setting

The shallow geologic materials in the study area include unconsolidated alluvial and eolian materials of Holocene age (Lindvall, 1980 and 1983), which unconformably overlie bedrock of Cretaceous age (Robson and Romero, 1981). These geologic materials are discussed in the following sections.

2.3.1 Bedrock Materials

The study area is on a northern flank of the Denver Basin, a regional scale closed structural depression that affects the attitude of all of the bedrock units within the vicinity (Robson and Romero, 1981). The shallowest bedrock unit in the study area is the Denver Formation, consisting mostly of claystones and siltstones with intermittent sandstones and lignites (Robson and Romero, 1981). The Denver Formation, like the deeper bedrock units below it, dips to the southeast at an angle of approximately one degree. This late Cretaceous unit is believed to have been originally about 900 feet thick within the study area, but has been severely eroded since the time of its deposition and prior to the deposition of the unconsolidated materials. Today, only 200 to 250 feet of the Denver Formation remain within the study area (Morrison-Knudsen Engineers, 1988). The gently rolling surface topography slopes to the west toward the South Platte River. Two paleochannels that were formed during the time of Denver Formation erosion are the First Creek and northern paleochannels, which cross the study area from the southeast to the northwest (Figure 2.2). Two other less well documented paleochannels parallel the First Creek paleochannel, to the north and south. Because these paleochannels have not been named, they are

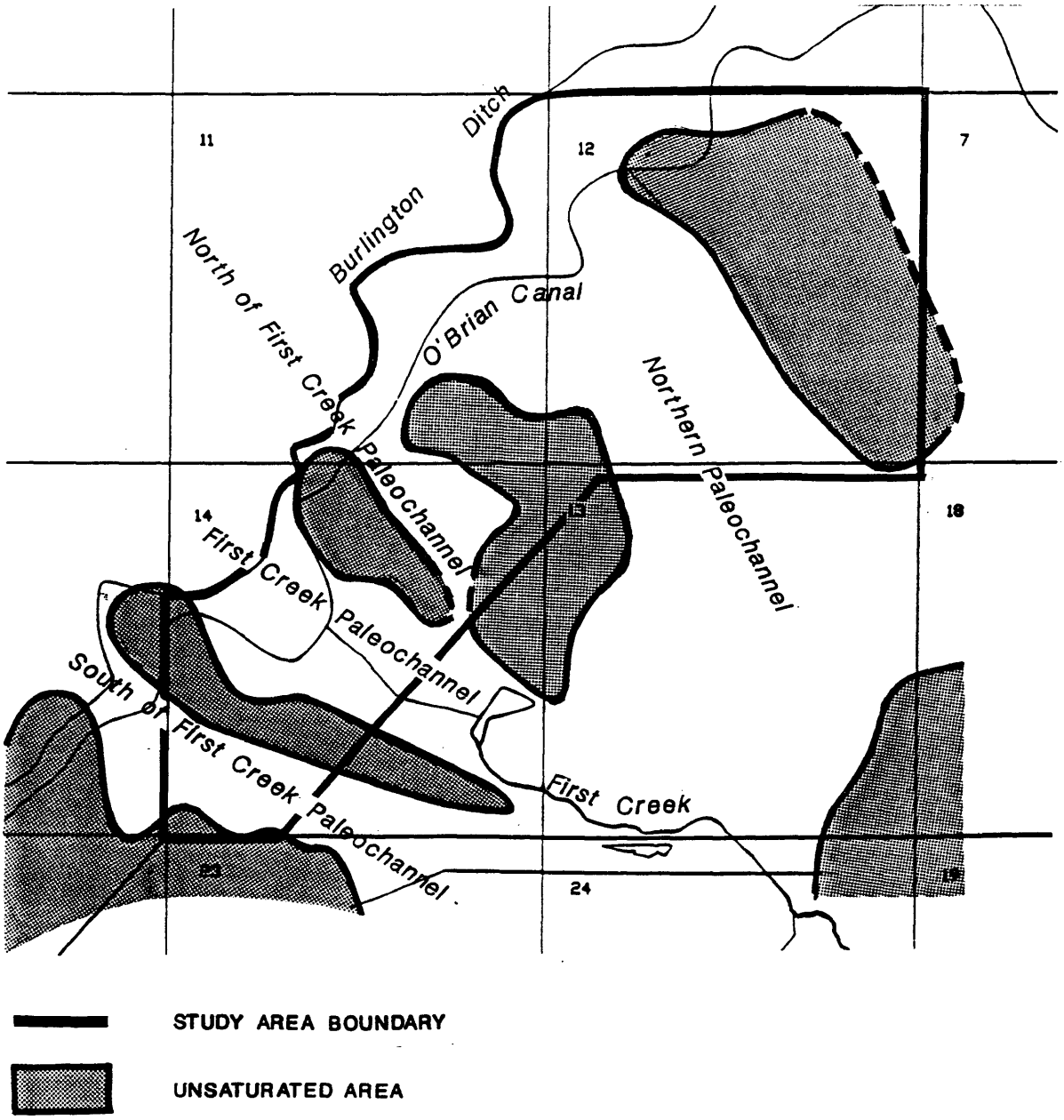

Figure 2.2 Study Area Features (Modified from HLA, 1992)

referred to as the north of First Creek (NFC) and south of First Creek (SFC) paleochannels in this report.

2.3.2 Unconsolidated Materials

Four units consisting of unconsolidated materials are present within the study area: (1) the Slocum Alluvium, an Illinoian age mixture of coarse gravel interlayered with thin lenses of fine- to medium-grained arkosic sands (Lindvall, 1971b); (2) a Pleistocene to early Holocene age loess unit consisting of sandy silt, with clay and silty clay within the upper portion; (3) a late Pleistocene to early Holocene age eolian sand unit consisting of sandy silt to gravel; and (4) the Piney Creek Alluvium, a Holocene age mixture of clay, silty fine-grained sand, and gravel (Figure 2.3). The Slocum Alluvium is generally 10 to 15 feet (3 to 4.5 meters) thick; the loess unit is generally less than 10 feet (3 meters) to as much as 20 feet (6 meters) thick; the eolian unit ranges in thickness up to 5 feet (15 meters); and the Piney Creek Alluvium is generally less than 10 feet (3 meters) thick (Lindvall, 1971a and 1971b). The Slocum Alluvium generally occupies the tops of bedrock highs and has been removed in stream channels. The loess and eolian sand units were deposited within the First Creek and northern paleochannels, and subsequently the First Creek paleochannel was partially filled by Piney Creek Alluvium (ESE, 1988; Lindvall, 1983). Bedrock highs form the boundaries of the saturated portions of the paleochannels (Figure 2.4).

2.4 Hydrogeologic Setting

The hydrogeologic framework and hydrologic flow model for the study area are based on previous work by Konikow (1977), ESE (1988), and HLA (1992). These topics are discussed in the following sections.

2.4.1 Hydrogeologic Framework

A conceptual model of the study area includes a two-layered hydrogeologic system in which a partially saturated, permeable, unconsolidated eolian and alluvial layer (hereafter referred to as the unconsolidated unit, and the saturated portion as the unconsolidated aquifer) overlies a partially saturated, low permeability, semiconsolidated bedrock unit (Denver Formation). The Denver Formation is continuous across

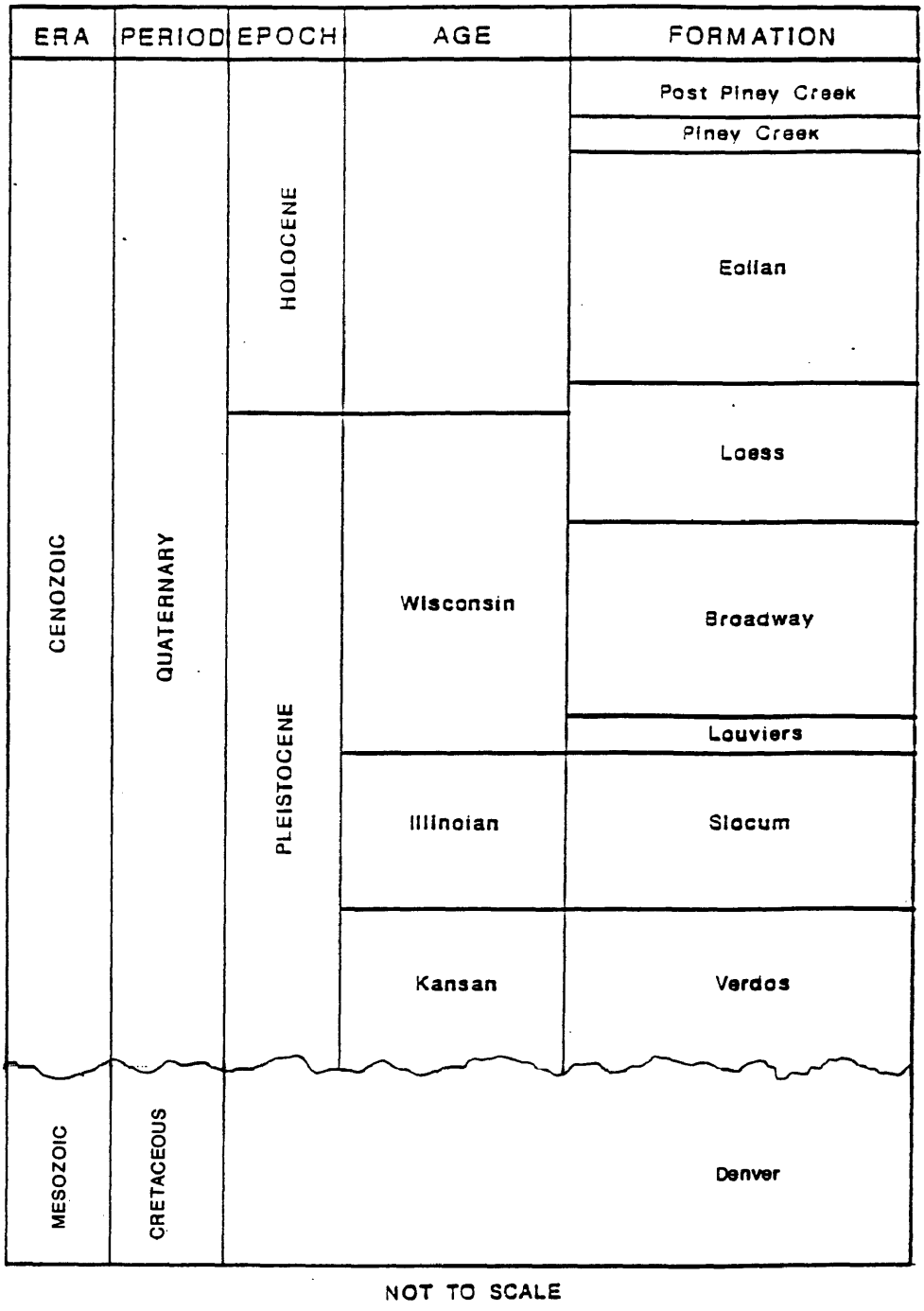

Figure 2.3 Stratigraphic Column for Unconsolidated and Shallow Bedrock Materials within the Study Area

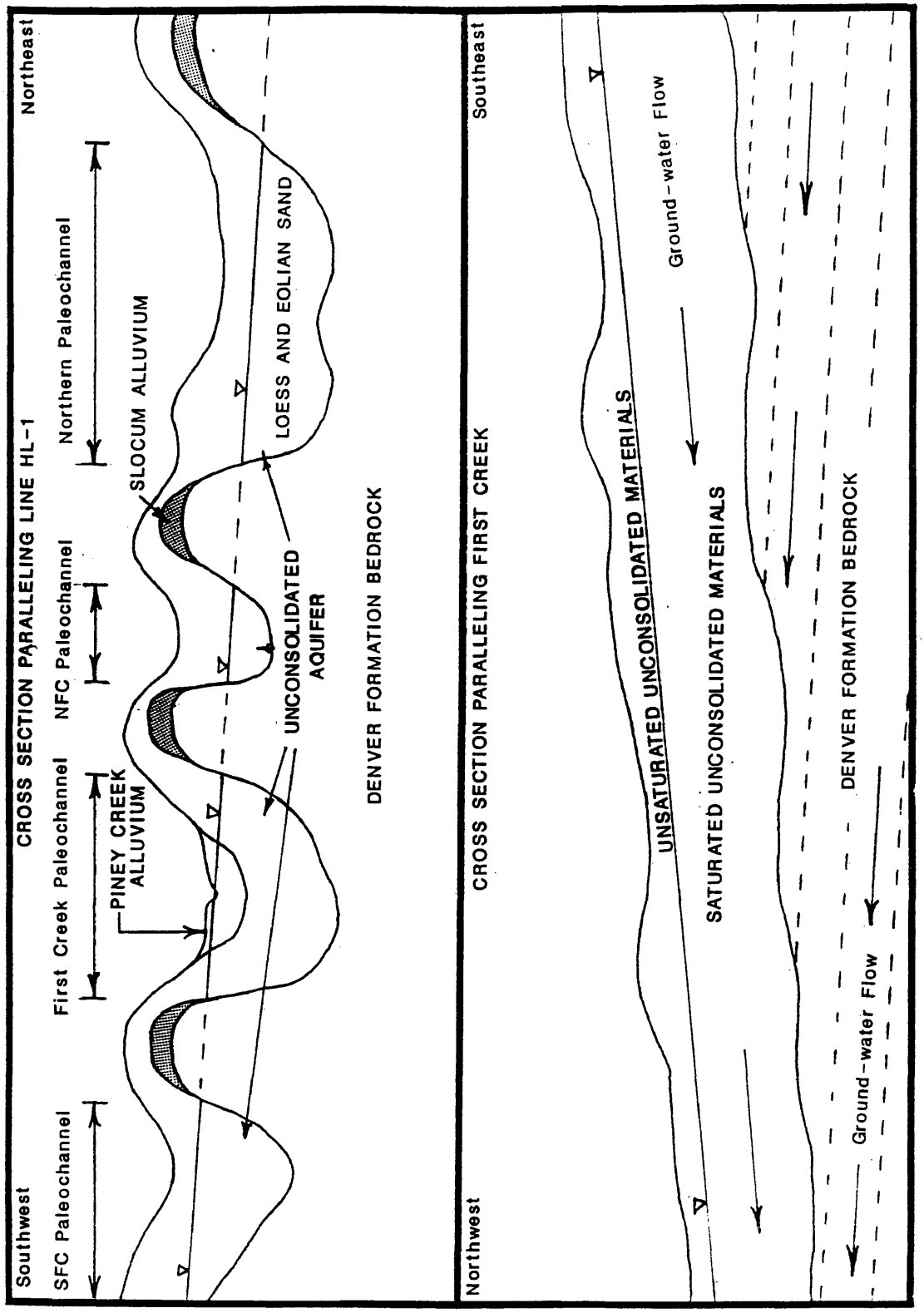

Figure 2.4 Diagrammatic Geologic Cross Sections Across the Study Area (Based on Lindvall, 1980 and 1983; and ESE, 1988)

the study area, although its lithology is not uniform and its aquifer characteristics vary (ESE, 1988).

Even though the unconsolidated unit is continuous, the materials comprising it are not saturated everywhere within the study area (HLA, 1992). Therefore, the unconsolidated aquifer is not a continuous layer. The ground water within this unit is unconfined, and several previous studies (ESE, 1988; HLA, 1992) have included the weathered portion of the upper Denver Formation with the saturated alluvial/eolian materials as components of the unconfined flow system.

The northern paleochannel is no longer an active surface-water drainage pathway. However, in the First Creek paleochannel, First Creek flows until it is intercepted by O'Brian Canal. The water table is as shallow as 1.5 feet within a large portion of the First Creek area and is approximately 20 feet deep or more within the northern paleochannel.

2.4.2 Hydrologic Flow System Model

Ground water within the study area flows from southeast to northwest, which is consistent with the regional flow pattern (Konikow, 1977; HLA, 1992), as illustrated in Figure 2.5. The bedrock highs separating the paleochannels cause the shallow ground-water flow to split between the channels. The flow within the channels may reunite downgradient of the study area; the downgradient extent of the unsaturated areas is not well known.

Ground water within the Denver Formation flows updip from southeast to northwest (ESE, 1988). As the water reaches the top of the Denver Formation, it discharges into the shallow unconfined flow system. The regional discharge area for the unconfined flow system is the South Platte River, which is approximately 2 miles northwest of the study area boundary. The interpreted unconfined potentiometric surface within the study area is shown in Figure 2.5.

There is a distinct difference in aquifer characteristics between the Denver Formation hydrogeologic unit and the unconsolidated aquifer. Hydraulic conductivities have been estimated to range from 10^{-7} to 10^{-5} cm/sec for Denver Formation claystones, and from 10^{-6} to 10^{-4} cm/sec for Denver Formation sandstones. Hydraulic conductivities have been estimated to range from 10^{-3} to 10^{-1} cm/sec within the eolian materials and the Piney Creek Alluvium (ESE, 1988).

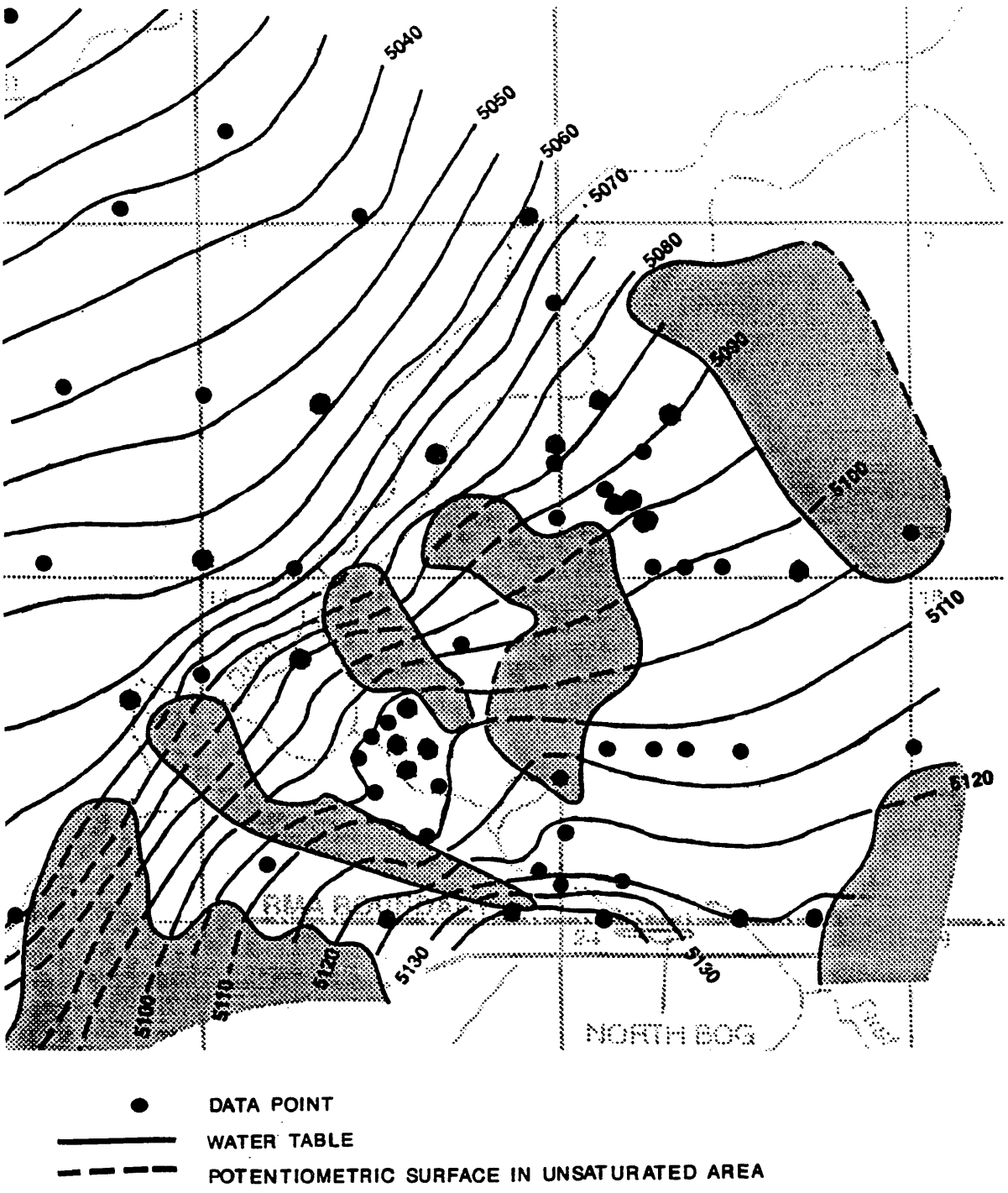

Figure 2.5 Potentiometric Surface of the Unconfined Aquifer in the Vicinity of the Study Area (After HLA, 1992)

Chapter 3.
GEOPHYSICAL METHODS

3.1 Background

Three geophysical techniques: borehole induction logging, EM profiling, and vertical electrical soundings (VES), were used in this study to evaluate subsurface geochemical and lithologic parameters within the study area. These techniques are discussed in the following sections.

3.1.1 Electrical Conduction in Earth Materials

For most rocks near the earth's surface, conduction of electricity is entirely through ground water contained in the pores of the rocks (Keller and Frischknecht, 1966). Resistivity is inversely proportional (thus, conductivity is proportional) to the number of charge carriers available, with the constant of proportionality being determined by the mobility of the ions. The resistivity of a conductor or semiconductor is the same whether measured with direct or alternating current.

The electrical properties of a water-bearing rock are describable in the same terms as the electrical properties of an electrolyte. For most rocks near the earth's surface, conduction is electrolytic, the conductive medium being a common salt. The resistivity of a water-bearing rock depends on the amount of water present, the salinity of the water, and the distribution of water within the rock (Keller and Frischknecht, 1966). A salt dissociates into ions when it goes into solution and these ions are free to move around independently in the solution. When an electric field is applied, cations accelerate toward the negative pole and anions toward the positive pole. The ions soon reach a terminal velocity, which is called the mobility of the ions. Mobility depends on both temperature and concentration. When an electric field is applied to an electrolyte, the amount of current that flows is found by multiplying the number of ions present (concentration) by the ion's mobility.

The concept of equivalent salinity is frequently used in discussing the resistivity of ground water. Ground water may have a variety of salts in solution; the equiva-

lent salinity of a solution is the salinity of a sodium chloride solution that would have the same resistivity as the solution being tested. For a given salt, the logarithm (log) of resistivity is linearly related with a slope of approximately -1 to the log of salinity. The log of conductivity is linearly related, with a slope of approximately +1, to the log of salinity. This implies that, approximately,

$$\sigma = k * s,$$

where σ = conductivity, k = a constant, and s = salinity. Type curves for the resistivity of various salts as a function of salinity are found in Keller and Frischknecht (1966). A graph illustrating the linear relation between TDS and electrical conductivity for ground water in the Denver Basin is presented in Figure 3.1 (Romero, 1976).

3.1.2 Borehole Induction Logging

The applicability of the EM method was initially assessed by logging 11 existing polyvinyl chloride-cased monitoring wells using an EM39 downhole induction tool made by Geonics Limited (Geonics, 1993), which measures the apparent conductivity of the earth around a borehole. These logs were performed to provide data to assess the electrical conductivity contrast between the various lithologic units. The results of this downhole logging indicated that the conductivity of the Denver Formation bedrock was 2 to 10 times the conductivity of the unconsolidated unit. The ranges of conductivity measured for the various geologic units are summarized below:

Geologic Unit	Apparent Conductivity
Unsaturated Unconsolidated Unit	20 to 75 mmhos/m
Saturated Unconsolidated Unit	48 to 105 mmhos/m
Denver Formation	150 to 225 mmhos/m

Because of the logging results, it was believed that the EM technique could be used to evaluate depth to bedrock. Because of the contrast in conductivities for the two lithologic units, bedrock can be interpreted to be shallower in areas where the apparent conductivity increases, and deeper in areas where apparent conductivity decreases. Because of the closeness in conductivities between unsaturated and saturated unconsolidated materials, the technique may not be able to resolve between unsaturated and saturated conditions in the unconsolidated unit. Resolving unconsolidated unit saturation was not a primary objective of the original study.

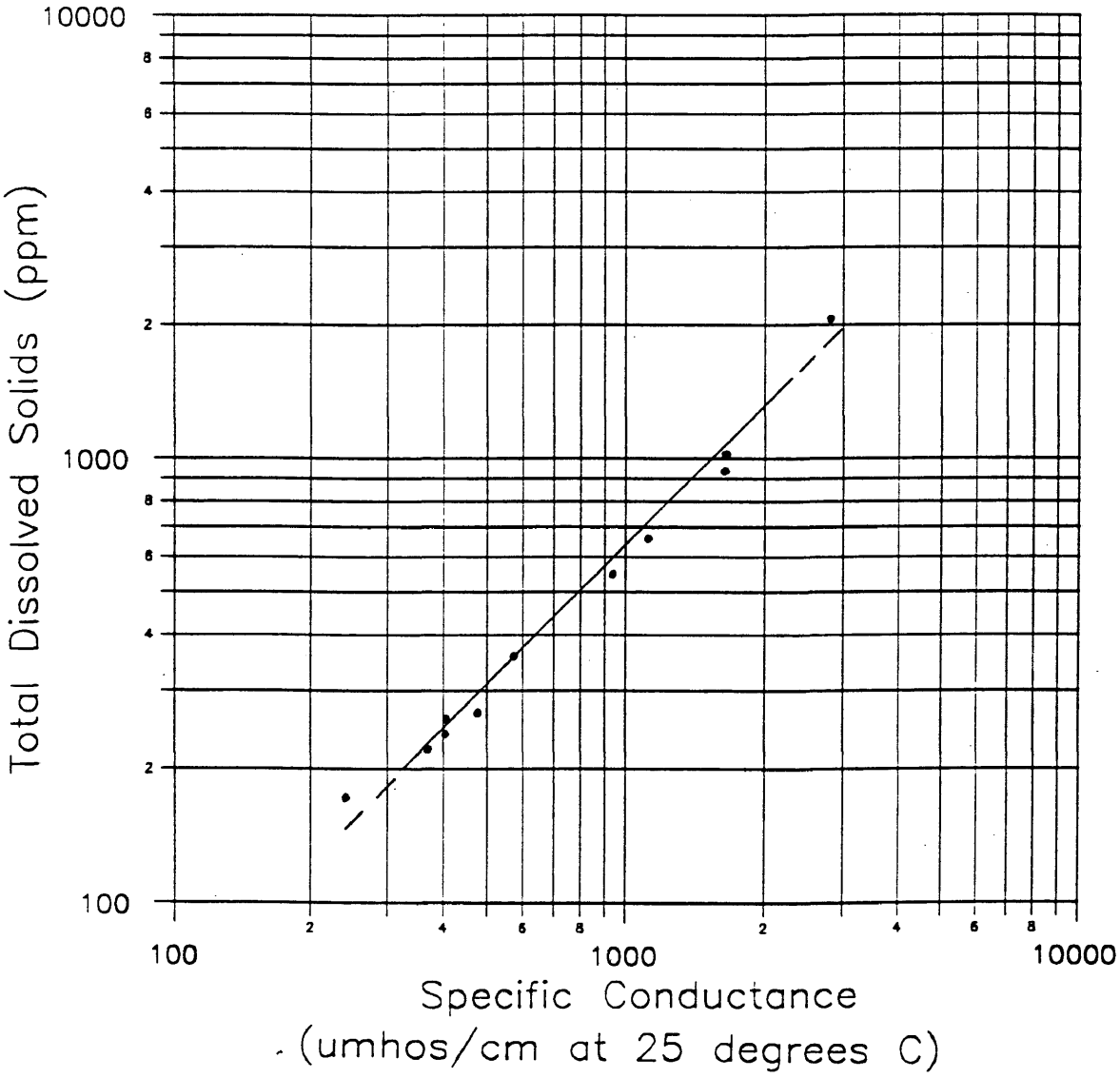

Figure 3.1 Relation of Specific Conductance to Dissolved Solids for Water from the Denver Formation (After Romero, 1976)

3.1.3 Electromagnetic Profiling

The EM conductivity measurement technique used in this study employed two different instruments made by Geonics Limited to measure the apparent electrical conductivity of subsurface materials. The EM31-D instrument has a transmitter coil and a receiver coil that are spaced a set distance of 3.67 meters apart (Geonics, 1991a). The EM34-3 instrument has a transmitter coil and a receiver coil whose separation can be varied to 10, 20, and 40 meters (Geonics, 1991b). For the EM method, the depth of investigation is proportional to the coil separation and can be changed by varying the coil separation and signal frequency.

The skin depth, the depth at which the induced EM field is equal to e^{-1} times the source EM field, is related to magnetic permeability μ, conductivity σ, and signal frequency ω. Skin depth is generally regarded as the depth below which no appreciable contribution to the apparent conductivity is made. The skin depth δ can be calculated using the following equation:

$$\delta = \sqrt{\left(\frac{2}{\mu\sigma\omega}\right)}$$

(Kaufman and Keller, 1983). The calculated skin depth values (assuming a conductivity of 100 mmhos/m) for the various coil spacings and frequencies are summarized below:

Coil spacing (meters)	Instrument	Frequency (Hz)	Skin Depth (meters)
0.50	EM39	39,200	8.04
3.67	EM31-D	9,800	16.1
10	EM34-3	6,400	19.9
20	EM34-3	1,600	39.8
40	EM34-3	400	79.6

The transmitter coil uses an alternating electrical current of a specific frequency and the associated magnetic field to induce an electrical current in the ground (Figure 3.2). This electrical current in turn creates a secondary current in the receiver coil. The coils are linked by a reference cable; this cable is also connected to a meter. The meter calculates the apparent conductivity of the earth between the coils, which is proportional to the quadrature magnetic field generated in the earth by the current in the transmitter coil (McNeill, 1980b).

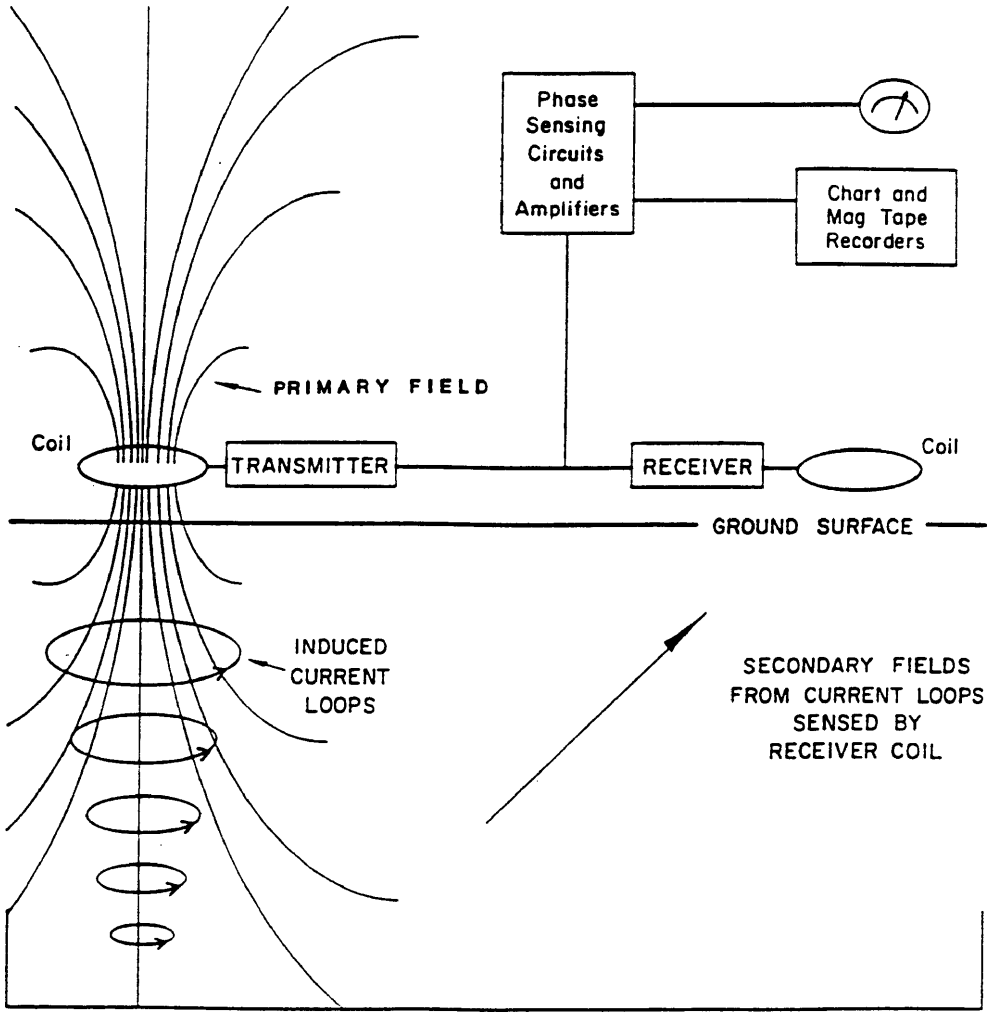

Figure 3.2 Block Diagram Showing Principles of Electromagnetic Conductivity Measurement Systems (After Benson and Others, 1982)

Conductivity measurements made on the ground surface are influenced by both bedrock depth and the presence of highly ionic ground water. The depth to water table and the unconsolidated and bedrock lithology may also affect the conductivity measurements (Keller and Frischknecht, 1966; McNeill, 1980a, 1980b, 1982).

Conductivity profiles were performed in the study area by HLA as part of design data collection for a ground-water intercept and treatment system (HLA, 1990). Profiles were positioned parallel to each other approximately perpendicular to the interpreted paleochannel axes in an effort to assess the configuration and lateral extent of the saturated portions of the channels in the vicinity of the intercept and treatment system. This orientation was believed to provide more of the type of data necessary for system design than an axial orientation. The immediate use of the conductivity data was to provide a rapid, cost-effective assessment of paleochannel configuration and to guide the drilling effort, in which borings were drilled to bedrock to provide more exact data on paleochannel configuration, and monitoring wells were installed to allow ground water to be collected for analysis. In total, four profiles (Lines HL-1, HL-3, HL-4, and HL-5) were performed in June 1989 to provide data for design of the ground-water extraction and recharge systems (HLA, 1990). Four additional profiles (Lines MWP-1, MWP-2, MWP-3, and MWP-4) were performed in October and November 1992 (HLA, personal communication) to provide data for a well network to monitor ground-water quality in the vicinity of the intercept and treatment system.

The locations of these profiles are shown in Plate 1, and information pertinent to the profiles is summarized below:

Profile	Stations	Length (feet)	Coil Spacings (meters)
HL-1	0 to 137	13,700	10 and 20
HL-3	0 to 109	10,900	10 and 20
HL-4	0 to 111	11,100	10 and 20
HL-5	0 to 54	5,400	10 and 20
MWP-1	94 to 144	5,000	3.67, 10, and 20
MWP-2	194 to 224	3,000	3.67, 10, and 20
MWP-3	276 to 347	7,100	10, 20, and 40
MWP-4	398 to 443	4,500	3.67, 10, and 20

3.1.4 Vertical Electrical Soundings

As an additional source of subsurface data, VESs were conducted using a Schlumberger electrode arrangement at 10 locations within the study area (Plate 1). The VES technique uses measurements of direct current applied into the ground

between two distantly spaced current electrodes and voltage differences between two more closely spaced potential electrodes to calculate apparent resistivities within the earth materials in the test area (Figure 3.3). By moving the current and potential electrodes to greater spacings, measurements are made that represent deeper and deeper materials. The technique is less rapid than the EM method, but the results give a profile of resistivity versus depth.

Interpretation of VES data involves plotting the logarithm of one-half of the current electrode spacing against the calculated apparent resistivity and matching the plot to a series of type curves (Keller and Frischknecht, 1966). The VES technique provides an estimate of the depths to and the resistivities of the different geo-electric layers in the vicinity of the center of the electrode spread. VES data, along with borehole and well data, were used to calibrate EM data to the conditions specific to the study area and to constrain the interpretation of the EM data.

3.2 Field Procedures

The procedures used to acquire field data for the EM profiling and VES techniques are described in the following sections. Extensive discussions of each procedure are available in Keller and Frischknecht (1966) and McNeill (1980b and 1985).

3.2.1 Electromagnetic Profiling

The data collection procedures for the EM technique are relatively simple. First, the survey lines are positioned with a constant station spacing. The stations are surveyed topographically to provide horizontal and vertical control for each measurement station. Data are then collected by occupying each station in turn and making conductivity measurements using several coil spacings (Figure 3.3). The data used in this study were collected from two to four coil spacings, as listed in Section 3.1.2.

For each coil spacing, the transmitter and receiver coils are held equidistant from the staked station location. The EM34-3 system can be used to measure the vertical dipole by laying the coils flat on the ground, or to measure the horizontal dipole by holding the coils vertically with their axes perpendicular to the survey line. The depths of penetration for the two orientations are different; therefore, it is desirable to collect data in both orientations when possible. In this study, however,

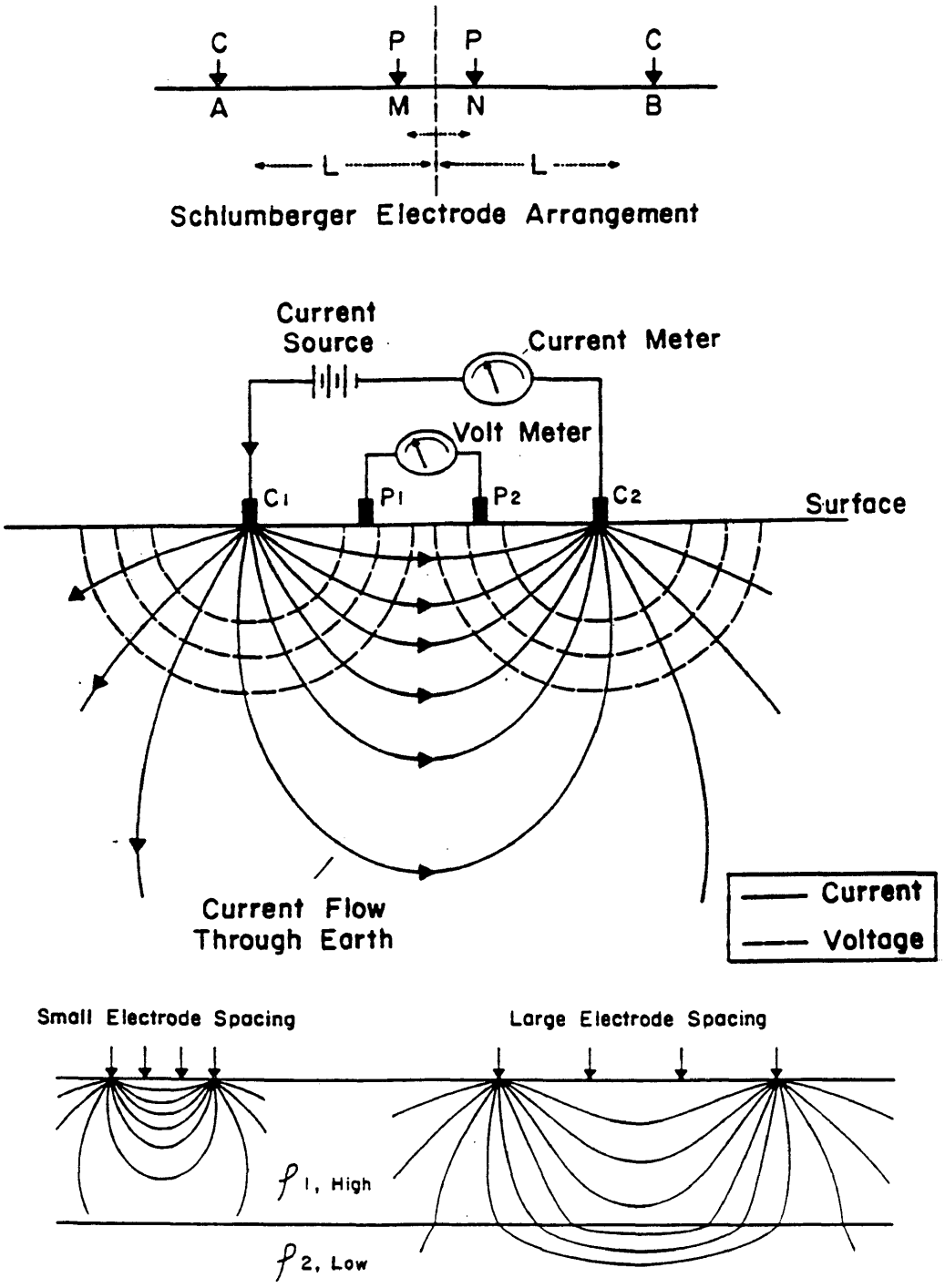

Figure 3.3 Vertical Electrical Sounding Configuration (After Benson and Others, 1982)

data were only collected in the latter mode after initial testing indicated that the vertical dipole data may be noisy, and therefore of minimal use. Each coil spacing uses a different signal frequency, and the coil separation can be adjusted accurately by using a tuning function built into the instrument. Data from each station can be collected within a few minutes, and the survey team may then move to the next station.

Each profile line in this study had a 100-foot station spacing, and as many as 12,000 line feet of data were collected in a day. For all profile lines, horizontal dipole data were collected at 10- and 20-meter coil spacings, and 40-meter coil-spacing data were collected on Line MWP-3. The EM31-D system, which has a fixed 3.67-meter spacing, was used to obtain additional data on Lines MWP-1,-2, and -4. The EM31-D system provides data with a shallower depth of penetration than the EM34-3 system; the addition of the 3.67-meter data from the EM31-D and the 40-meter EM34-3 data provided additional points with which to draw a conductivity curve (Kaufman and Keller, 1983). EM data for all eight profiles are listed in Appendix A.

3.2.2 Vertical Electrical Soundings

VES data were collected at 10 selected locations to supplement and calibrate the EM data and to aid in data interpretation where EM data were ambiguous. Six soundings (VES-A through VES-F) were conducted in 1989, and four (VES-1 through VES-4) were conducted in 1992 (HLA, 1990 and personal communication). The data were collected using potential electrode spacings in combinations of 0.30, 1.21, 1.52, and 1.83 meters (1, 4, 5, and 6 feet), and current electrode spacings from 0.66 to 141.43 meters (2.15 to 464 feet). These spacings allowed for depths of penetration ranging from approximately 0.33 to 70 meters (Dobrin, 1976). VES soundings have an advantage over EM profiling methods in that the method is not sensitive to alternating current power lines. Because the technique does not provide areal information as rapidly as EM profiling, only a limited number of VESs were conducted. VES data tables are presented in Appendix A, and data plots are presented in Appendix B.

Chapter 4.
RESULTS AND DISCUSSION

4.1 Conceptual Geophysical Model

Because of previous work in the vicinity of the study area and the downhole EM logging conducted in 1989, a simple two-layer geophysical model (Figure 4.1) was hypothesized. This model is based on the assumption that because bedrock is composed of mostly claystones and siltstones, which have a high ion content associated with the clay minerals, it has a relatively high electrical conductivity. The near-surface alluvial and eolian units, which consist of unconsolidated sandy silts to gravels, have lower electrical conductivities. Because of this favorable conductivity contrast, conductivity measurements made at the ground surface are expected to be higher where bedrock is shallower and lower where bedrock is deeper. This model is supported by data gathered in the study area (Figures 4.2 and 4.3).

A complicating factor to this simple model is that ground water within the shallow unconfined system is, in places, high in ionic concentration. In particular, the First Creek paleochannel has areas where ground-water TDS exceeds 5000 parts per million (ppm) (ESE, 1988; HLA, 1990, 1992). A large portion of this ionic concentration is chloride, with the remainder consisting of calcium, magnesium, sodium, and various other anions and cations. In the 52 wells used in this study for which ground-water data are available, chloride concentration ranges from 55 to 1700 ppm, with a mean of 464.7 ppm and a standard deviation of 419.7 ppm. The percentage of TDS represented by chloride ranges from 6.92% to 35.5%, with a mean of 20.1% and a standard deviation of 6.67%. The relatively high TDS within areas of the First Creek paleochannel raises the measured apparent conductivity and makes the interpretation of EM data problematic. In these areas, the geophysical model must be revised to a three-layer system: (1) unsaturated alluvium and eolian materials, (2) saturated alluvium and eolian materials (unconsolidated aquifer), and (3) bedrock materials (Figure 4.4). The electrical conductivity of high-TDS ground water may locally exceed that of bedrock. Where ground-water TDS concentration is low, the unconsolidated aquifer may have nearly the same conductivity as the unsaturated portion of

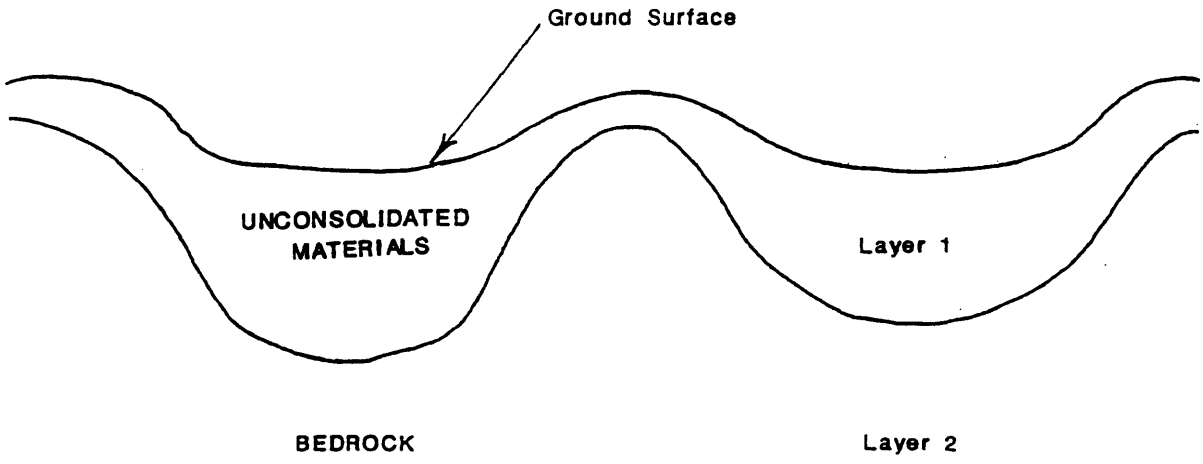

Figure 4.1 Two-Layer Geophysical Model Based on 1989 Borehole Logging Data

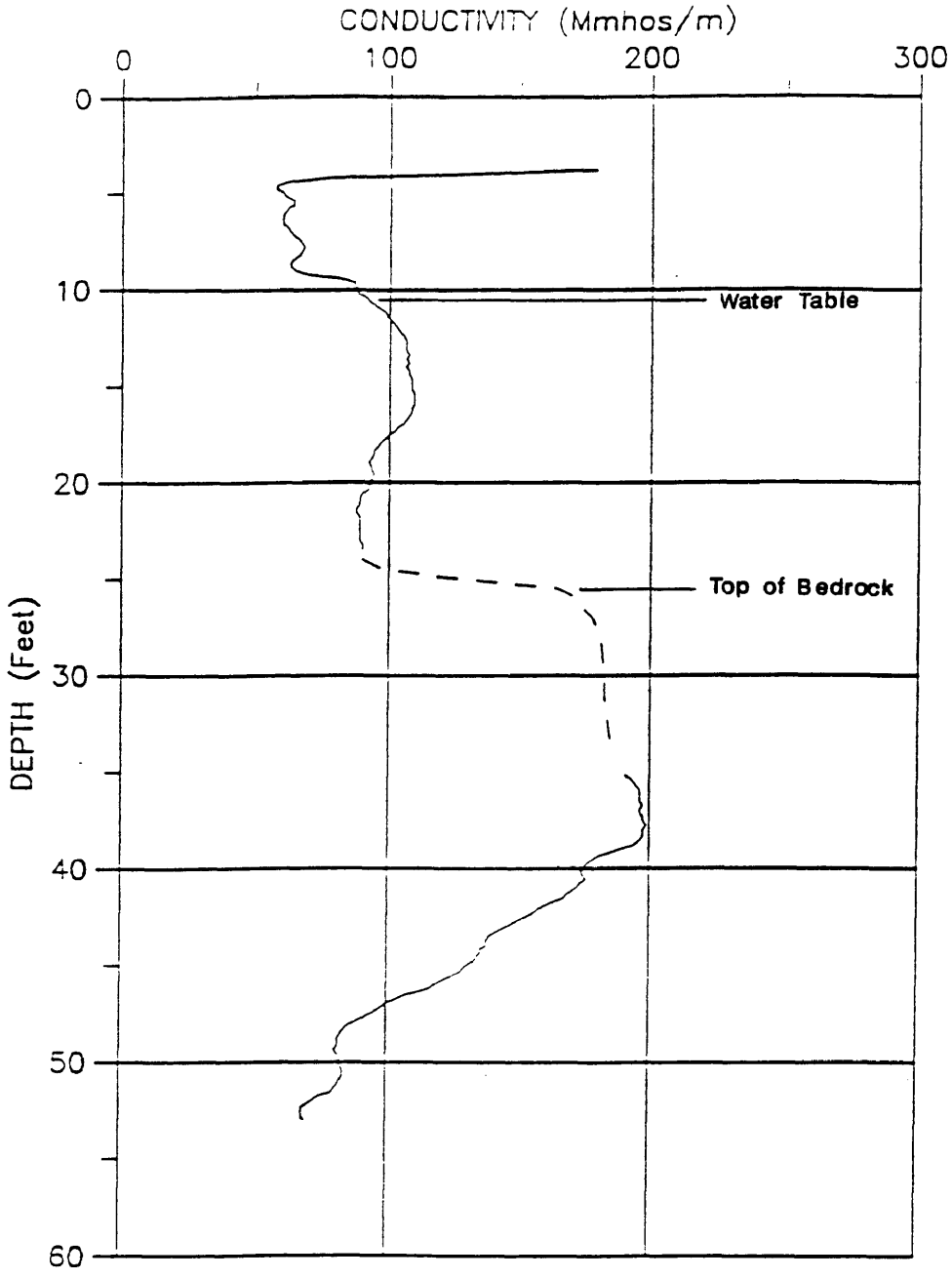

Figure 4.2 Composite Borehole Electromagnetic Log from Wells 37374 and 37379 (After HLA, Personal Communication)

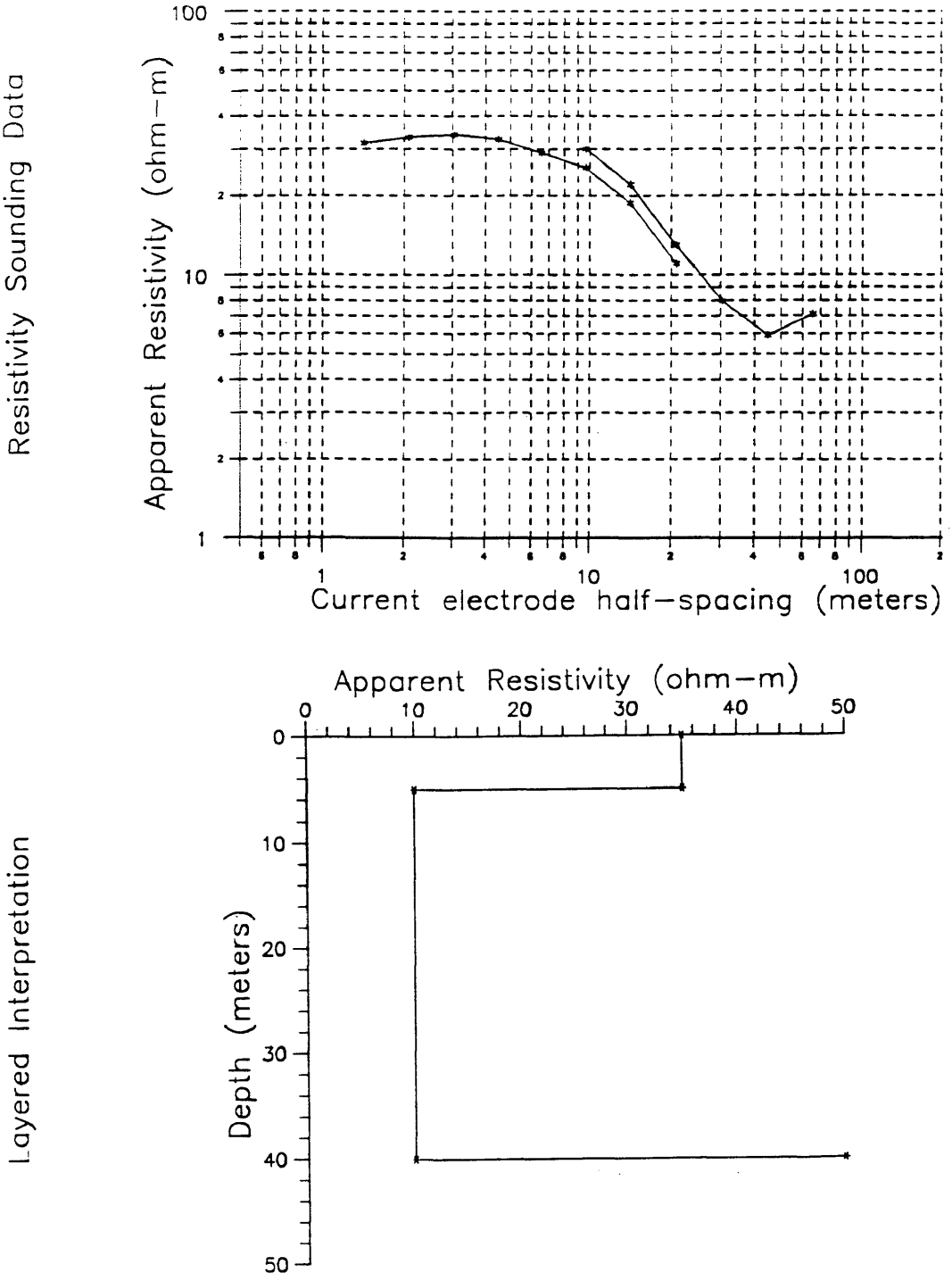

Figure 4.3 Resistivity Sounding Data and Interpretation for VES-3

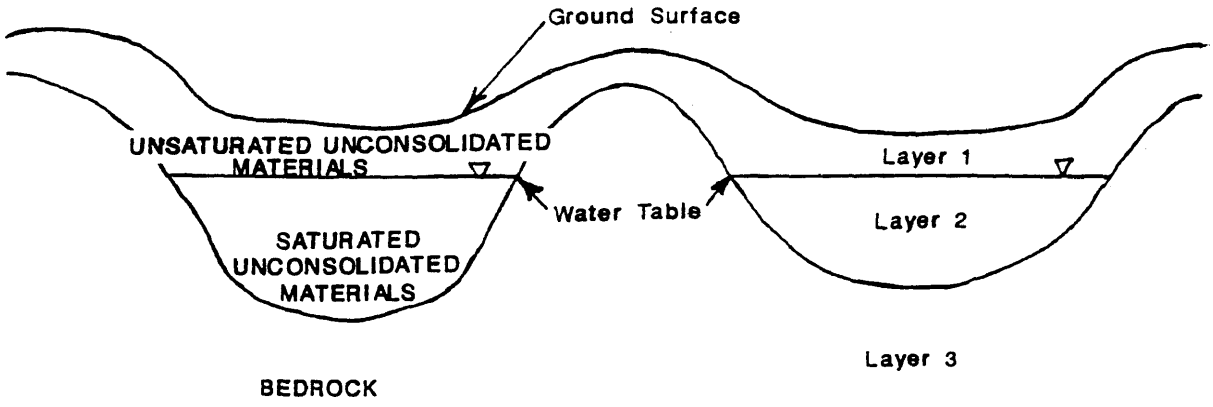

Figure 4.4 Three-Layer Geophysical Model

the unconsolidated unit. The three-layer model is supported by data presented in Figures 4.5 and 4.6.

4.2 Development of Geophysical Model for Test Area

The techniques used for evaluating the data obtained from the northern paleochannel include selection of parameters for analysis, assessments of data distributions, forward geophysical modeling, and assessment of lithologic and geochemical properties. These techniques and the results of the data evaluation are discussed in the following sections.

4.2.1 Parameter Selection

Parameters to be used for analysis were selected by examining the variations in the various types of field and analytical data. The northern paleochannel was used as the test area for developing the geophysical model and evaluating the data obtained during the study. This area was chosen because of its relative simplicity in relation to the First Creek area. The ground-water ionic concentrations are lower in the northern paleochannel than in the First Creek paleochannel; thus it was expected that the geophysical model would be less complex. From borehole induction logs from wells 37320, 37321, 37395, and 37397 (Appendix A) in the northern paleochannel, the measured apparent conductivities ranged from approximately 20 to 75 mmhos/m for unsaturated unconsolidated deposits, from 48 to 105 mmhos/m for saturated unconsolidated deposits, and from approximately 150 to 225 mmhos/m for the Denver Formation. Although there is some variation in conductivity between lithologies in the unconsolidated unit, and between Denver Formation subunits, there is a more pronounced contrast between unconsolidated deposits as a group and Denver Formation subunits as a group (Figure 4.6).

As shown by apparent conductivity data ranges shown in Section 3.1.2, the measured conductivity of the unconsolidated units is lower than that of the bedrock by a factor of 2 to 10, which suggests that the EM method is capable of distinguishing between the two in the absence of interferences that will be subsequently described. However, these data suggest that the EM method may not be able to resolve unsaturated versus saturated unconsolidated materials. In some of the borehole induction logs, a response indicating the location of the water table is not apparent.

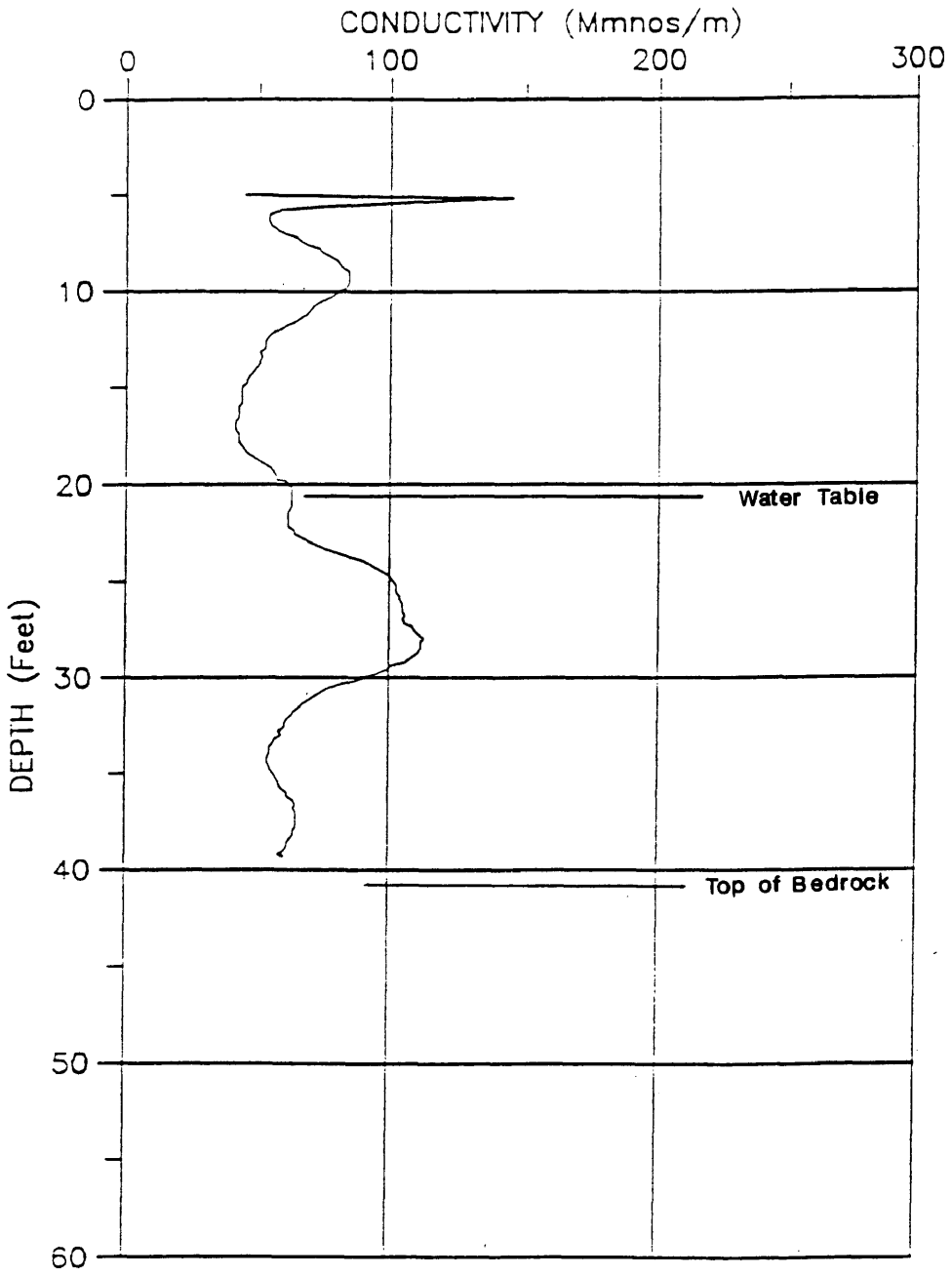

Figure 4.5 Borehole Electromagnetic Log from Well 37344 (After HLA, Personal Communication)

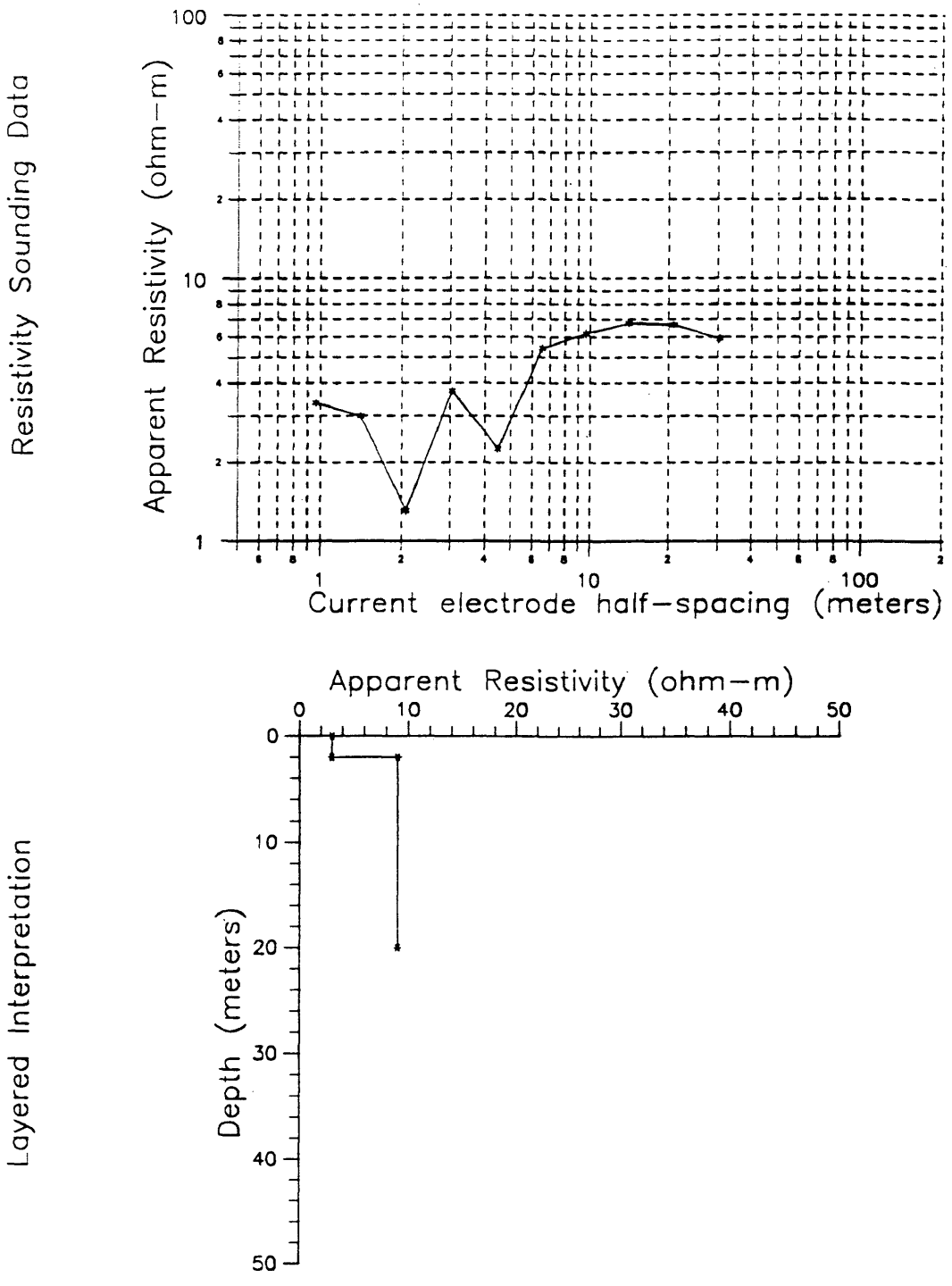

Figure 4.6 Resistivity Sounding Data and Interpretation for VES-D

However, logs from wells 37395, 37313, and 37374 (Appendix A) show an increase in conductivity at the water table. This response is hypothesized to be the result of high-TDS ground water. Because of this response, depth to bedrock, TDS, and apparent conductivity were chosen as the primary parameters for analysis. Other parameters for analysis include depth to water table and ground-water conductivity.

4.2.2 Data Analysis

The approach used for data analysis in this study consisted of several steps. The first step was to examine data distributions of the selected parameters, including apparent conductivity, depth to bedrock, ground-water conductivity, TDS concentration, and depth to water table. The second step was to examine cross-parameter relations and perform regression analyses using various combinations of parameters. The third step was to use the field data and the conceptual geophysical models discussed in Section 4.2.1, to perform forward geophysical modeling using a computer modeling program. The fourth step was to integrate the results of the data distribution assessment, the regression analyses, and the computer modeling assessment to arrive at an interpretation of the apparent conductivity data within the study area.

Parallel approaches were used for the northern paleochannel (used as the model development area) and the First Creek paleochannel (used as the model confirmation and refinement area). The results of the northern paleochannel assessment are discussed in the following subsections.

Assessment of Data Distributions

The examination of distributions for the various data types, presented in Table 4.1, indicated the following:

(1) Based on the distributions of apparent conductivity data for the 10-meter coil spacing, a value of greater than 64 mmhos/m may be considered anomalous for the 10-meter data, and a value of greater than 74 mmhos/m may be considered anomalous for the 20 meter data.

Table 4.1 Statistics for Northern Paleochannel Data

Parameter	Low Value	High Value	Mean	Variance	Standard Deviation	Number of Samples
Apparent Conductivity (mmhos/m)						
10-meter coil spacing	15.0	82.0	36.4	185.4	13.6	161
20-meter coil spacing	31.5	98.0	49.6	144.8	12.0	161
Residual conductivity (mmhos/m)						
10-meter coil spacing	-7.6	56.5	11.7	166.8	12.92	161
20-meter coil spacing	9.5	41.2	7.6	107.1	10.35	161
Standardized residual conductivity						
10-meter coil spacing	-.336	2.22	.472	.283	.532	161
20-meter coil spacing	-.202	1.04	.185	.065	.255	161
Depth to bedrock (feet)						
	23.0	54.0	39.0	31.6	5.62	45
Ground-water conductivity (mmhos/m)						
	120.0	222.5	151.9	536.36	23.16	25
Total dissolved solids in ground water (parts per million)						
	1004.0	2806.0	1467.2	192397.2	438.6	25
Water table depth (feet)						
	13.4	32.6	24.9	19.27	4.39	45

(2) Measured ground-water electrical conductivities greater than 1982 μmhos/cm (198.2 mmhos/m) are considered anomalous. This value is the sum of the mean plus twice the standard deviation.

(3) Ground-water TDS data greater than approximately 2344 ppm (see Figure 4.7) are considered anomalous for the area; this value is the sum of the mean value plus twice the standard deviation (Davis, 1986).

Cross-plots of different data types were made to examine the relationships between parameters. The following relationships were observed:

(1) Apparent conductivity measured at the ground surface is inversely, nonlinearly related to bedrock depth and depth to water table (Figures 4.8 and 4.9).

(2) Apparent conductivity is significantly directly related to ground-water TDS and ground-water electrical conductivity (Figure 4.10).

(3) Ground-water electrical conductivity (GC) is directly related to ground-water TDS, and this relationship can be described by a linear function with a correlation coefficient of 0.9141. A linear regression was performed on the GC and TDS data from the northern paleochannel, and the best-fit equation is as follows:

$$GC(\text{in } \mu\text{mhos/cm}) = 0.565 * TDS(\text{in ppm}) + 731.36$$

This relation is discussed further in Section 4.4.

Multivariate regressions involving 10- and 20-meter coil spacing apparent conductivity data as the dependent variables and bedrock depth, TDS concentration, and depth to water table as regression variables, were performed on the data points from the entire study area. Regressions using one, two, and all three variables were performed. The data for these regressions are summarized in Table 4.2, and indicate that all three regression variables are significant in determining apparent conductivity. However, the correlation coefficients, especially for the 20-meter data, suggest that the correct relation is not linear.

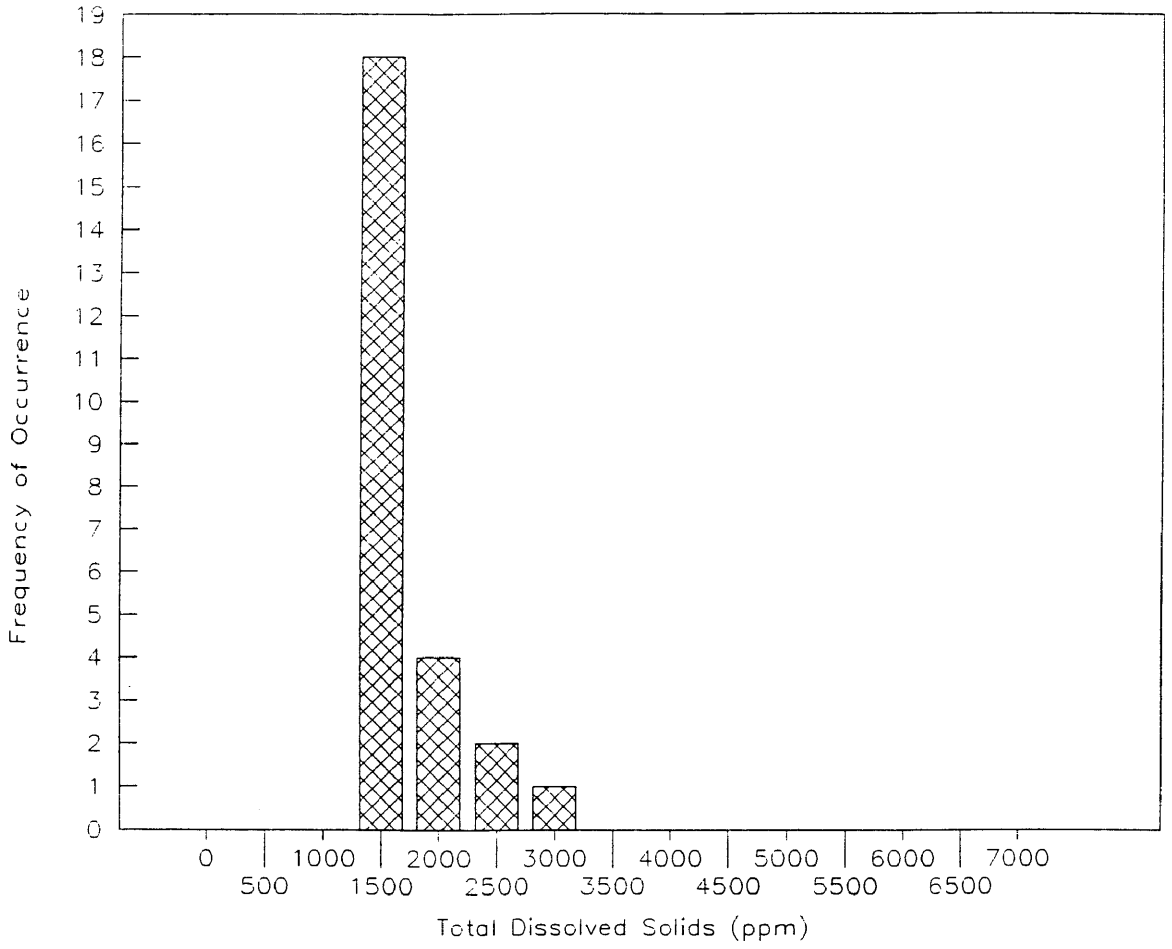

Figure 4.7 Histogram for Total Dissolved Solids in Ground Water for the Northern Paleochannel

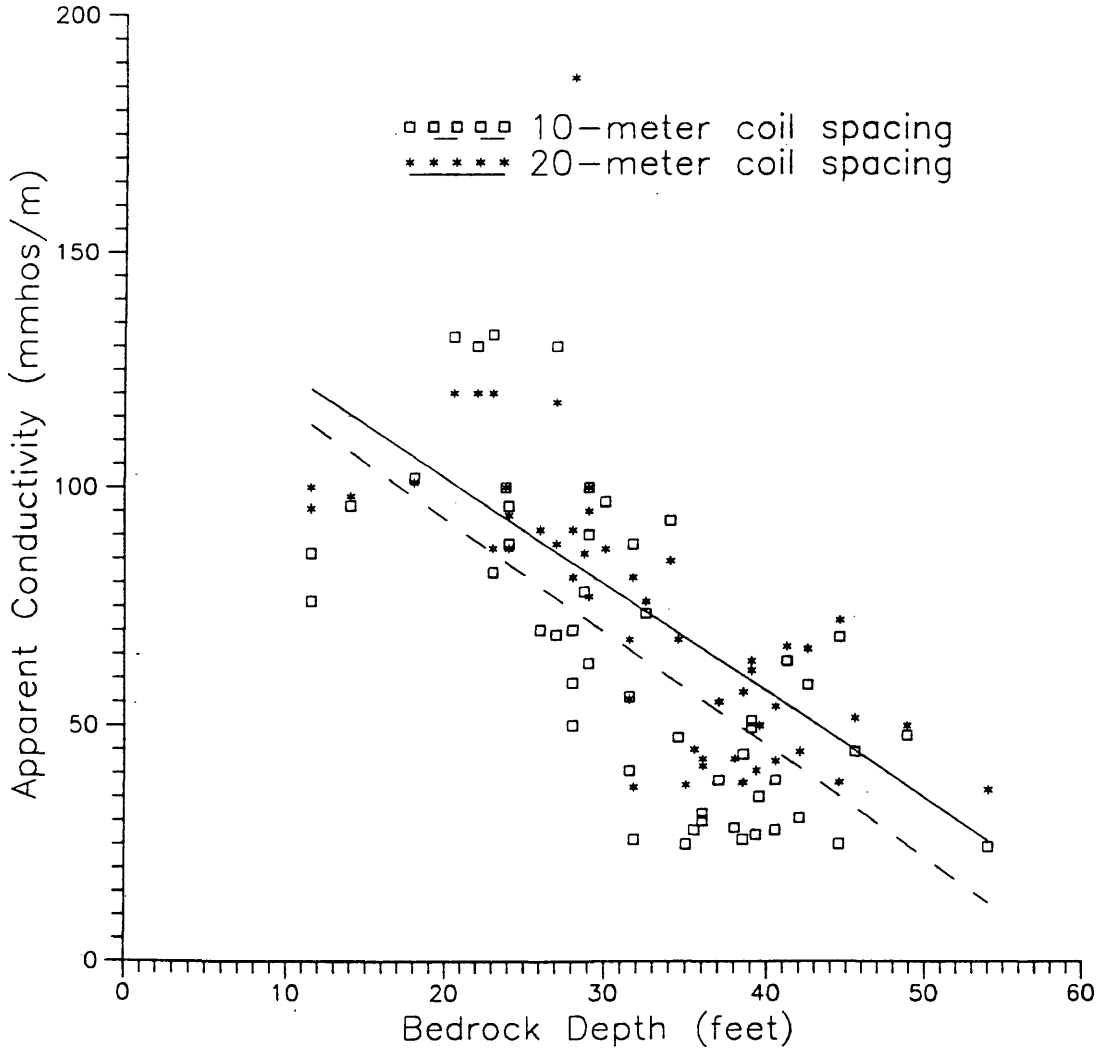

Figure 4.8 Relation of Apparent Conductivity to Bedrock Depth for All Data Points in the Study Area

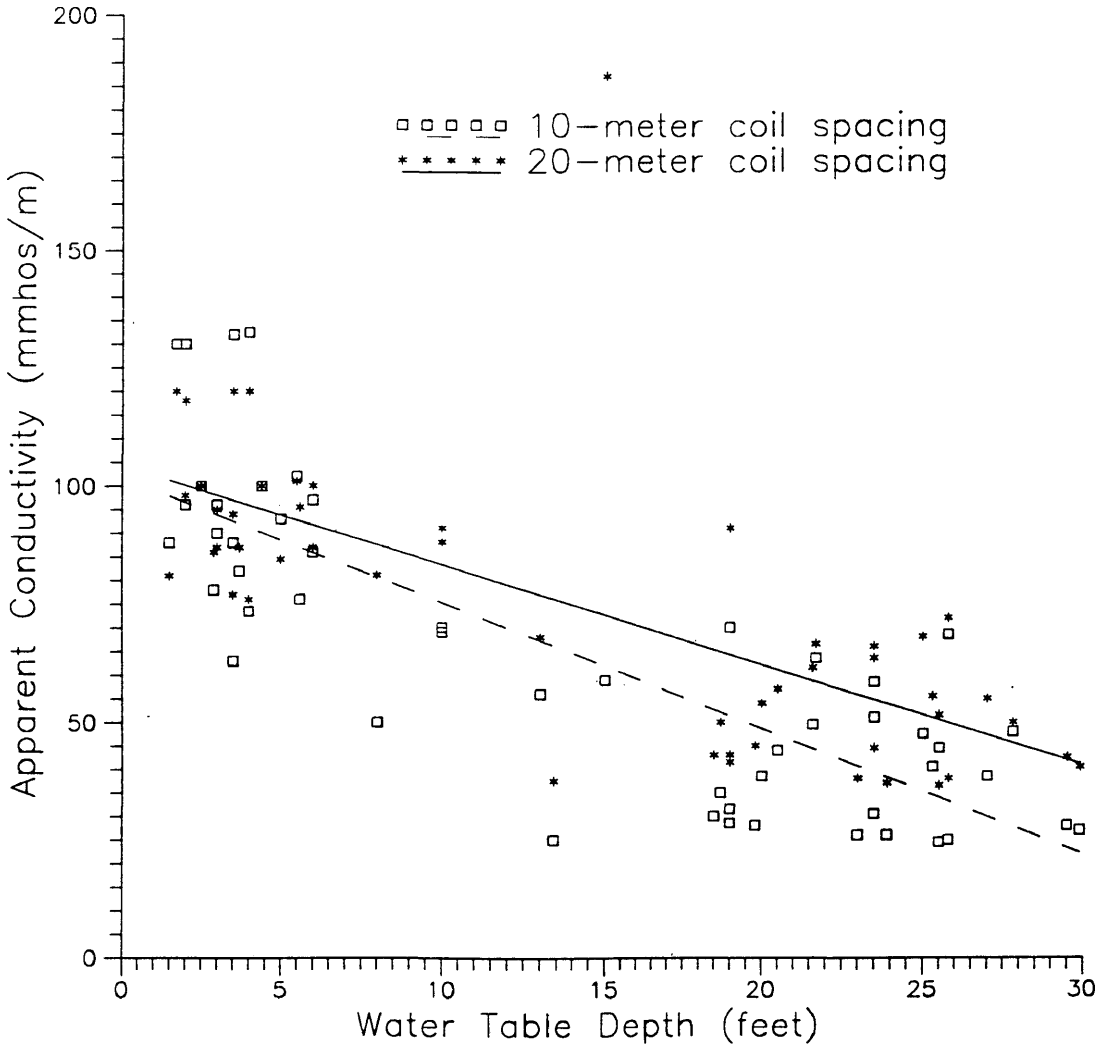

Figure 4.9 Relation of Apparent Conductivity to Water-Table Depth for All Data Points in the Study Area

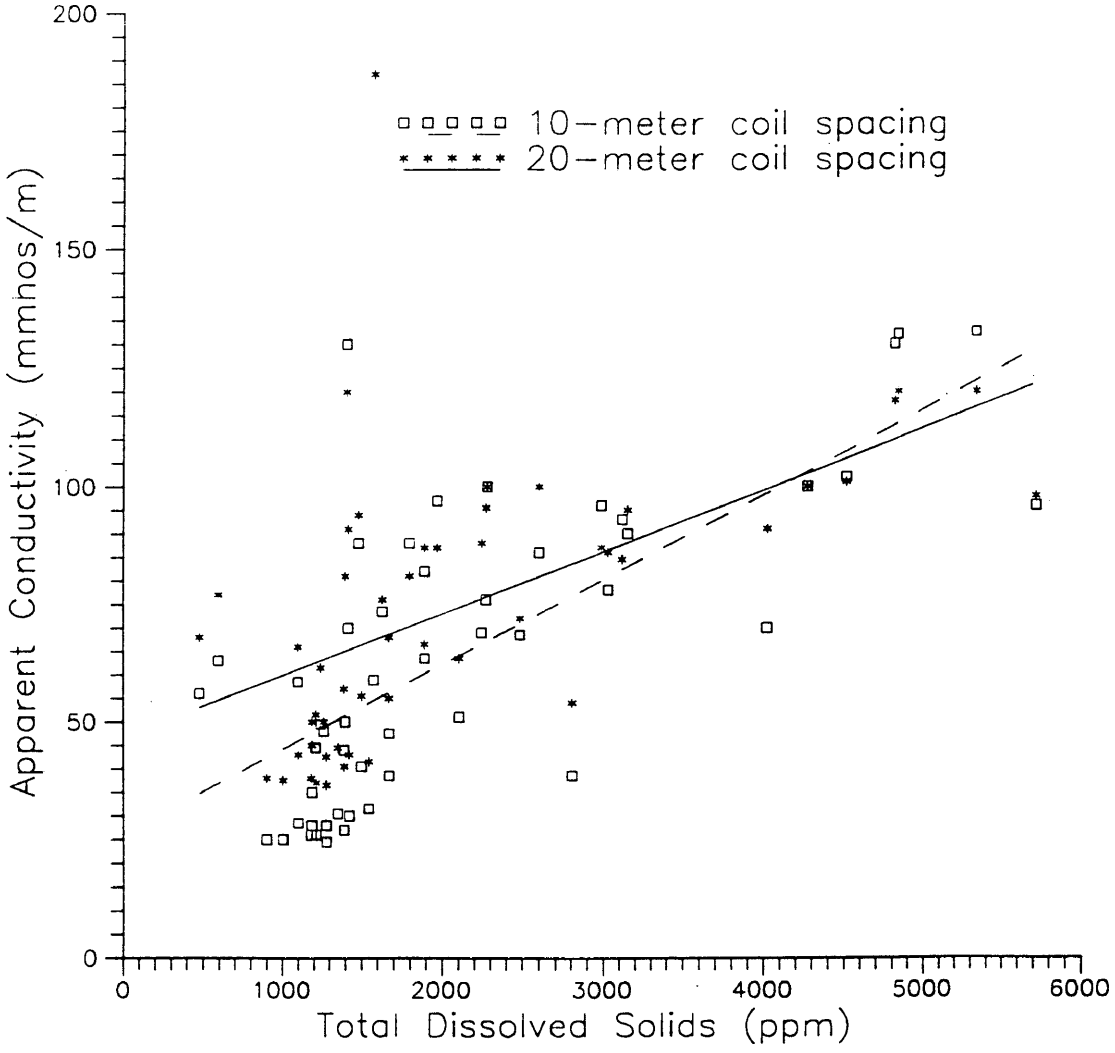

Figure 4.10 Relation of Apparent Conductivity to Total Dissolved Solids in Ground Water for All Data Points in the Study Area

Table 4.2 Multivariate Regression Results for All Data Points in the Study Area

A. Regression Relations with Apparent Conductivity (10-meter coil spacing) as the Dependent Variable:

	Standardized Partial Regression Coefficients for Regression Variables							
	Constant	Bedrock Depth	TDS	Water Table Depth	Correlation Coefficient	F-Test	F_{crit} (α=.05)	Degrees of Freedom
Equation:	AC = 70.65 +.0342 BR + .0098 TDS - 1.99 WT							
SRCs	0.0	.0099	.3897	-.6094	.8774	52.38	2.81	3,47
Equation:	AC = 71.53 + .0097 TDS - 1.97 WT							
SRCs	0.0	none	.3878	-.6026	.8774	80.23	3.20	2,48
Equation:	AC = 84.74 - 1.43 BR + .0122 TDS							
SRCs	0.0	-.4171	.4840	none	.7968	41.72	3.20	2,48
Equation:	AC = 140.41 -2.36 BR							
SRCs	0.0	-.6887	none	none	.6887	44.22	4.04	1,49
Equation:	AC = 101.0 -2.66 WT							
SRCs	0.0	none	none	-.8152	.8152	97.06	4.04	1,49
Equation:	AC = 26.12 + .0180 TDS							
SRCs	0.0	none	.7181	none	.7181	52.17	4.04	1,49

SRC = Standardized Partial Regression Coefficient; TDS = Total Dissolved Solids (ppm);
AC = Apparent Conductivity (mmhos/m); BR = Bedrock depth (feet); WT = Water Table Depth (feet)

Table 4.2 Multivariate Regression Results for All Data Points in the Study Area (continued)

B. Regression Relations with Apparent Conductivity (20-meter coil spacing) as the Dependent Variable:

	Standardized Partial Regression Coefficients for Regression Variables							
	Constant	Bedrock Depth	TDS	Water Table Depth	Correlation Coefficient	F-Test	F_{crit} (α=.05)	Degrees of Freedom
Equation:	AC = 113.32 -1.069 BR + .0046 TDS - .9887 WT							
SRCs	0.0	-.3306	.1931	-0.3213	.7462	19.68	2.81	3,47
Equation:	AC = 85.65 + .0060 TDS -1.6863 WT							
SRCs	0.0	none	.2544	-0.5481	.7197	25.78	3.20	2,48
Equation:	AC = 120.31 - 1.797 BR +.0057 TDS							
SRCs	0.0	-.5557	.2428	none	.7206	25.92	3.20	2,48
Equation:	AC = 146.62 - 2.238 BR							
SRCs	0.0	-.6920	none	none	.6920	45.03	4.04	1,49
Equation:	AC = 104.39 - 2.115 WT							
SRCs	0.0	none	none	-.6875	.6875	43.92	4.04	1,49
Equation:	AC = 46.76 + .0131 TDS							
SRCs	0.0	none	.5548	none	.5548	21.79	4.04	1,49

SRC = Standardized Partial Regression Coefficient; TDS = Total Dissolved Solids (ppm);
AC = Apparent Conductivity (mmhos/m); BR = Bedrock depth (feet); WT = Water Table Depth (feet)

Forward Modeling Results

On the basis of the relationships described above, forward modeling was conducted for all eight EM lines, using the computer program EMIX34P, written by Interpex, Ltd. of Golden, Colorado. The input parameters for each station for the model were station location, surface elevation, number of layers, layer conductivities, layer thicknesses, and coil spacings. The program calculates theoretical EM34-3 and EM31-D responses for each coil spacing based on the input model parameters (Interpex, 1993).

The analytical technique used during the forward modeling portion of the study was to compare the actual EM apparent conductivity data obtained in the field with the synthetic data calculated by EMIX34P. The synthetic data were then subtracted from the actual data, and the differences or residuals were examined, posted on a map, and contoured. The residuals were then interpreted by assessing their distributions and lateral variations and by comparing them to other parameters. Positive residuals or anomalies are present where the actual data exceed the synthetic data, and negative residuals occur where synthetic data exceed actual data. Standardized residuals were calculated for each station by dividing the residual for that station by the synthetic apparent conductivity value for that station. The standardized residual represents the residual as a fraction of the synthetic value. Plots of the actual data, synthetic data, and residual and standardized residual data are presented in Appendix B.

The geophysical model that was input to the forward modeling program was a two-layer model representing unconsolidated materials overlying bedrock (see Figure 4.11). The conductivities selected for the two layers were 30 mmhos/m for alluvium and 200 mmhos/m for bedrock, based on the responses observed in borehole induction logs. The thickness of the unconsolidated layer was calculated by subtracting the mapped bedrock surface elevation from the ground-surface elevation. The bedrock surface map was obtained from a previous study (HLA, personal communication) and was constructed based on accumulated borehole information. The topographic values were a combination of professionally surveyed data and data estimated from a detailed topographic map of the study area (HLA, 1990).

The two-layer input conductivity model generated synthetic curves that, in places, agree well with the actual field data (see Figure 4.12). However, positive and negative residuals were observed (see Figures 4.13 and 4.14 and Appendix B). The areas where the absolute value of the residual exceeds approximately 10 to 20

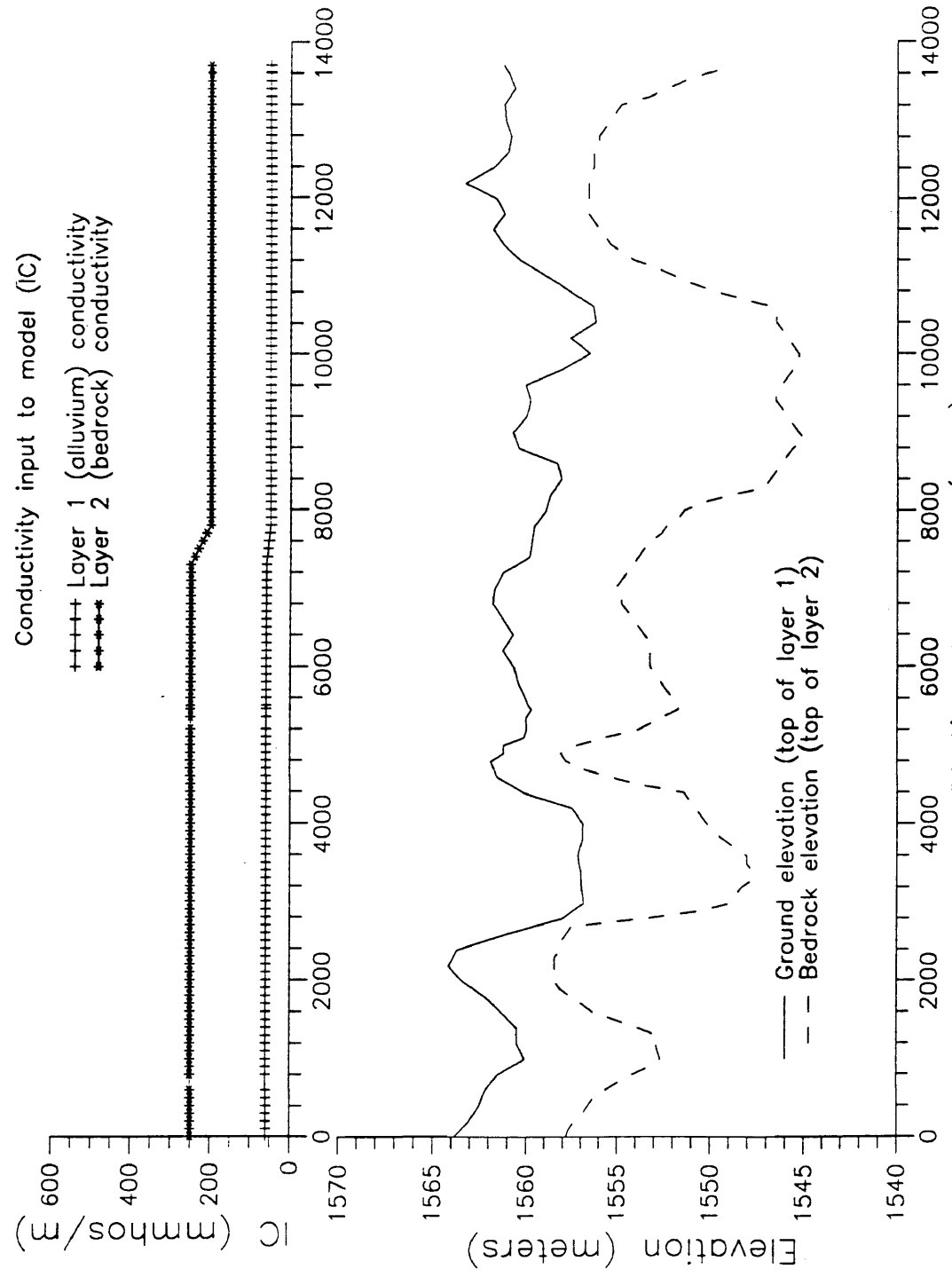

Figure 4.11 Input Data for Two-Layer Geophysical Model for Line HL-1

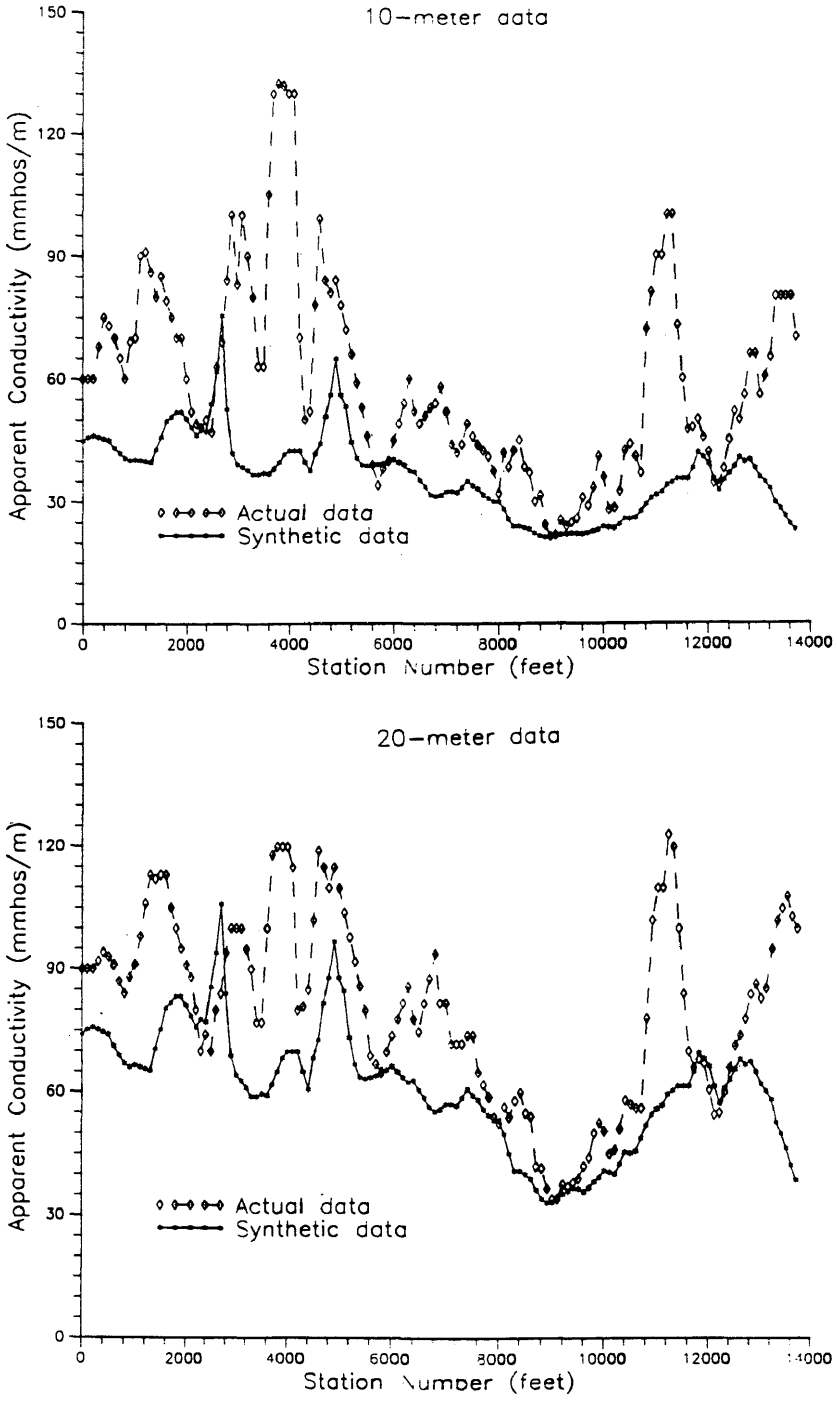

Figure 4.12 Actual and Synthetic Apparent Conductivity Data for Line HL-1

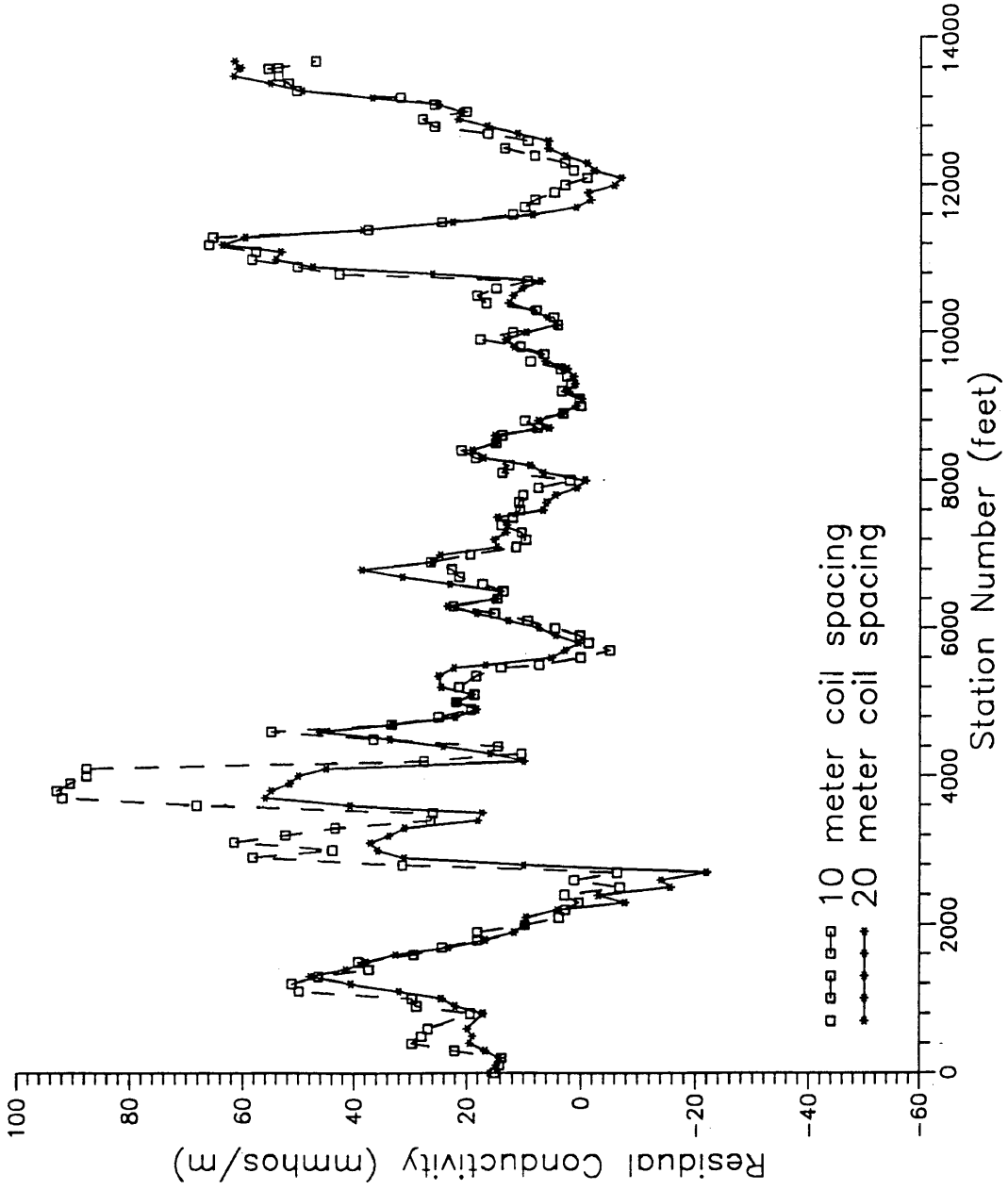

Figure 4.13 Residual Apparent Conductivity Data for Line HL-1

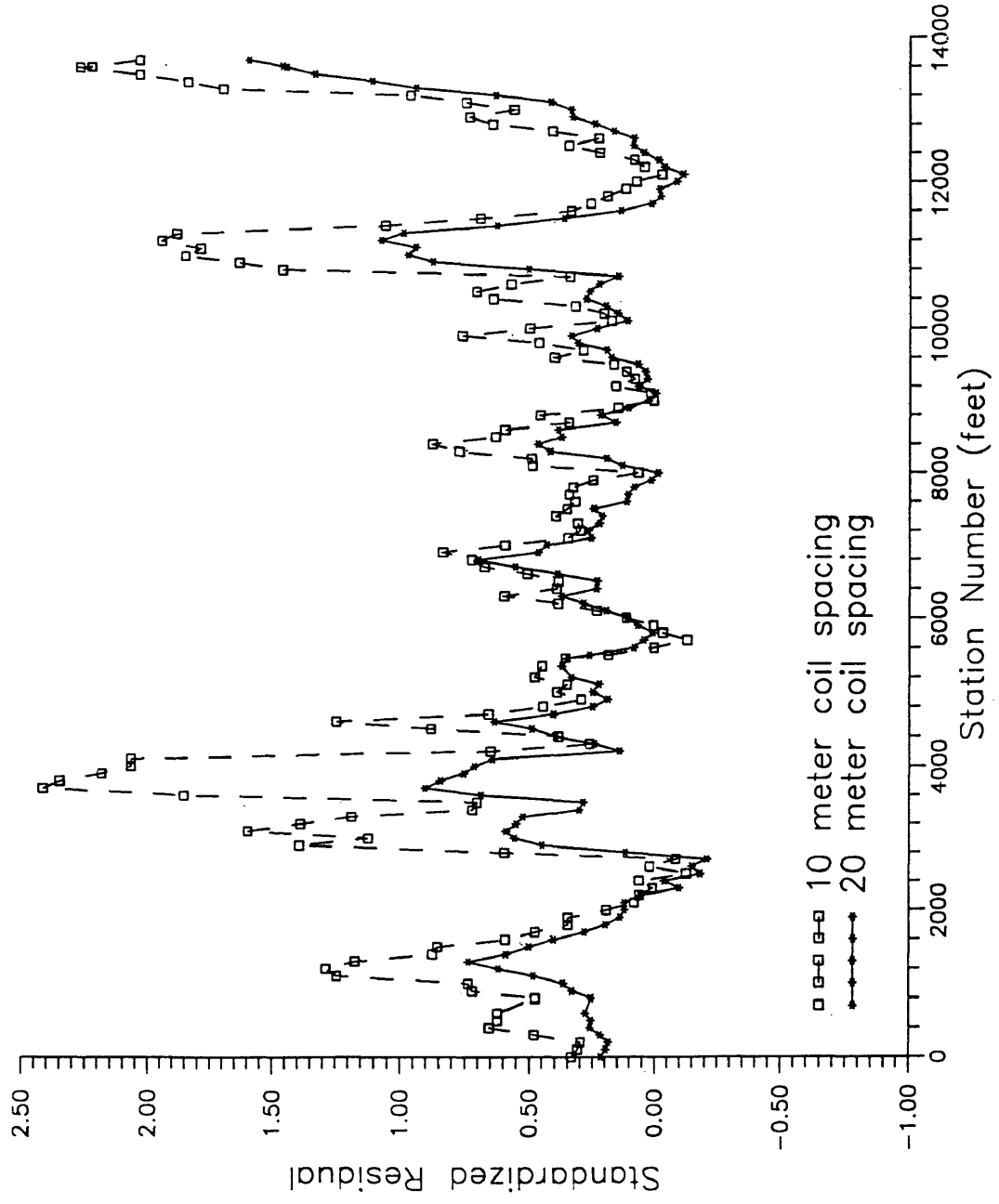

Figure 4.14 Standardized Residuals for Line HL-1

mmhos/m were interpreted to be most meaningful. This is the level at which residuals were interpreted to represent, with a greater degree of confidence, physical phenomena not due to model input data inaccuracies The positive residuals can be caused by three different factors: (1) high-TDS ground water creates a third layer with high conductivity between the alluvium and the bedrock, (2) bedrock depth is shallower than has been mapped on the basis of borehole data, or (3) a higher than normal conductivity exists in the unsaturated unconsolidated layer. The first type of residual was observed most often, particularly on lines HL-1, HL-3, and MWP-3 (see Plate 1). The second type of residual anomaly is believed to occur in unsaturated areas on lines HL-1, HL-3, HL-4, and MWP-3. The third residual anomaly type may occur in the unsaturated area at the northeast edge of the northern paleochannel on lines HL-1, HL-3, HL-4, and MWP-3. The reason that high conductivity in the unconsolidated unit is suspected is that a large cattle feedlot and a manure pile from past feedlot operations are present in the areas of anomalously high conductivity data near the northeast ends of these EM lines. The three types of anomalies and the areas affected by them are discussed in Section 4.4 and are posted on Plate 3. The standardized residuals calculated for each EM station did not prove to be useful in interpreting the forward modeling results. Standardized residuals exhibited the same relationships between coil spacings as did normal residuals, but could not be correlated from line to line.

4.2.3 Lithologic Properties

The only parameter that was varied across the northern paleochannel in the forward modeling simulations was depth to bedrock, the thickness of the uppermost model layer. For the majority of the length of four of the five lines that cross the northern paleochannel, the EMIX34P-generated synthetic data provide a fairly close match to the actual field data. This general match suggests that bedrock depth is an important parameter in the geophysical model. The importance of bedrock as a significant parameter in determining apparent conductivity is supported by the multivariate regression results for the area, as shown in Table 4.2.

The variations in unconsolidated unit lithology and bedrock lithology do not appear to correlate well with residual conductivity anomalies, where the modeled data deviate appreciably from the actual data. However, large lateral conductivity changes within the unconsolidated materials are not expected. Nearly all of the borehole data

examined show a degree of vertical inhomogeneity, but suggest that the area is relatively laterally homogeneous.

4.2.4 Geochemical Properties

The residual conductivity anomalies were compared with ground-water TDS data from wells within 300 feet of the EM profile lines. In nearly every case where a positive residual anomaly (Figure 4.13) occurs in an area of saturated alluvium and eolian materials, the anomaly can be correlated with high TDS in ground water (Plate 2). Several positive residual anomalies occur within the saturated portions of the paleochannels where no ground water data exist (Plate 3), and because of the linear relationship between TDS and electrical conductivity observed in ground-water sample data, it is interpreted that high-TDS ground water is the primary factor responsible for the residual conductivity anomalies. The data indicate that high-TDS ground water causes a high-conductivity layer, and that a large thickness of this high-conductivity layer creates an anomalously high EM apparent conductivity response that overshadows the small responses that may occur from saturated unconsolidated material conditions alone.

4.3 Refinement of Geophysical Model in Confirmation Area

The techniques for refining the geophysical model in the First Creek paleochannel were similar to those used in model development. As with the northern paleochannel, several steps were performed using First Creek paleochannel data. First, data distributions were examined. Regressions were not performed separately for First Creek data, because the regressions performed for model development (Section 4.2.1) included data from the entire study area. Results of forward modeling were examined and combined with the data distribution assessment to arrive at an interpretation and a refined model for the area. The results of the model refinement are presented in the following sections.

4.3.1 Data Analysis

Ground-water TDS data for the First Creek paleochannel were plotted against GC data, and a linear regression was performed (Figure 4.10). The best-fit equation for the data was found to be the following:

$$GC \text{ (in } \mu\text{mhos/cm)} = TDS \text{ (in ppm)} * 0.983 + 490.54$$

This equation, with a correlation coefficient of 0.9543, is more significant than the equation for the northern paleochannel. This relation is discussed further in Section 4.4.

The two-layer geophysical model developed for the northern paleochannel was applied to the First Creek paleochannel (Figure 4.11) to confirm the areal extent where the model appears to be valid. In general, the model produced synthetic data with broad depressions corresponding to the paleochannels, and peaks corresponding to the bedrock high areas between paleochannels. Several areas of positive residual anomalies were produced within the saturated unconsolidated portion of the paleochannel, and another anomalous condition was noted in this area. In the portion of the paleochannel where high ground-water TDS has been identified as the highest, the following conditions were observed: (1) the residual conductivity anomalies are the greatest, (2) the 10-meter data are greater than the 20-meter data (Figure 4.12), and (3) the 10-meter residuals are greater than the 20-meter residuals (Figure 4.13). Where 3.67-meter spacing data were collected, the 3.67-meter data were also greater than the 10-meter data and the 3.67-meter residuals were greater than the 10-meter residuals. This crossover effect is consistent across all six EM profile lines that traverse the First Creek paleochannel. The effect is interpreted to indicate that a highly conductive third layer is present between the two modeled layers (Figure 4.15).

A two-layer model with conductivities of 50 mmhos/m for the unconsolidated layer and 250 mmhos/m for the bedrock provides a better fit between modeled and actual data than does the 30/200 mmhos/m model used for the northern paleochannel (Figure 4.11). Using the 50/250 mmhos/m conductivities for model input, the low portions of the actual EM data (the valleys between the high residual areas) match the modeled data reasonably well (Figures 4.12 and 4.13). However, because of the higher TDS values present in the First Creek paleochannel, there are more anomalously high areas with higher residual anomalies than in the northern paleochannel

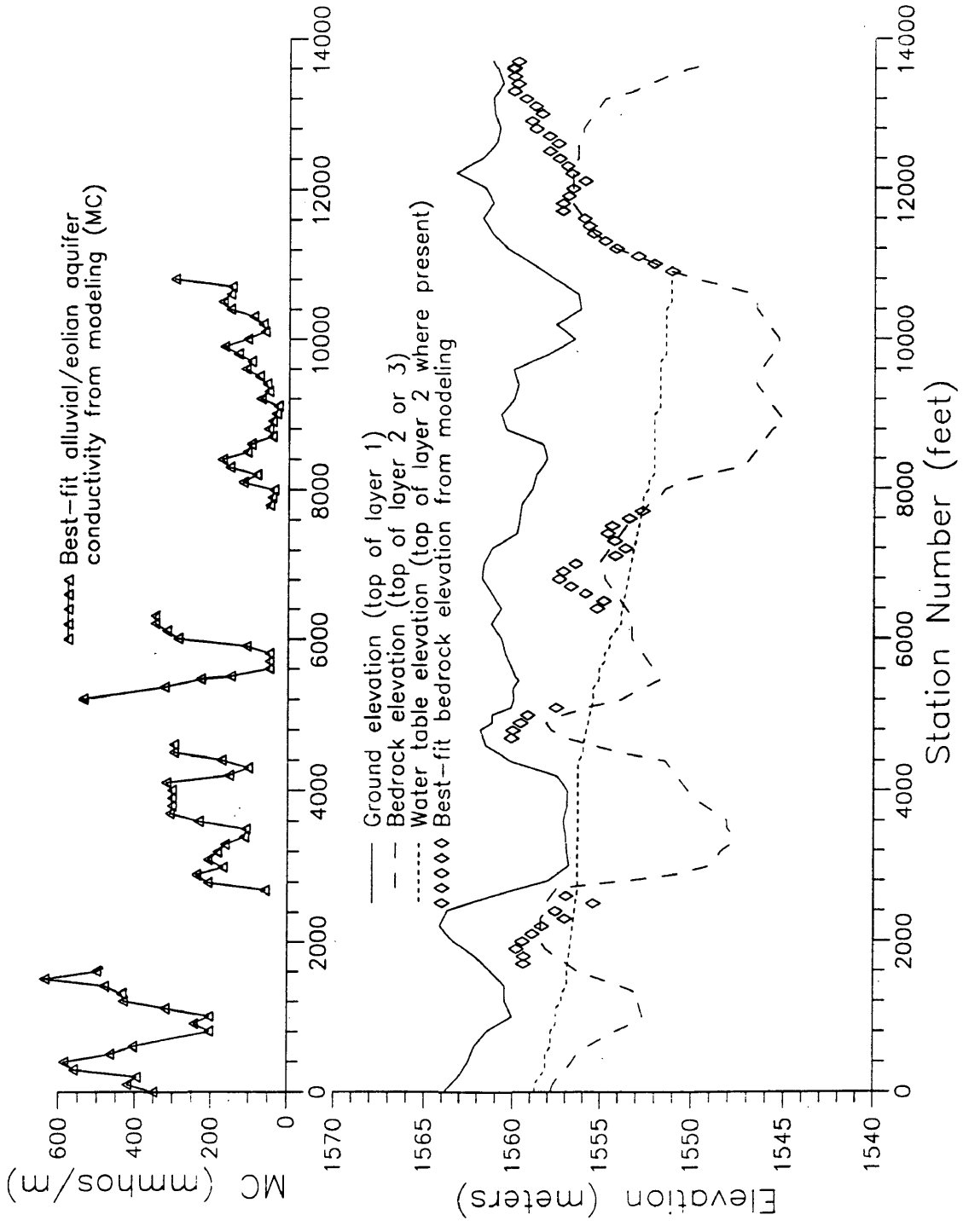

Figure 4.15 Three-Layer Geophysical Model for Line HL-1

(see Tables 4.1 and 4.3 and Figure 4.16). Therefore, the errors associated with using only a two-layered geophysical model are greater in the First Creek area.

4.3.2 Lithologic Properties

The main lithologic property affecting the apparent conductivity response is depth to bedrock. Comparison of synthetic conductivity data to actual data indicates that, in areas of unsaturated unconsolidated materials where there is no interference caused by high-TDS ground water, the two-layered geophysical model of unconsolidated materials over bedrock provides a relatively close match. Because this model does not take lithologic variation into account, it is interpreted that such variations do not have a major effect on the conductivities within either the unconsolidated unit or the bedrock. By varying the depth to bedrock by up to a few meters, the synthetic data can be made to match the actual data with a high degree of accuracy. This close match suggests that either (1) the model conductivities are very close to those of the actual geologic materials, and the model results can therefore be used to improve the estimate of the bedrock surface, or (2) the bedrock depths input to the model may be accurate and the conductivity values are incorrectly assumed. The data suggest that the former is true in the bedrock high areas where the unconsolidated unit is unsaturated and there is a lower density of borehole data to constrain the bedrock surface interpretation. In general, the limits of the mapped bedrock high areas agree with the interpretation of the conductivity data, although the positions of the bedrock crests may be shifted by as much as 200 feet and the bedrock depths may be inaccurate by as much as two meters (Figure 4.15).

4.3.3 Geochemical Properties

The combination of ground-water TDS and saturated unconsolidated thickness are interpreted to be the primary geochemical parameters affecting conductivity. The presence of high-TDS ground water is confirmed by ground-water analytical data from wells in the vicinity of the EM profile lines (Plate 2). The highest TDS value of 5713 ppm is from well 37072, which is approximately 50 feet from station 1500 on Line HL-3; this station has a residual apparent conductivity of 47.4 mmhos/m for the 10-meter coil spacing. Well 37069, with a TDS of 5332 ppm, is approximately 200 feet from station 3800 on Line HL-1; this station has a 10-meter residual apparent

Table 4.3 Statistics for First Creek Paleochannel Data

Parameter	Low Value	High Value	Mean	Variance	Standard Deviation	Number of Samples
Apparent conductivity (mmhos/m)						
10-meter coil spacing	29.0	132.5	65.97	482.4	21.96	197
20-meter coil spacing	52.0	120.0	80.59	179.96	13.41	197
Residual conductivity (mmhos/m)						
10-meter coil spacing	-6.4	92.9	26.0	453.7	21.3	197
20-meter coil spacing	-21.9	56.0	15.7	180.2	13.4	197
Standardized residual conductivity						
10-meter coil spacing	-.159	2.41	.652	.292	.541	197
20-meter coil spacing	-.207	.903	.245	.0432	.208	197
Depth to bedrock (feet)						
	11.0	34.0	24..44	41.12	6.41	30
Ground-water conductivity (mmhos/m)						
	85.0	610.0	318.65	24245.42	155.7	23
Total dissolved solids in ground water (parts per million)						
	476	5713	2743.9	2287073.0	1512.3	23
Water table depth (feet)						
	1.5	16.0	5.95	18.87	4.344	30

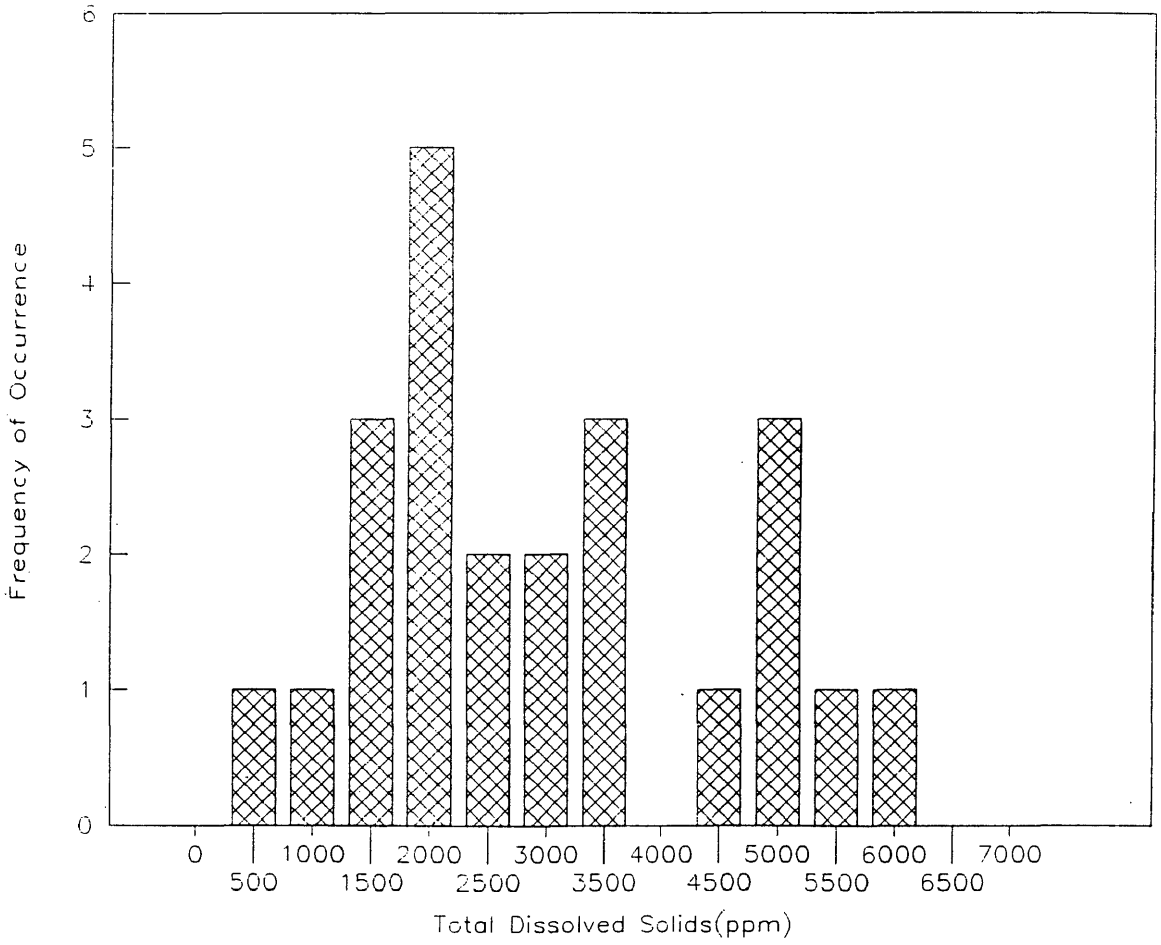

Figure 4.16 Histogram for Total Dissolved Solids in Ground Water for the First Creek Paelochannel

conductivity of 92.9 mmhos/m. The depth to ground water in the First Creek paleochannel is also shallower than in the northern paleochannel (see Tables 4.1 and 4.3), which makes the effect of the high-TDS ground water in the First Creek paleochannel more pronounced.

The saturated area of the First Creek paleochannel was modeled using an alternative three-layered model (Figure 4.15). The assumption was made that the saturated thickness of the unconsolidated unit (the unconsolidated aquifer) may represent a distinct conductivity layer, with the conductivity varying proportionally with ground-water TDS concentration. The model input thickness of the unconsolidated aquifer layer was calculated by subtracting the potentiometric surface values from a previous study (HLA, personal communication) from ground-surface elevation values. The results of this modeling effort indicated that a close match to actual apparent conductivity data could be achieved using this approach. The unconsolidated aquifer conductivities that provided the best match to actual apparent conductivity data are displayed in Figure 4.15.

The results of the modeling effort allowed the boundaries of the high-TDS residual anomalies to be estimated more accurately than before modeling was conducted. Likewise, the boundaries of the residual anomalies interpreted to represent excessive estimates of bedrock depths can be more accurately estimated. The extent and magnitudes of the anomalies, based on the interpretation of residual data, are summarized in Section 4.4 and displayed on Plate 3.

4.4 Application of Geophysical Model to Study Area

The conceptual geophysical model was applied to the study area in the same way as for the two paleochannels. The study area outside of the paleochannels has a much lower density of borehole data, so that there are fewer data points against which to judge an interpretation of the EM data. However, by using the two paleochannels as calibration areas, the EM interpretation was extrapolated to the sparse-data areas to enhance the understanding of the bedrock configuration and the ground-water TDS concentration within the study area. The statistics for parameters in areas of unsaturated unconsolidated materials are listed in Table 4.4.

Table 4.4 Statistics for Areas of Unsaturated Unconsolidated Materials

Parameter	Low Value	High Value	Mean	Variance	Standard Deviation	Number of Samples
Apparent conductivity (mmhos/m)						
10-meter coil spacing	27.9	106.0	58.2	273.8	16.5	260
20-meter coil spacing	35.9	123.0	79.6	276.7	16.6	260
Residual conductivity (mmhos/m)						
10-meter coil spacing	-23.1	74.0	17.20	301.89	17.37	260
20-meter coil spacing	-33.2	63.6	12.01	320.39	17.90	260
Standardized residual conductivity						
10-meter coil spacing	-.376	2.39	.500	.300	.548	260
20-meter coil spacing	-.330	1.59	.216	.104	.322	260
Depth to bedrock (feet)						
	8.5	33.0	15.32	45.41	6.74	11

4.4.1 Lithologic Properties

The depth to bedrock estimates throughout the study area have been evaluated on the basis of the EM conductivity modeling results. The modeling results indicate that depth to bedrock is accurately estimated throughout the majority of the study area. However, there are some notable exceptions that will be discussed.

Positive and negative residual conductivities in the area of unsaturated unconsolidated materials at the southwest boundary of the First Creek paleochannel (see Plate 3) suggest that bedrock may be shallower in the southwestern portion and deeper in the northeastern portion than is currently estimated. An inaccurate estimate in this area is plausible because of the lack of borehole data in this area. The objectives of past studies have not focused on the accurate depiction of the bedrock surface in unsaturated areas, but rather on the assessment of paleochannel configuration and lithologic variation in saturated areas. Similar anomalies are present in unsaturated areas north of the First Creek paleochannel, south of the northern paleochannel, and particularly north of the northern paleochannel.

In the area north of the northern paleochannel, two high residual conductivity anomalies suggest that either (1) suspected high ionic concentration conditions exist in the soil, or (2) bedrock is actually shallower than is currently estimated (see Figure 4.17). Two variations on the basic geophysical model were input to EMIX34P, and the following two possibilities were found to produce good agreement between actual and synthetic data:

1. The conductivity of the unconsolidated layer is locally increased to approximately 200 mmhos/m, and the bedrock conductivity is increased to approximately 250 mmhos/m, or

2. The depth to bedrock is locally as shallow as 0.2 meter, rather than the approximately 6 meters estimated from the bedrock map.

Because of the consistency of the anomaly across lines MWP-3, HL-1, HL-3, and HL-4 (see Plate 3), and because the Denver Formation is known to outcrop at nearby Henderson Hill on Rocky Mountain Arsenal (ESE, 1988), the latter interpretation is more credible. However, because the residuals at both 10- and 20-meter spacings are both so high on Line HL-1, an element of increased conductivity

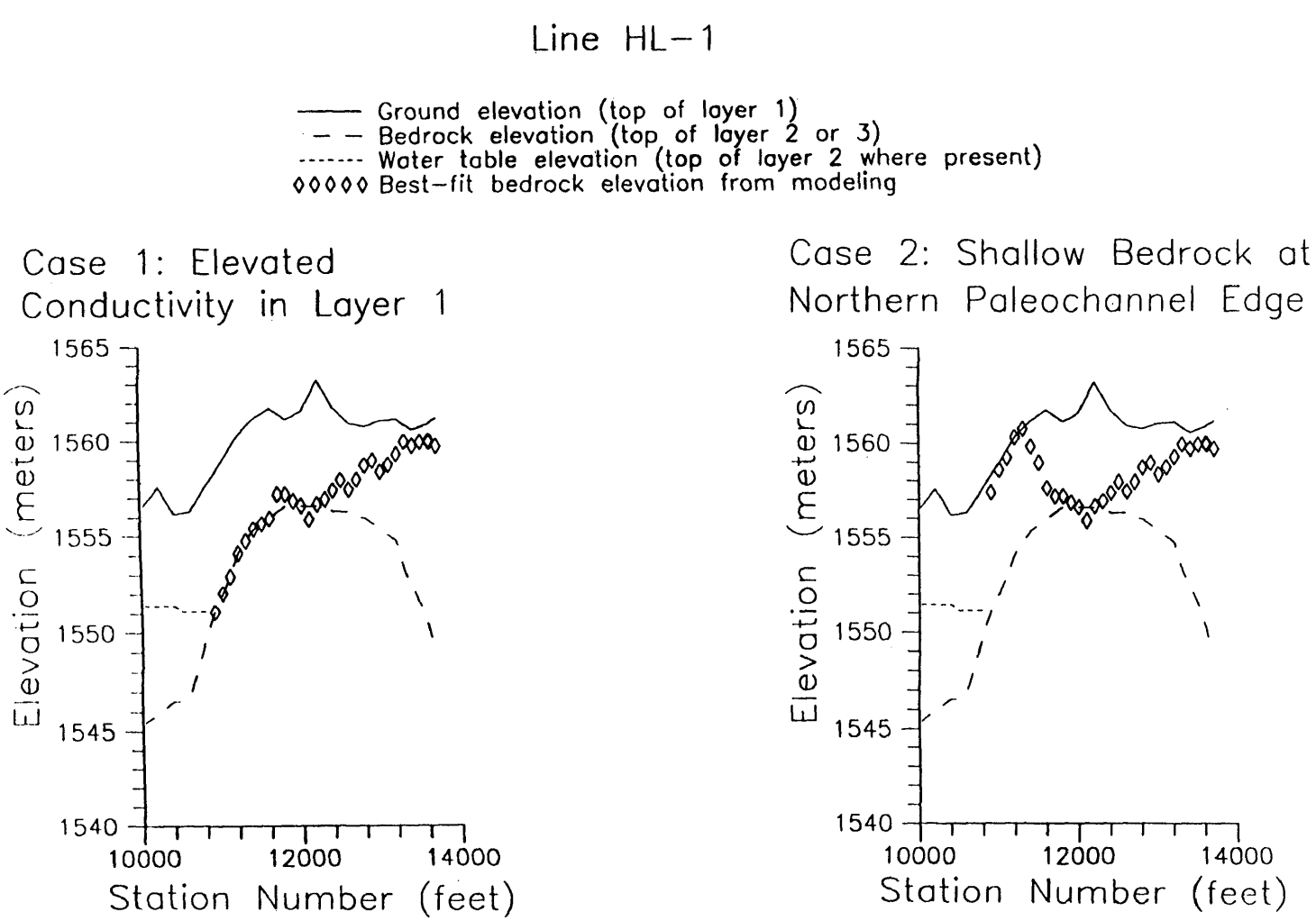

Figure 4.17 Alternative Models for Anomalous Area North of Northern Paleochannel

within the alluvium is suspected locally in the vicinity of station 11100 on Line HL-1. The resistivity data interpretation from VES-F supports a conductivity of 200 mmhos/m beginning at a depth of approximately one meter, but does not help to support one interpretation over the other.

4.4.2 Geochemical Properties

The understanding of ground-water TDS concentration within the study area has been advanced through evaluation of the conductivity modeling results. By examining the residual conductivity data, areas of apparent high-TDS ground water have been identified within the two primary paleochannels and the SFC and NFC paleochannels (see Plate 3). The residual conductivity data suggest that the SFC paleochannel has high-TDS ground water in two lobes, with the northeastern of the two lobes (near the northeastern paleochannel boundary) having the higher TDS. The southwestern boundary of the SFC paleochannel has been estimated on the basis of borehole data, but is outside of the study area. The SFC and NFC paleochannels apparently have high-TDS ground water near the channel edges, but the low residual conductivities in the center of the paleochannels are interpreted to represent low TDS concentrations (see Plate 3).

4.5 Uncertainty Analysis

There are uncertainties associated with several aspects of this study. Field data are subject to instrument precision and accuracy, and the ability of field personnel to accurately read the field instruments and record measurements. The analytical data used for TDS concentration calculation are subject to rigorous quality assurance/quality control requirements, but still are subject to a level of uncertainty. The parameters used for modeling are subject to uncertainty in that some of them, such as conductivity, were assumed and others such as bedrock depth were extracted from interpreted contour maps. Various types of uncertainties are discussed in this section.

The primary factors interpreted to cause positive residuals in the areas of unsaturated unconsolidated materials are an overestimate of depth to bedrock, or an underestimate of conductivities. The primary factor interpreted to cause positive residuals in saturated areas is high ground-water TDS, because depth to bedrock is well known. The primary factors interpreted to cause negative residuals are an

underestimate of depth to bedrock, or an overestimate of conductivities. If an abundance of negative anomalies were observed in the residual data, the model conductivities would be suspected to be overestimated. However, because both positive and negative residual anomalies are observed, the estimates of model conductivities are interpreted to be fairly realistic. The abundance of positive residual anomalies is therefore attributed to (1) overestimates of bedrock depths in unsaturated areas, and (2) high ground-water TDS within several portions of the paleochannels.

The uncertainty associated with choosing the correct conductivity model depends on the amount of corroborating data available. In the case of the HL lines, where the only coil spacings used were 10 and 20 meters, the model uncertainty can locally be high because numerous layer conductivity/layer thickness combinations may be found that yield synthetic data consistent with the actual conductivity data (see Figure 4.17). However, in areas where additional data such as bedrock depth, depth to water table, water chemistry data, induction logs, or VES data are available, the uncertainties associated with constructing an accurate conductivity model or geological interpretation are decreased. For this reason, the MWP lines, where three or four coil spacings were used, have an increased certainty in the conductivity models. The addition of more coil spacings and vertical dipole data for each coil spacing would provide several more data points for each station with which to construct an apparent conductivity curve. A conductivity curve could then be used to construct a more reliable conductivity model.

Various cross-parameter relations were assessed for the northern paleochannel, the First Creek paleochannel, and the combined data. Linear regression analysis was performed on 9 different types of relations, as summarized in Table 4.5 and presented in Figures 4.18 through 4.28. In addition, multivariate regressions were conducted for the combined data (Table 4.2), with 10 and 20 meter coil spacing data as the dependent variables and bedrock depth, depth to water table, and total dissolved solids as the regression variables. All 3 of the regression variables, as well as all 12 of the multivariate and single variable regressions, were found to be significant. The regression analyses yielded the following results:

(1) The most significant parameter for 10-meter conductivity is water-table depth. This is interpreted to be a result of high-TDS conditions in the First Creek area, which make the unconsolidated aquifer more conductive.

Table 4.5 Single Variable Regression Results for All Data Points in the Study Area

Relation	Equation	Goodness of Fit	Correlation Coefficient	F-Test	F_{crit} (α =.05)	Degrees of Freedom
GC vs TDS						
NP	GC=731.36+0.565TDS	.8355	.9141	106.69*	4.32	1,21
FCP	GC=490.54+0.983TDS	.9107	.9543	214.06*	4.32	1,21
All	GC=207.49+1.036TDS	.9222	.9603	521.73*	4.07	1,44
TDS vs RC (10 m)						
NP	TDS=1100.27+21.06RC	.2738	.5232	9.42*	4.24	1,25
FCP	TDS=1016.68+35.58RC	.3217	.5672	11.38*	4.26	1,24
All	TDS=965.21+35.31RC	.4936	.7026	49.71*	4.04	1,51
TDS vs RC (20 m)						
NP	TDS=1228.06+20.13RC	.2362	.4860	7.42*	4.26	1,24
FCP	TDS=1276.45+53.38RC	.2285	.4780	7.11*	4.26	1,24
All	TDS=1089.07+52.52RC	.3668	.6056	28.96*	4.04	1,50
TDS vs MC						
NP	TDS=1380.45+1.88MC	.0193	.1388	.0982	6.61	1,5
FCP	TDS=1285.72+6.52MC	.1166	.3414	1.45	4.84	1,11
All	TDS=1039.24+7.28MC	.2701	.5197	6.66*	4.41	1,18
GC vs MC						
NP	GC=1673.9-0.782MC	.0169	.1302	.0690	7.71	1,4
FCP	GC= 378.2+13.22 MC	.4017	.6338	5.37*	5.32	1,8
All	GC=628.5+11.9MC	.5433	.7371	16.65*	4.60	1,14

Table 4.5 Single Variable Regression Results for All Data Points in the Study Area (continued)

Relation	Equation	Goodness of Fit	Correlation Coefficient	F-Test	F_{crit} (α=.05)	Degrees of Freedom
GC vs RC (10 m)						
NP	GC=143.37+.733RC	.0942	.3069	2.18	4.32	1,21
FCP	GC=141.73+3.50RC	.2860	.5348	8.41*	4.32	1,21
All	GC=117.09+3.77RC	.5142	.7171	46.57*	4.07	1,44
GC vs RC (20 m)						
NP	GC=143.87+.907RC	.1227	.3502	2.94	4.32	1,21
FCP	GC=191.17+4.60RC	.1676	.4093	4.23	4.32	1,21
All	GC=130.71+5.63RC	.3655	.6046	25.35*	4.07	1,44
RC (10 m) vs MC						
NP	RC=-1.32+.123MC	.7646	.8744	19.49*	5.99	1,6
FCP	RC=17.74+.116MC	.1749	.4182	3.18	4.54	1,15
All	RC=3.24+.162MC	.3993	.6319	15.29*	4.28	1,23
RC (20 m) vs MC						
NP	RC=-.746+.0913MC	.5871	.7662	8.53*	5.99	1,6
FCP	RC=5.57+.0980MC	.3231	.5684	7.16*	4.54	1,15
All	RC=.2601+.115MC	.5201	.7212	24.93*	4.28	1,23

GC = Ground-water conductivity (µmhos/cm)
MC = Modeled unconsolidated aquifer conductivity (mmhos/m)
RC (10 m) = Residual conductivity (10 meters) (mmhos/m)
RC (20 m) = Residual conductivity (20 meters) (mmhos/m)
TDS = Total dissolved solids (parts per million)

* = Relation is statistically significant at α=.05 level
NP = Northern paleochannel data only
FCP = First Creek paleochannel data only
All = All data points within study area

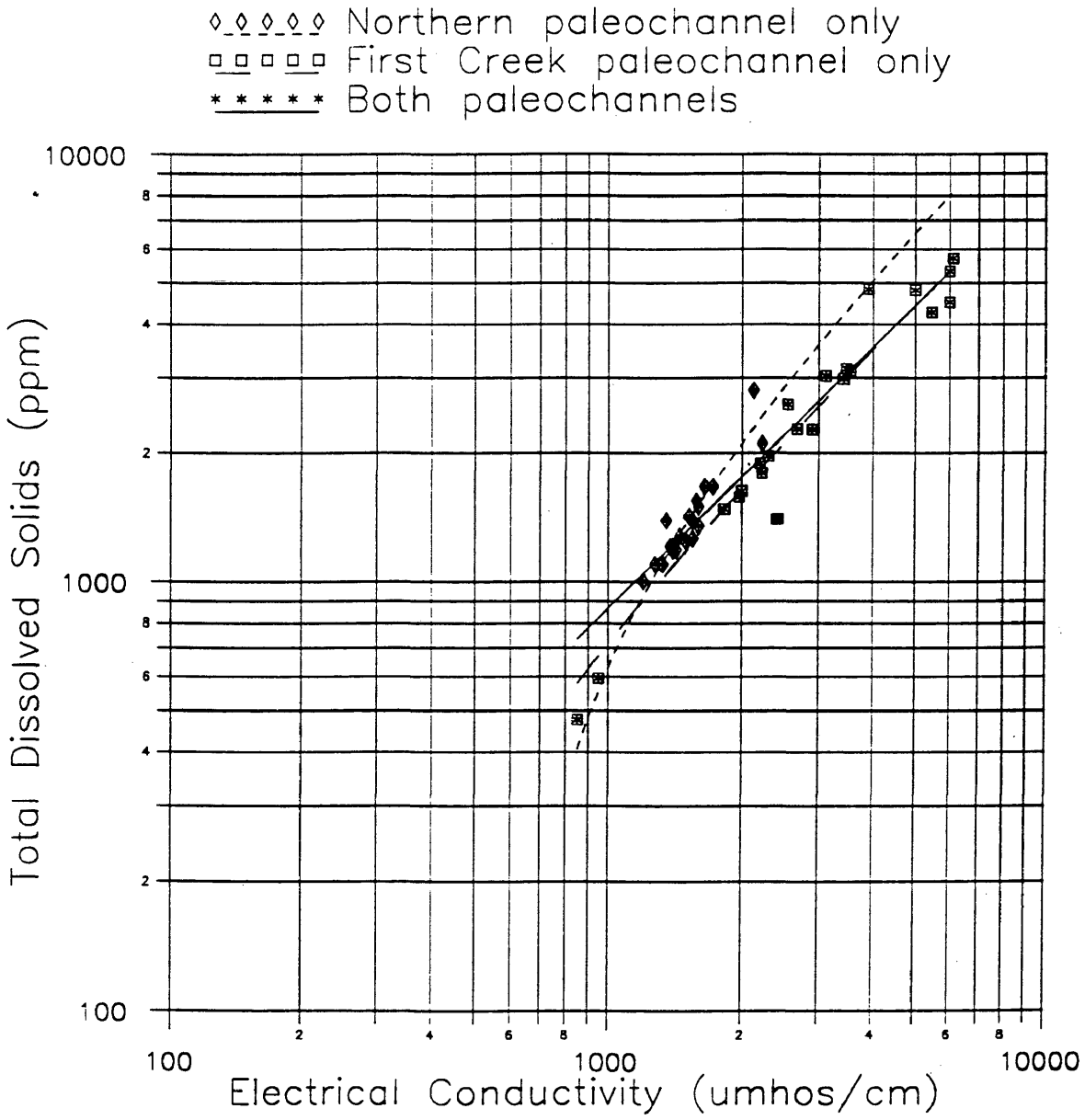

Figure 4.18 Total Dissolved Solids versus Gound-Water Conductivity (Logarithmic Scale)

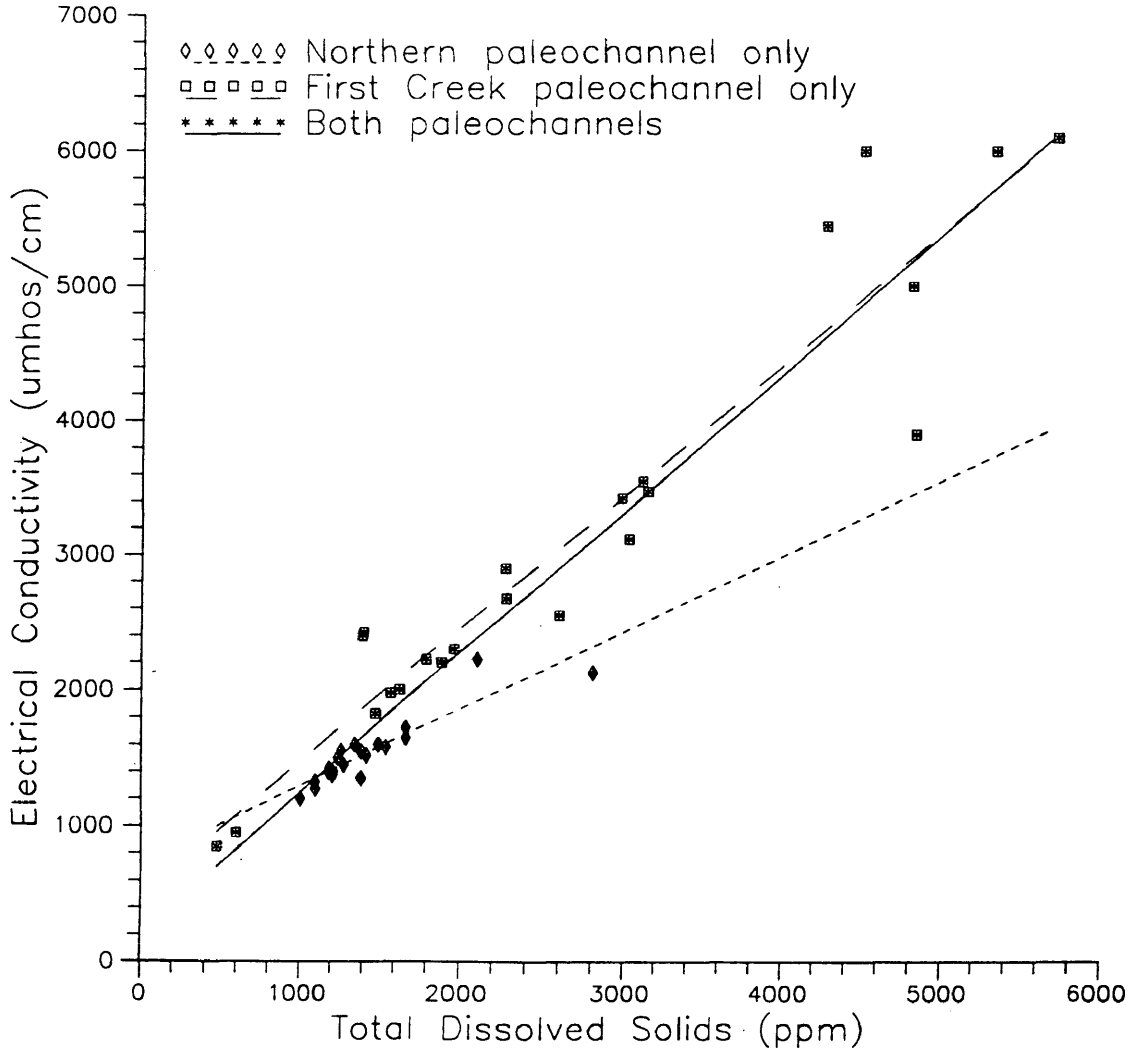

Figure 4.19 Total Dissolved Solids versus Ground-Water Conductivity (Linear Scale)

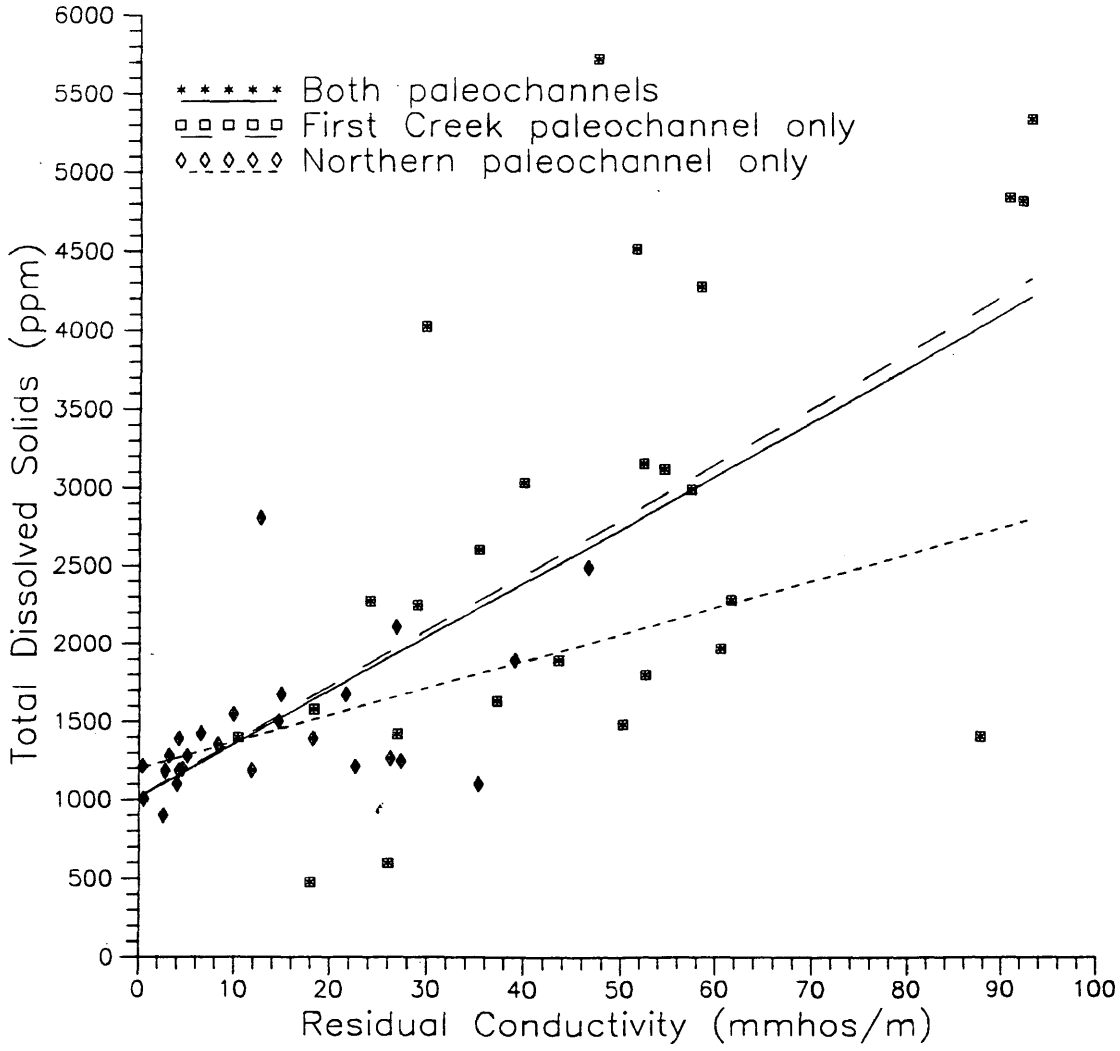

Figure 4.20 Residual Conductivity for 10-Meter Coil Spacing versus Total Dissolved Solids

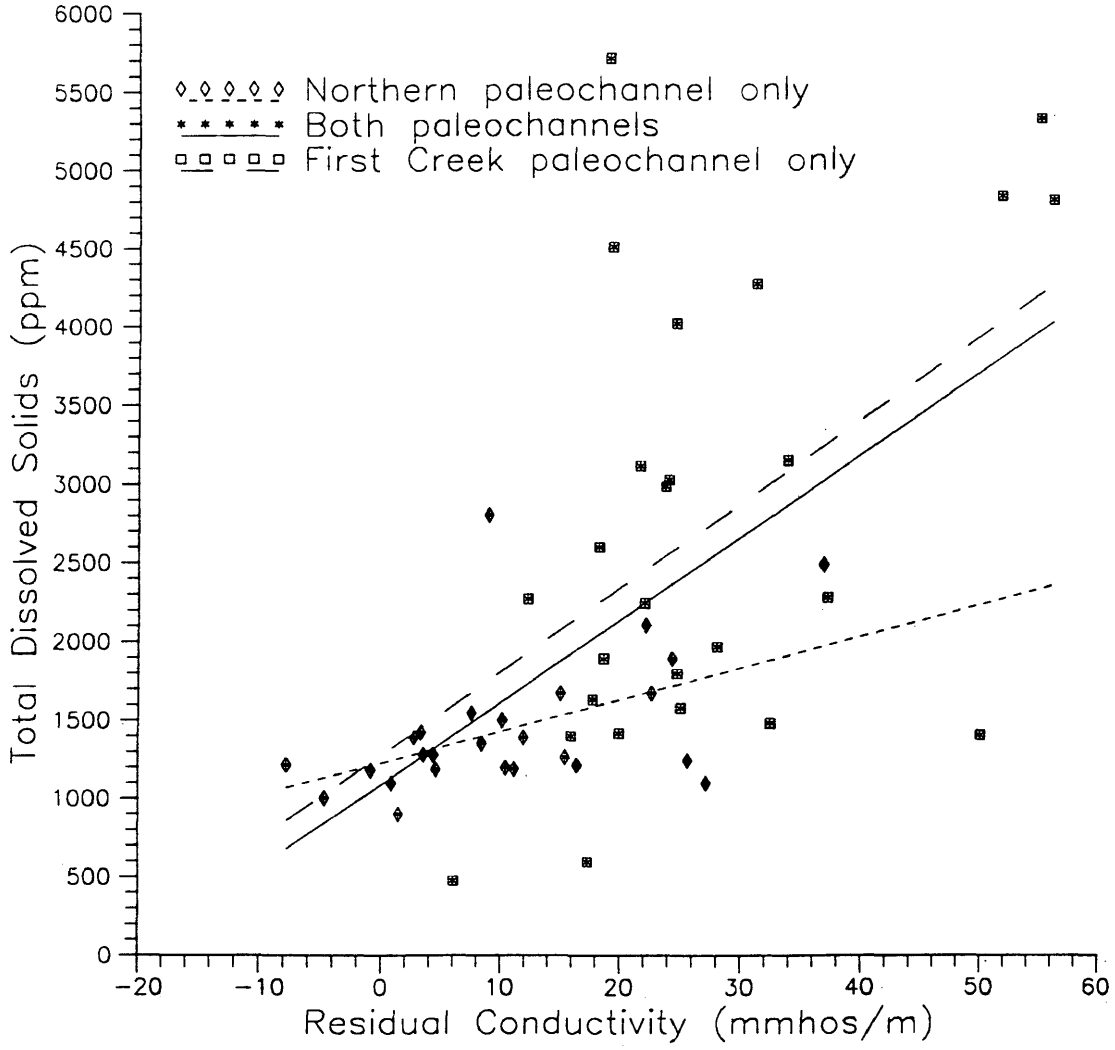

Figure 4.21 Residual Conductivity for 20-Meter Coil Spacing versus Total Dissolved Solids

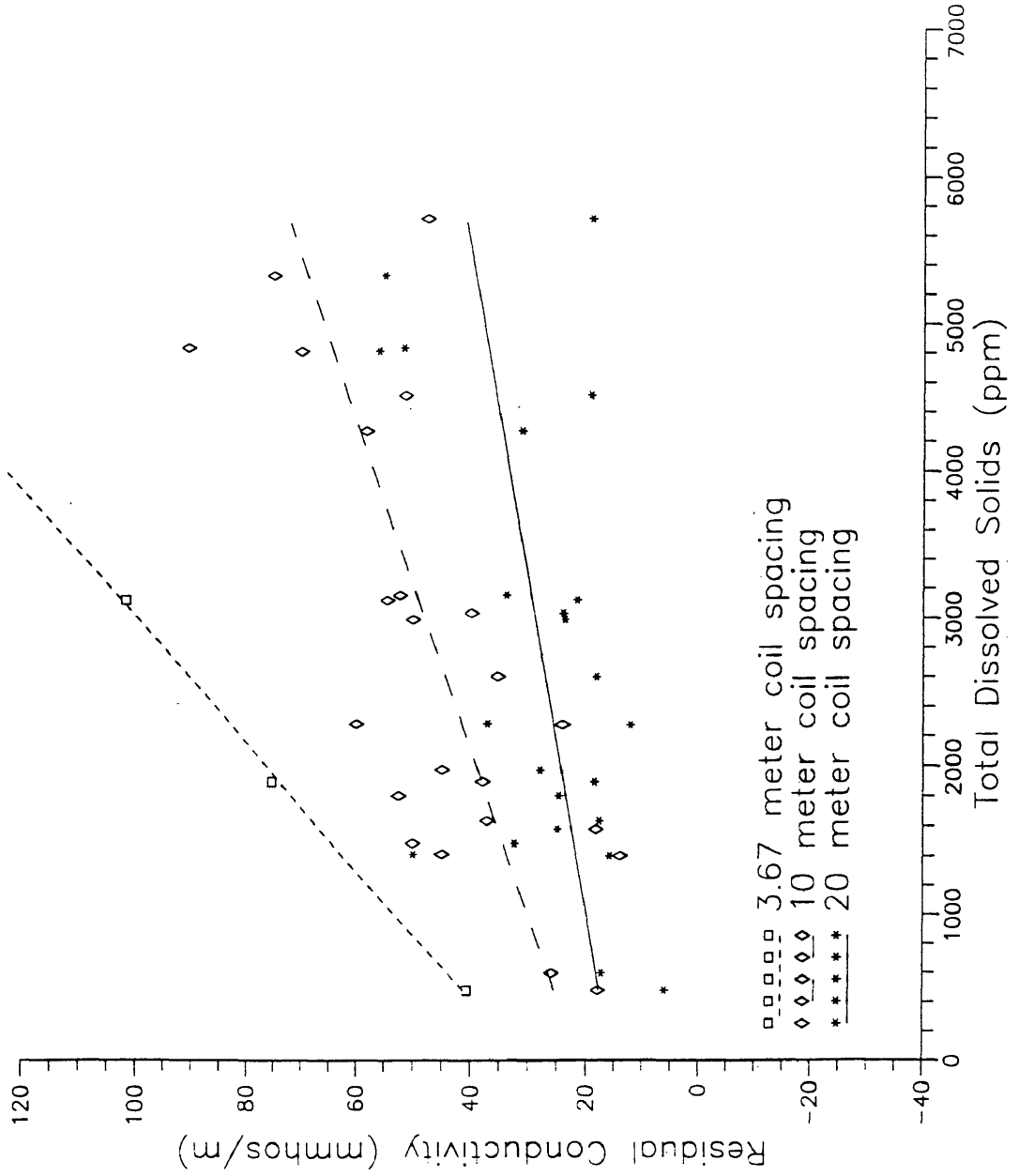

Figure 4.22 Total Dissolved Solids versus Residual Conductivity for the First Creek Paleochannel

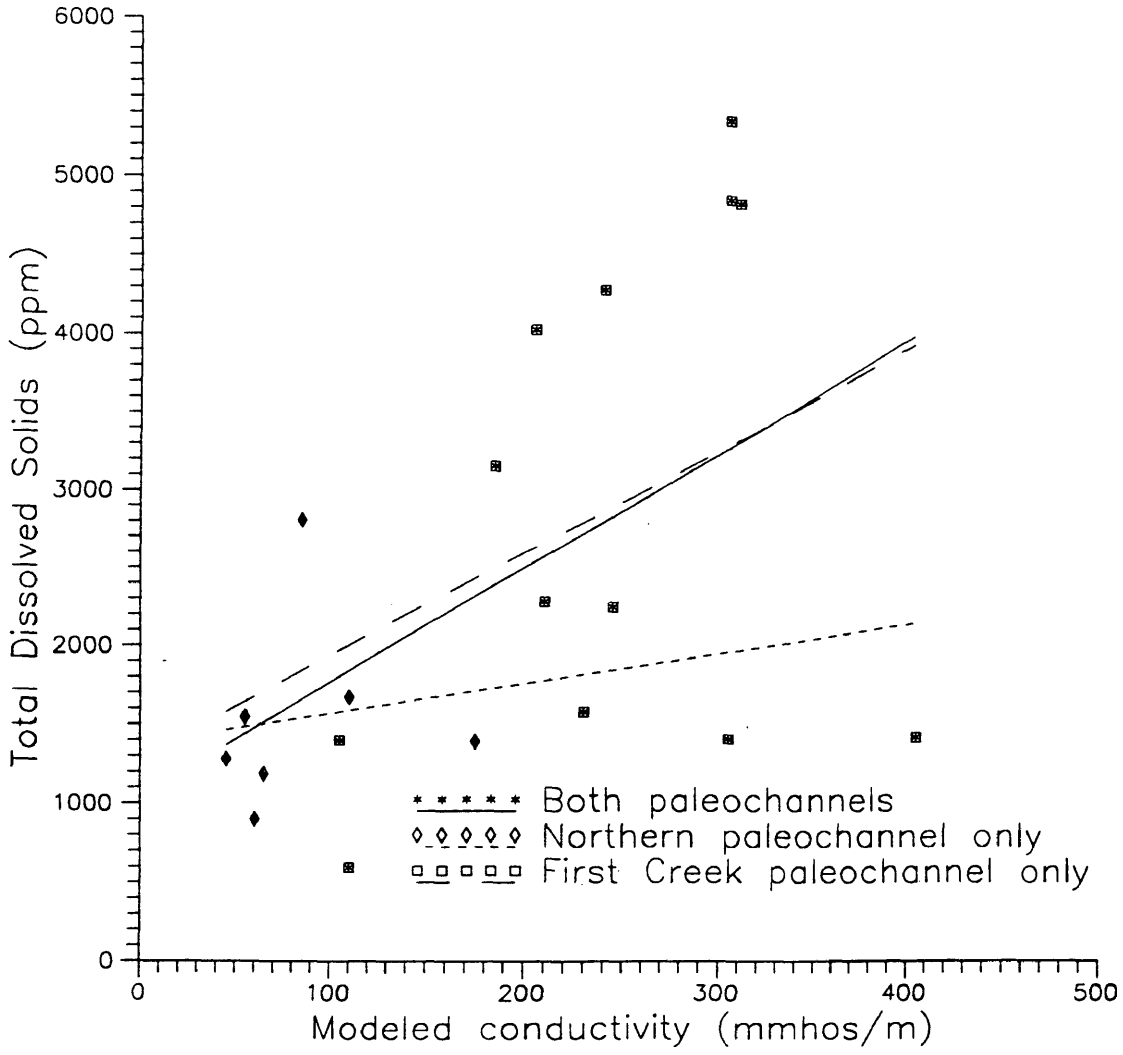

Figure 4.23 Modeled Unconsolidated Aquifer Conductivity versus Total Dissolved Solids in Ground Water

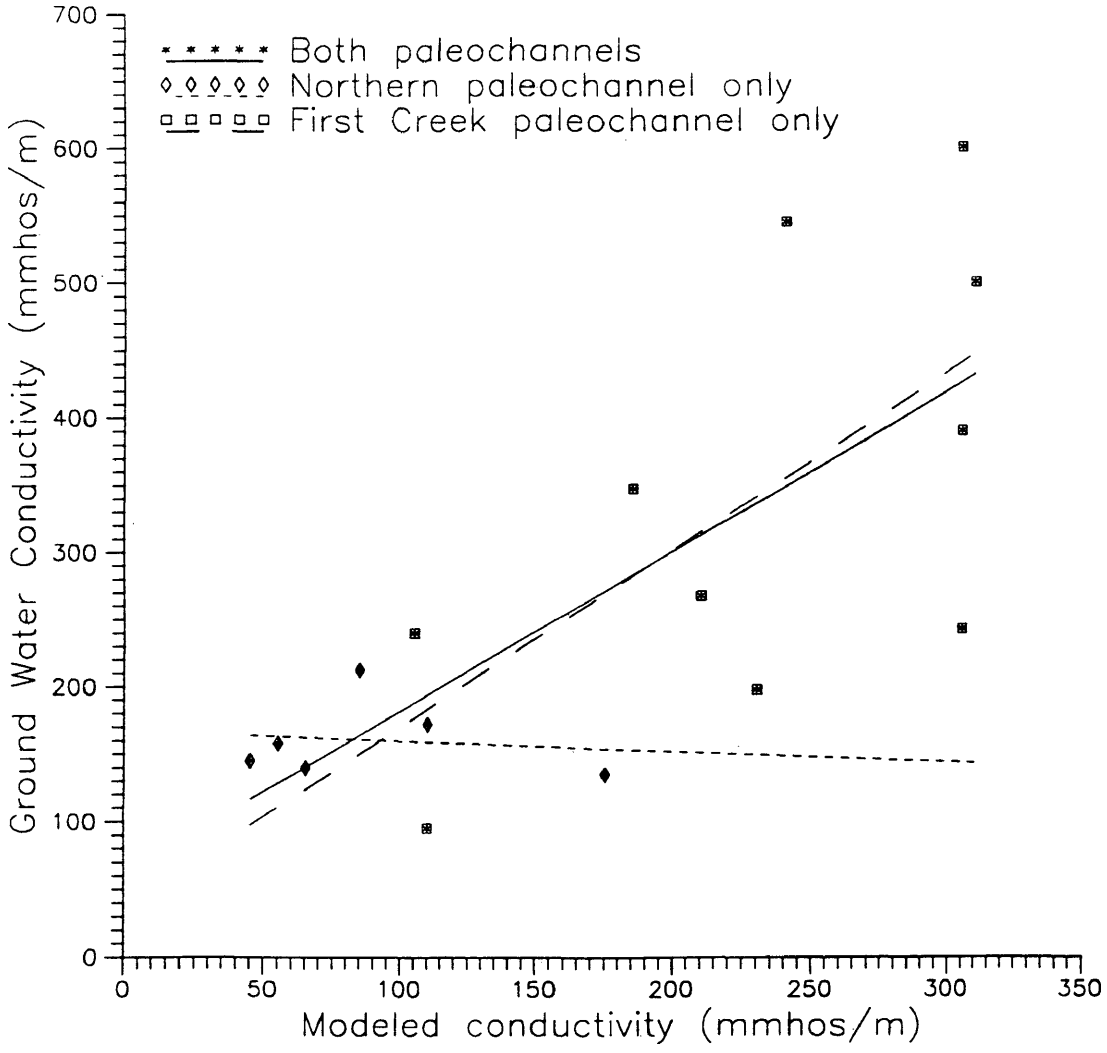

Figure 4.24 Modeled Unconsolidated Aquifer Conductivity versus Ground-Water Conductivity

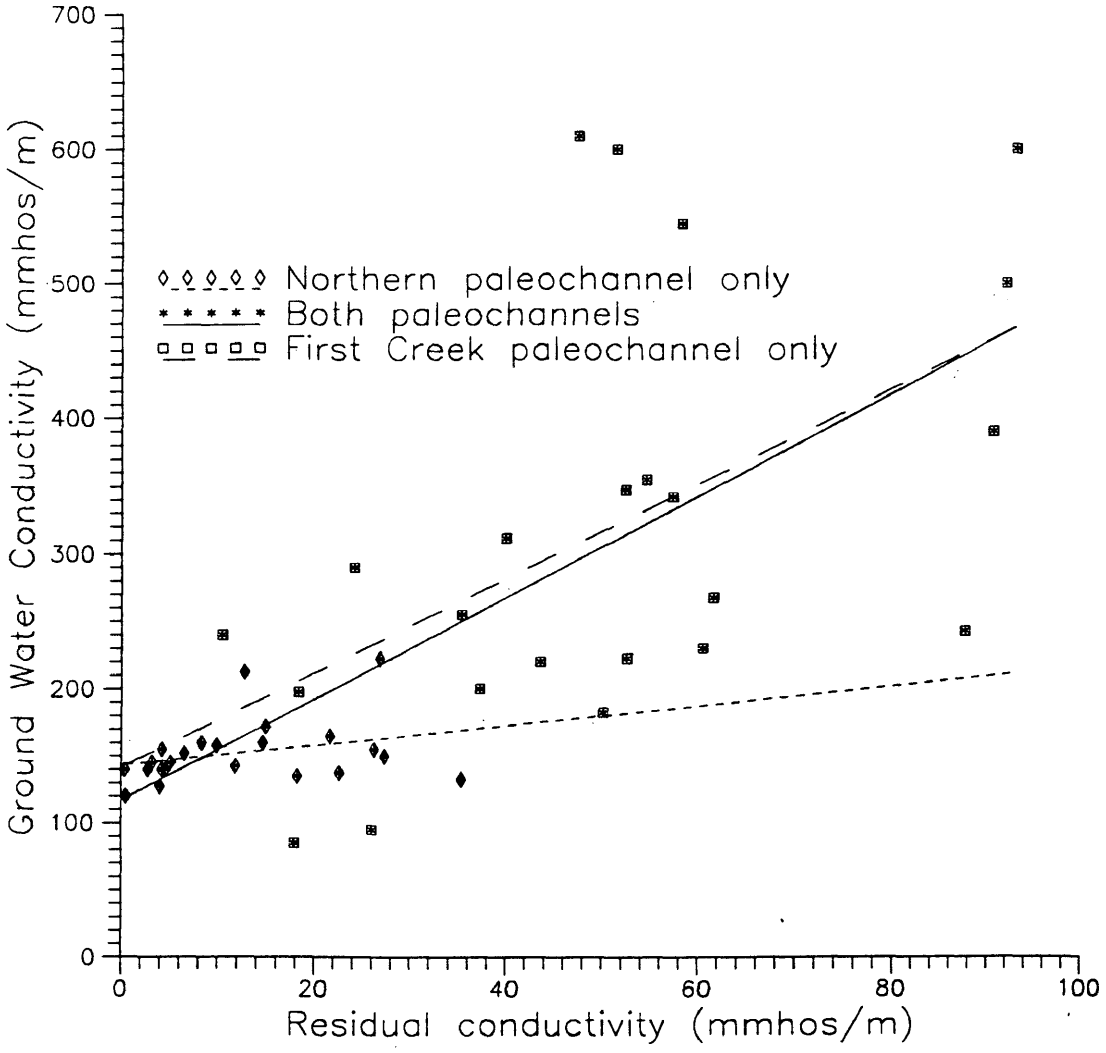

Figure 4.25 Residual Conductivity for 10-Meter Coil Spacing versus Ground-Water Conductivity

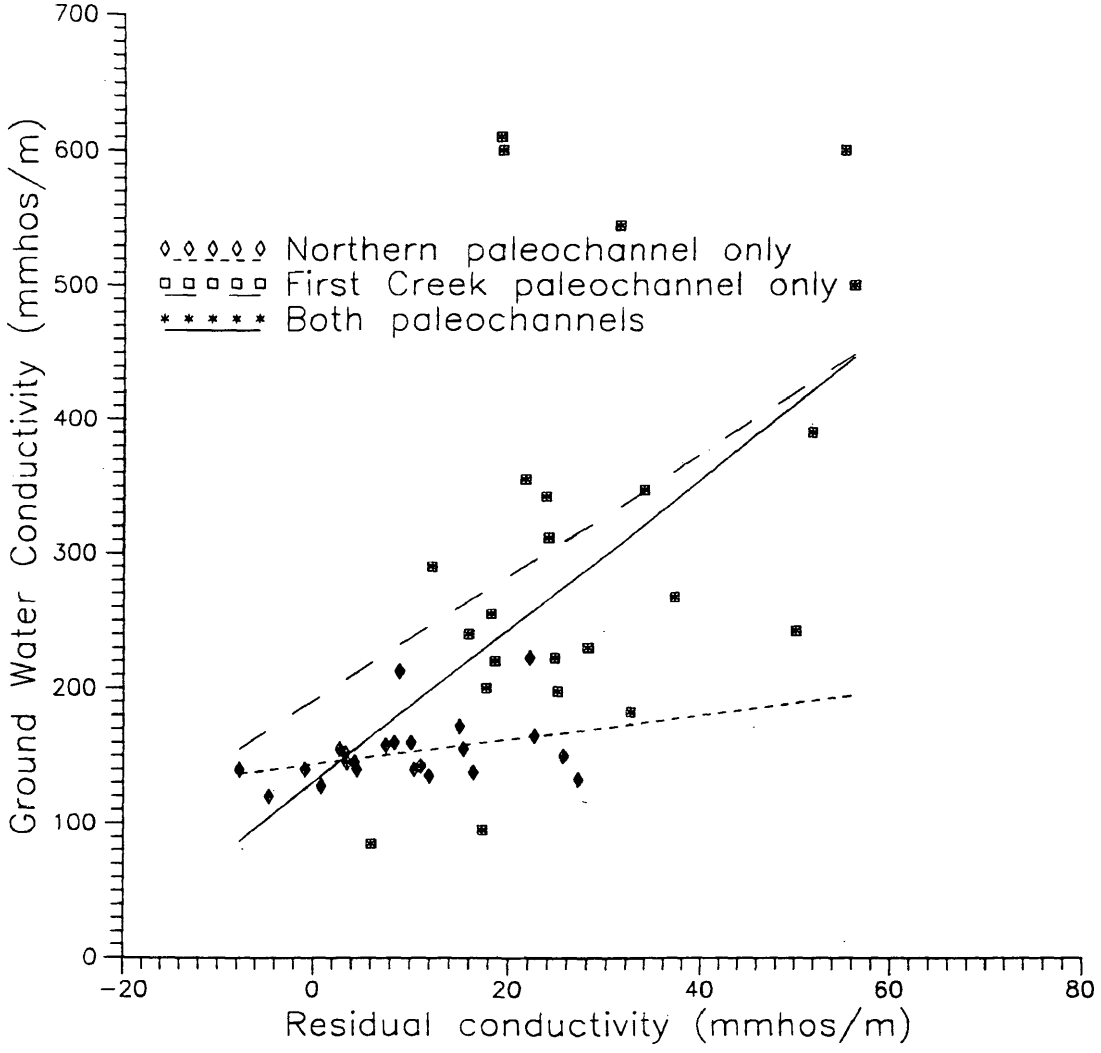

Figure 4.26 Residual Conductivity for 20-Meter Coil Spacing versus Ground-Water Conductivity

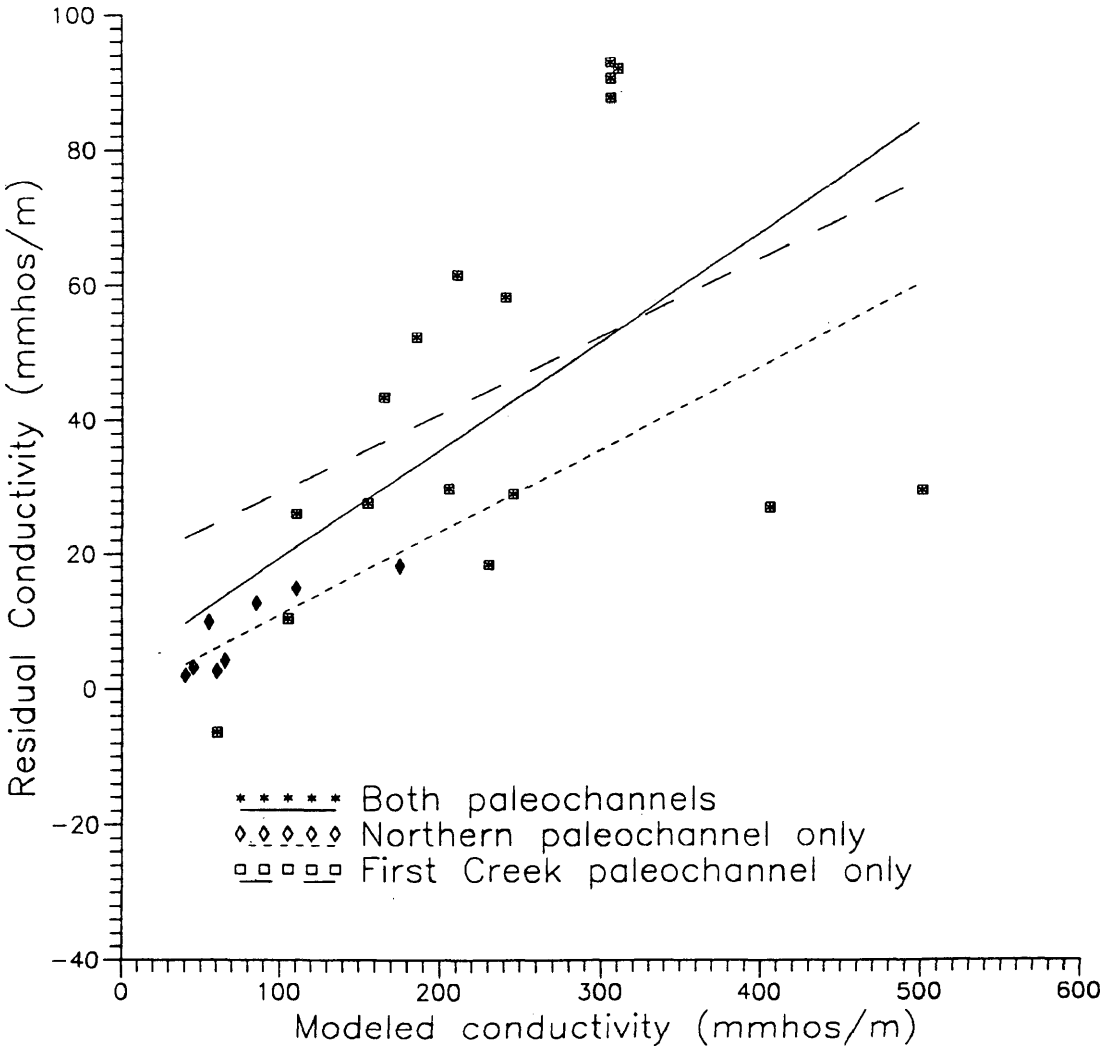

Figure 4.27 Modeled Unconsolidated Aquifer Conductivity versus Residual Conductivity for 10-Meter Coil Spacing

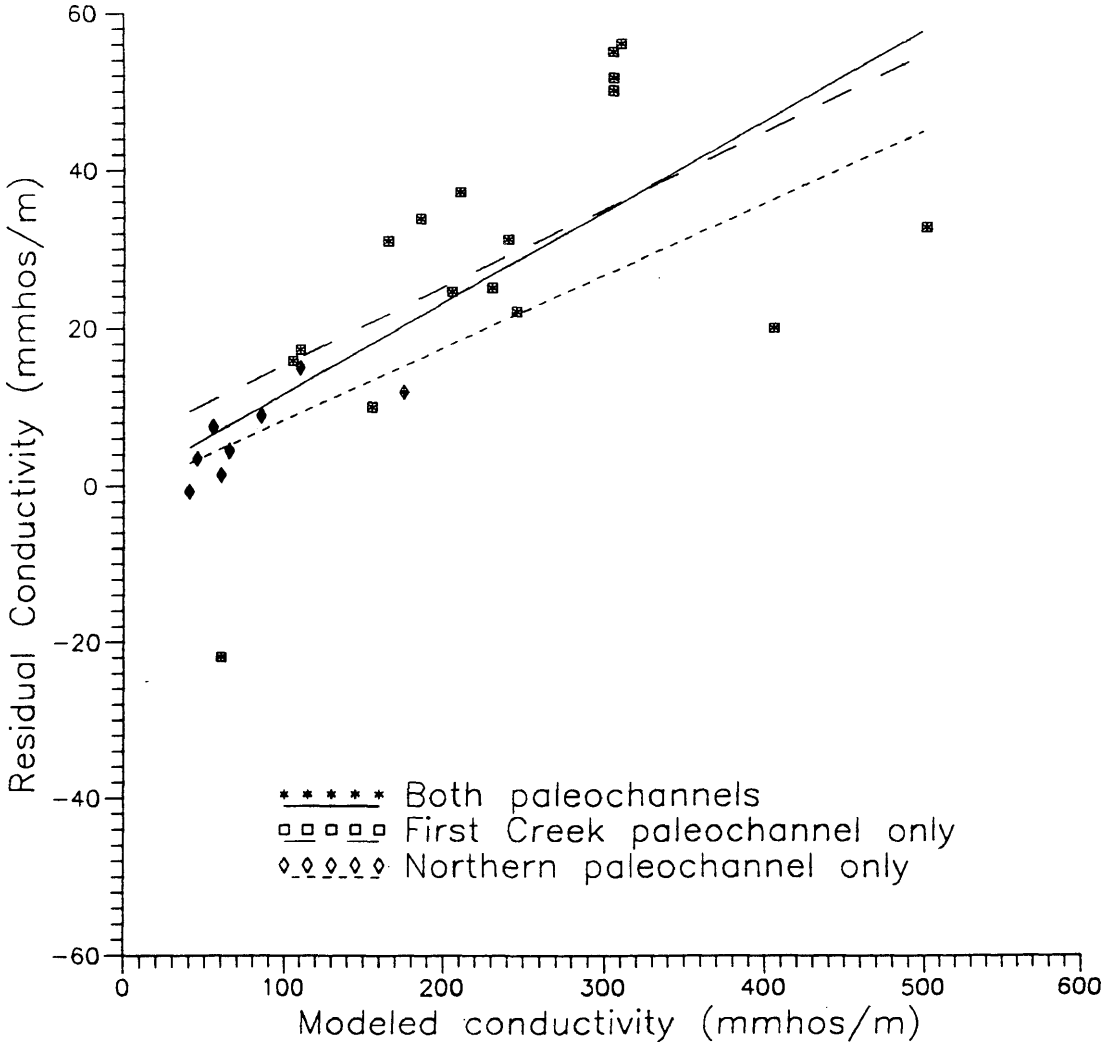

Figure 4.28 Modeled Unconsolidated Aquifer Conductivity versus Residual Conductivity for 20-Meter Coil Spacing

(2) The second most significant parameter for 10-meter data is TDS concentration.

(3) The third most significant parameter for 10-meter data is bedrock depth.

(4) The most significant parameter for 20-meter data is bedrock depth.

(5) The second most significant parameter for 20-meter data is water-table depth.

(6) The third most significant parameter for 20-meter data is TDS concentration.

The results indicate that bedrock depth, a parameter indicating conditions at depth, is more significant for the data gathered with long-spacing instruments. The plots of 40-meter synthetic data and actual data (Figures 4.29 and 4.30) indicate closer agreement between actual versus modeled data, suggesting that bedrock depth is a more significant variable for the 40-meter conductivity data. The data also indicate that TDS concentration and/or water-table depth are more significant variables for short-spacing data.

The single variable regressions for the study area, summarized in Table 4.5 and displayed in Figures 4.18 through 4.28, indicate that the ground-water TDS versus ground-water conductivity relation is the best of all those analyzed (see Figure 4.18). Although the regression relations for both individual paleochannels are significant, the relation is improved by combining the data from the entire study area. The same pattern of improvement is observed in all relations except residual conductivity versus modeled conductivity; for this relation, the northern paleochannel data provided the most significant results.

Many of the regression relations in Table 4.5 indicate a significant trend at the $\alpha = .05$ level, but the correlation coefficients are not high. This is interpreted to be the result of nonlinearity in the relations. Also, because several factors such as bedrock depth, water-table depth, and TDS concentration can collectively influence apparent conductivity, a significant relation with a high correlation coefficient based on only one variable may not be feasible. As stated previously, a reliable conductivity model (and hydrogeologic model) is dependent on the collection of several types of data to constrain the different possible interpretations of the EM data.

The synthetic data for all data points for all coil spacings were plotted on the same graphs with actual field data; these plots are presented in Figures 4.29 and 4.30

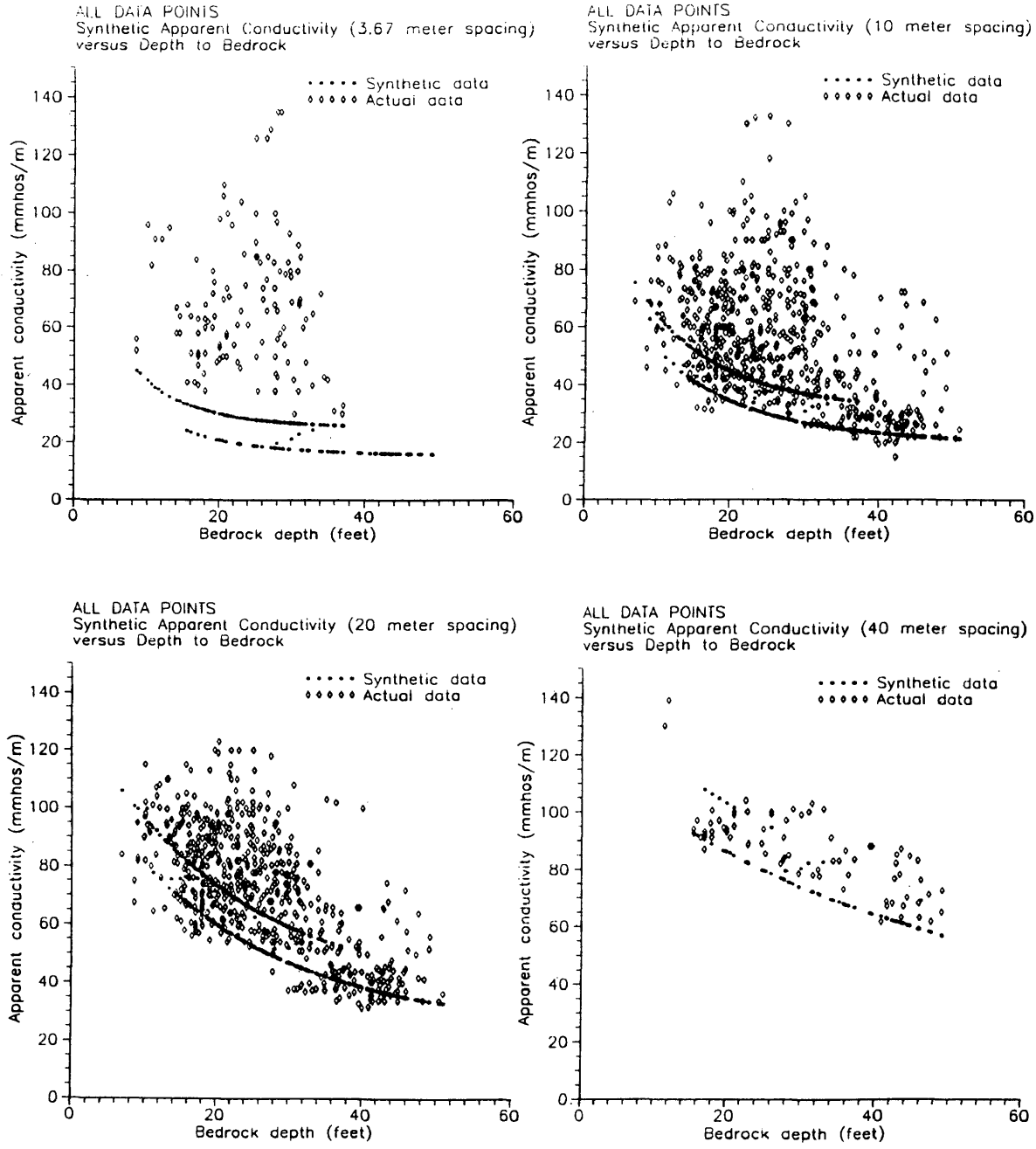

Figure 4.29 Actual and Synthetic Apparent Conductivity Data versus Interpreted Depth to Bedrock for All Points in the Study Area (Linear Scale)

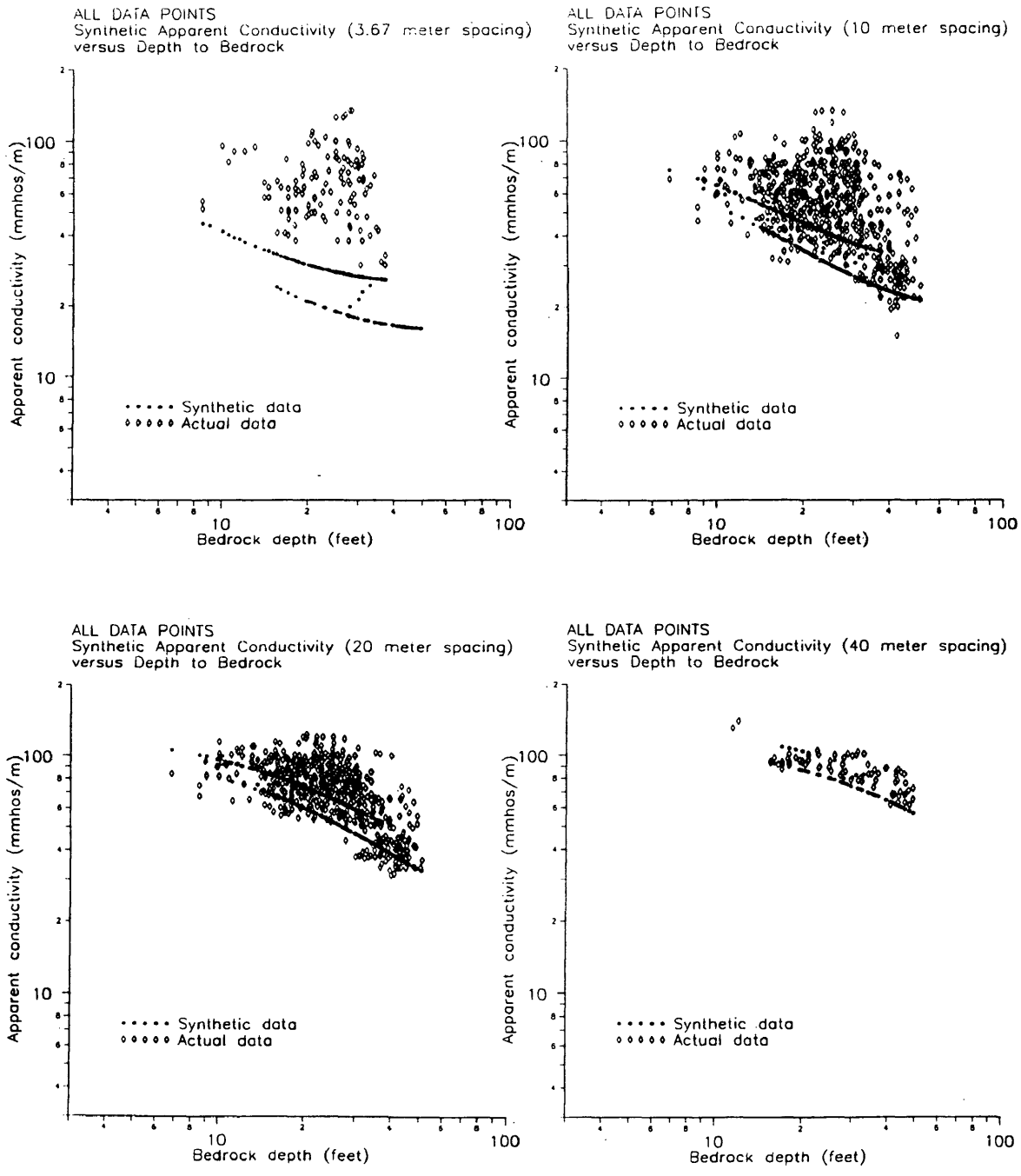

Figure 4.30 Actual and Synthetic Apparent Conductivity Data versus Interpreted Depth to Bedrock for All Points in the Study Area (Logarithmic Scale)

and Appendix B. These plots confirm that the "true" relation of bedrock depth to apparent conductivity, as represented by the model-generated synthetic data, is not linear. Rather, it is a ridge-regression function (McNeill, 1980c) that is clearly not linear when plotted on a linear-linear scaled graph. However, plotted on a log-log scale, the synthetic data closely resemble a straight line with a negative slope of 0.4 to 0.6. This slope indicates that the apparent conductivity may be approximated by a function of the form,

$$\sigma_a = k * h^{-x}$$

where σ_a is apparent conductivity, k is a constant, h is depth to bedrock, and x is a number between approximately 0.4 and 0.6. However, such a function would be an approximation only; a more accurate representation would require a more elaborate relation (McNeill, 1980c).

4.6 Revisions to Conceptual Geophysical Model

The conceptual geophysical model for the study area has been refined during this study through the evaluation of ground-water TDS and electrical conductivity data. Specifically, the following interpretations have been made:

(1) Ground-water electrical conductivity is linearly proportional to TDS concentration;

(2) The apparent conductivity of the saturated unconsolidated section is proportional to the TDS of the ground water;

(3) The conductivity of the bedrock does not appear to be affected by the TDS concentration of the ground water in the unconsolidated section overlying it; the bedrock apparent conductivity remains relatively constant throughout the study area;

(4) The apparent conductivity measured at the ground surface is a superposition or arithmetic sum of the effects of the unconsolidated layer and the bedrock layer; and

(5) Shallow high-conductivity anomalies are more apparent and result in higher apparent conductivities on instruments with shorter coil spacings; this phenomenon has been termed the crossover effect.

4.7 Revisions to Hydrogeologic Model

The results of this study have improved the hydrogeologic model for the study area, in terms of the conceptualization of flow within paleochannels. As evidenced in the First Creek, northern and SFC paleochannels, TDS does not exhibit an even or smooth distribution across the width of the channel (see Plates 2 and 3). Rather, it is partitioned into individual lobes of high-TDS water separated by narrow bands of low-TDS water. The explanation for this phenomenon is not clear, but it may be caused by variations in hydraulic conductivity within the unconsolidated sediments. The EM profile lines that cross First Creek, O'Brian Canal, and Burlington Ditch exhibit low residual apparent conductivities within 50 to a few hundred feet of the water courses. Therefore, it appears that these surface-water bodies have lowered the TDS level in the area adjacent to them by providing an influx or recharge of relatively fresh, low TDS ground water into the unconsolidated aquifer. A list of residual conductivity anomalies and interpretations is presented in Table 4.6.

The type of low-TDS ground water evidenced near First Creek and the canals is also apparently present in a zone north of the creek parallel to the First Creek paleochannel boundary. The same type of partitioning is apparent in the SFC paleochannel and the northern paleochannel. These effects suggest that there are preferential flow pathways within the paleochannels, that these pathways are more well flushed than the surrounding materials, and that TDS concentrations are lower within these preferential pathways.

Table 4.6 Summary of Interpretations for
Residual Conductivity Anomalies
(See Plate 3)

Positive Residual Anomalies	Interpretation
1. Three areas in the First Creek paleochannel with residuals up to 93 mmhos/m.	High-TDS ground water is present in the shallow alluvial aquifer (<5 feet deep).
2. Residuals up to 50 mmhos/m in the SFC paleochannel.	High-TDS ground water is present at a relatively shallow depth.
3. Residuals up to 30 mmhos/m in the NFC paleochannel.	High-TDS ground water is present.
4. Three areas in the northern paleochannel with residuals up to 46 mmhos/m.	High-TDS ground water is present in channelized flow paths.
5. Two high-residual ridges north of the northern paleochannel, with residuals up to 66 mmhos/m.	TDS content in soil is high, or bedrock is shallower than mapped.
6. An area at the north edge of the First Creek paleochannel with residuals up to 54.9 mmhos/m.	Bedrock is shallower than mapped, or ground-water TDS is high.
Negative Residual Anomalies	
Various negative anomalies in areas of unsaturated alluvium, especially south of First Creek paleochannel on line MWP-1.	Bedrock is deeper than mapped, or model conductivities are slightly high.

Chapter 5.
CONCLUSIONS

The results of this study indicate that the EM conductivity profiling technique can be used to estimate the following types of information:

(1) Locations of channel edges
(2) Channel widths
(3) Locations of the deepest portions of the channels
(4) Bedrock topography
(5) Locations of the high-TDS portions of ionic contaminant plumes.

The following general interpretations have been made on the basis of the results of this study:

(1) Ground-water electrical conductivity is proportional to TDS concentration.

(2) The apparent conductivity of the saturated unconsolidated section is proportional to the TDS of the ground water.

(3) The conductivity of the bedrock does not appear to be affected by the TDS concentration of the ground water in the unconsolidated section overlying it. The bedrock apparent conductivity remains relatively constant throughout the study area.

(4) The apparent conductivity measured at the ground surface is approximately an arithmetic sum of the effects of the unconsolidated layer and the bedrock layer.

(5) Shallow high-conductivity anomalies are more apparent and result in higher apparent conductivities on instruments with shorter coil spacings.

This phenomenon has been termed the crossover effect. Residual conductivities from modeling are higher for those data obtained using shorter coil spacings.

(6) Modeling data (based on the response due only to depth to bedrock) are more consistent with actual data for those data obtained using longer instrument coil spacings. This results in lower residual conductivities for longer coil spacing instruments.

The following location-specific conclusions were made on the basis of the results of this study:

(1) The First Creek paleochannel is a 1700- to 2500-foot wide, well defined pathway with a water table as shallow as 1.5 feet.

(2) The high TDS (locally as much as 5700 ppm) in portions of the paleochannel creates an anomalously high EM conductivity that locally obscures bedrock response and makes depth-to-bedrock estimates unreliable in those locations. The conductivity crossover phenomenon (shallow conductivity measurements are greater than deep conductivity measurements) has been observed to occur where ionic TDS exceed approximately 2000 ppm in the shallow unconfined groundwater. The response indicating high TDS concentration is indicated by local EM conductivity highs (spikes) superimposed on the broad paleochannel response curve.

(3) The observed conductivity crossover effect between 3.67-meter and 10-meter spacing data, and between 10-meter and 20-meter spacing data, and elevated EM conductivity readings in high-ionic TDS areas are consistent across all six EM lines that cross the First Creek paleochannel.

(4) The northern paleochannel is a less well-defined pathway that is 2500 to 4000 feet wide. A high-conductivity anomaly was observed near the northern edge of the northern paleochannel during both the 1989 and

1992 surveys, and the conductivity crossover effect was observed in this area during both surveys. This phenomenon may be an indication of high-ionic TDS (such as nitrate) in soil or ground water resulting from extended feedlot operations, which ended in approximately 1991. The anomaly may also be caused by bedrock depth shallower than currently estimated.

(5) A more subtle high-conductivity anomaly toward the southern edge of the northern paleochannel is apparently related to groundwater ionic TDS in excess of approximately 2000 ppm.

(6) As in the First Creek area, the northern paleochannel high-TDS responses are high-conductivity anomalies superimposed on the broad paleochannel response curve.

The results of the 1989 and 1992 geophysical surveys indicate that the EM technique is useful for assessing bedrock depth, in the absence of interfering factors and presence of high ionic concentrations in ground water within the study area. Other factors such as water-table depth and unconsolidated and bedrock lithology may influence EM readings, but their effects appear to be relatively minor within the study area.

The VES (or resistivity) data provided interpretations of resistivity with depth and bedrock depth and a constraint to the multiple possible interpretations of the EM data. The VES method is also less susceptible to cultural noise (e.g., caused by electrical power lines), which can limit the use of the EM method near such utilities.

The original objective of the EM surveys in the study area was to qualitatively evaluate bedrock depth to aid in assessing paleochannel configuration in the First Creek and northern paleochannels. The rationale for this approach was the favorable conductivity contrast between unconsolidated materials (low) and bedrock (high) that was observed in monitoring well induction logs. Throughout much of the study area, the conductivity effect caused by the depth to the unconsolidated unit/bedrock interface is the most consistent and strongest effect. This case can be approximated by a two-layered geophysical model.

Exceptions to the normal two-layered interpretation of bedrock depth based on EM results must be made, however, in areas of ground-water contaminant plumes.

This type of anomaly is most observable and may be distinguishable from bedrock effects, in areas where TDS exceeds approximately 2000 ppm. Unfortunately, where this anomalous effect occurs, it masks the bedrock effect and makes an estimate of depth to bedrock unreliable. In this case, a three-layered geophysical model is necessary to simulate the system, and to make an accurate interpretation of the data.

In the study area, it is possible to estimate the high-TDS portions of shallow contaminant plumes by identifying the areas where short-spacing conductivities approach or exceed long-spacing conductivities for the same locations. In these locations the conductivity values are directly related to the TDS in ground water. Because of the crossover in data from two coil spacings, the data can be interpreted to indicate that the data should not be used to interpret bedrock depth at that location and a high-TDS groundwater contaminant plume may be inferred. The location of the high-TDS portion of the plume may be estimated on the basis of areas of conductivity data crossover.

Water-table depth influences the apparent conductivity measured by the EM method. The ground-water table causes a noticeable EM conductivity response in areas where the ground-water TDS is high (greater than approximately 2000 ppm). However, in areas where ground-water TDS is lower, the contrast between the saturated and unsaturated unconsolidated materials is not normally large enough to interpret.

Variations in lithology within the unconsolidated unit (clays, sands, and gravels) and within bedrock (claystones, siltstones, and sandstones) may be expected to cause a measurable EM conductivity response. However, based on the current data set, the response caused by such variations is small in comparison to the response caused by the difference between unconsolidated materials (as a whole) and bedrock (as a whole). The variations in conductivity caused by either unconsolidated or bedrock lithology differences do not appear to be large enough to be conclusive.

Recommendations

The EM method can be effectively used to estimate depth to bedrock within the study area, using long coil-spacing instruments. Coil spacings of 20 and 40 meters have provided the data that are the most consistent with this objective. The EM method can be effectively used to map areas with high TDS in ground water, using short coil spacing instruments. Coil spacings of 3.67 and 10 meters have provided the data that are the most consistent with this objective. For either objective, or for both

objectives combined, a greater amount of information could be obtained and a more reliable conductivity model could be produced by collecting more EM data at each station. For example, using the EM31-D and EM34-3, the same two EM instruments used in this study, eight values for each station could be gathered using the 3.67-, 10-, 20-, and 40-meter spacings in both horizontal and vertical dipole modes. The data would take only slightly longer to gather, and would provide data with which to construct a conductivity curve to make an easier, more reliable interpretation. With such data, a computer modeling program such as EMIX34P could be used to perform inverse modeling.

The forward modeling technique developed in this study offers a means to separate the effects of two different parameters, such as depth to bedrock and ground-water TDS. The method could be used in other areas where one parameter is reasonably well known and another is not. A system could be modeled using one parameter, the synthetic data subtracted from actual data, and the residuals then assessed in terms of the other parameter. Within the study area, or near it, the EM method could perhaps be combined with microgravity data. Using gravity data to estimate depth to bedrock, the estimated bedrock depths could be forward modeled for EM data. The synthetic data could then be subtracted from actual data, and the resulting residuals could be assessed in terms of ground-water TDS. A small number of boreholes could be drilled to calibrate both the EM and gravity methods, and the calibration could be extrapolated to provide an areal interpretation.

As in this study, VES soundings are recommended to accompany the EM data. For the depth of investigation of this study, several VES soundings could be performed in a day, and the data so obtained would provide support to the EM interpretation. The combined geophysical methods offer a relatively rapid means to assess the subsurface conditions in an area of investigation.

Chapter 6.

BIBLIOGRAPHY

Benson, R.C., Glaccum, R.A., and Noel, M.R. 1982. Geophysical Techniques for Sensing Buried Waste and Waste Migration. Technos, Inc. for Lockheed Engineering and Management Services Company, Inc. and U.S. Environmental Protection Agency. Las Vegas, Nevada. 236 p.

Davis, J.C. 1986. Statistics and Data Analysis in Geology, Second Edition. John Wiley and Sons. New York, New York. 646 p.

Dobrin, M.B. 1976. Introduction to Geophysical Prospecting, Third Edition. McGraw-Hill, Inc. New York, New York. 630 p.

Environmental Science and Engineering, Inc. 1988. Offpost Operable Unit Remedial Investigation and Chemical Specific Applicable or Relevant and Appropriate Requirements, Final Report (Version 3.1) Volume I. Prepared for U.S. Army Program Manager's Office for Rocky Mountain Arsenal. December.

Geonics Limited. 1991a. EM31 Operating Manual. Ontario, Canada. November. 59 p.

Geonics Limited. 1991b. EM34-3 and EM34-3XL Operating Instructions. Ontario, Canada. October. 14 p.

Geonics Limited. 1993. EM39-Borehole Conductivity Logger (Four Conductor Model) Operating Manual. Ontario, Canada. August. 34 p.

Harding Lawson Associates. 1992. Offpost Operable Unit Remedial Investigation, Proposed Final Addendum, Volume I of II. Prepared for Program Manager for Rocky Mountain Arsenal. March. 124 p.

Harding Lawson Associates. 1990. Results of Pilot-Scale Hydraulic and Treatment Testing North of Rocky Mountain Arsenal, Interim Response Action A. Draft Final Report. Two Volumes. Prepared for Program Manager for Rocky Mountain Arsenal. June.

Harding Lawson Associates. Personal communication: Unpublished geophysical field data and analytical data from 1989 and 1992 programs. Collected for Program Manager for Rocky Mountain Arsenal. Used by permission.

Interpex, Limited. 1993. EMIX34P User's Manual and EMIX34P, Version 1.33 Software. Golden, Colorado.

Kaufman, A.A. and Keller, G.V. 1983. Frequency and Transient Soundings. Elsevier Science Publishers, B.V. New York, New York. 685 p.

Kaufman, A.A. and Keller, G.V. 1989. Induction Logging. Elsevier Science Publishers, B.V. New York, New York. 600 p.

Keller, G.V. 1968. Electrical Prospecting for Oil. Quarterly of the Colorado School of Mines. Golden, Colorado. 268 p.

Keller, G.V. and Frischknecht, F.C. 1966. Electrical Methods in Geophysical Prospecting. Pergamon Press. New York, New York. 519 p.

Konikow, L.F. 1977. Modeling Chloride Movement in the Alluvial Aquifer at the Rocky Mountain Arsenal, Colorado. United States Geological Survey Water-Supply Paper 2044. 43 p.

Lindvall, R.M. 1980. Geologic Map of the Commerce City Quadrangle, Adams and Denver Counties, Colorado. Map GQ-1541. United States Geological Survey.

Lindvall, R.M. 1983. Geologic Map of the Commerce City Quadrangle, Adams and Denver Counties, Colorado. Map GQ-1567. United States Geologic Survey.

McNeill, J.D. 1980a. Electrical Conductivity of Soils and Rocks. Technical Note TN-5. Geonics Limited. Ontario, Canada. 22 p.

McNeill, J.D. 1980b. Electromagnetic Terrain Conductivity Measurement at Low Induction Numbers. Technical Note TN-6. Geonics Limited. Ontario, Canada. 15 p.

McNeill, J.D. 1980c. EM34-3 Survey Interpretation Techniques. Technical Note TN-8. Geonics Limited. Ontario, Canada. 7 p.

McNeill, J.D. 1982. Electromagnetic Resistivity Mapping of Contaminant Plumes. In: Proceedings of National Conference on Management of Uncontrolled Hazardous Waste Sites, Washington, D.C. pp. 1-6.

McNeill, J.D. 1983. Use of EM31 Inphase Information. Technical Note TN-11. Geonics Limited. Ontario, Canada. 2 p.

McNeill, J.D. 1985. EM34-3 Measurements at Two Inter-Coil Spacings to Reduce Sensitivity to Near-Surface Material. Technical Note TN-19. Geonics Limited. Ontario, Canada. 3 p.

McNeill, J.D. 1992. Rapid, Accurate Mapping of Soil Salinity by Electromagnetic Ground Conductivity Meters. In: Advances in measurement of Soil Physical Properties: Bringing Theory into Practice. Soil Science Society of America. Madison, Wisconsin. pp. 209-229.

Mills, T., Hoekstra, P., Blohm, M., and Evans, L. 1988. The Use of Time Domain Electromagnetic Soundings for Mapping Sea Water Intrusion in Monterey County, California. Ground Water, Volume XXVI, Number 6. pp. 771-782.

Morrison-Knudsen Engineers, Inc. 1988. Geology of the Rocky Mountain Arsenal, Adams County, Colorado. Prepared for Holme, Roberts, and Owen. Denver, Colorado. 55 p.

Robson, S.G. and Romero, J.C. 1981. Geologic Structure, Hydrology, and Water Quality of the Denver Aquifer in the Denver Basin, Colorado. Prepared for the United States Geological Survey and the Colorado Division of Water Resources.

Romero, J.C. 1976. Report on the Ground Water Resources of the Denver Basin, Colorado. Colorado Department of Natural Resources, Division of Water Resources. Denver, Colorado. 109 p.

APPENDIX A
DATA BASE

APPENDIX A - DATA BASE

The data base for the study includes the following:

Figures A-1 through A-7:

- Borehole induction logs (from 4 wells in the northern paleochannel, 3 in the First Creek paleochannel, and 4 south of First Creek)

Diskette Files

EMDATA.WK1:

- Eight electromagnetic conductivity profiles (2 crossing the northern paleochannel, 3 crossing the First Creek paleochannel, and 3 crossing both)

  Lithologic descriptions from approximately 16 soil borings in unsaturated unconsolidated unit areas

  Lithologic descriptions from approximately 49 monitoring wells drilled to bedrock (23 in the First Creek area and 26 in the northern area)

  Water quality (total dissolved solids) data for 49 wells (23 in the First Creek paleochannel and 26 in the northern paleochannel)

VESDATA.WK1:

- Resistivity sounding data for 10 vertical electrical soundings.

NOTES:

The locations of the data points are shown in Plate 1.

The field surveys were performed using feet as the unit of measure. However, for data analysis, feet were converted to meters.

The data used in this study are presented in Lotus spreadsheet format on the enclosed diskette entitled Appendix A. The actual EM data, synthetic EM data, borehole, and analytical data are contained in the file EMDATA.WK1. VES data are contained in a spreadsheet file named VESDATA.WK1. Both files are write-protected.

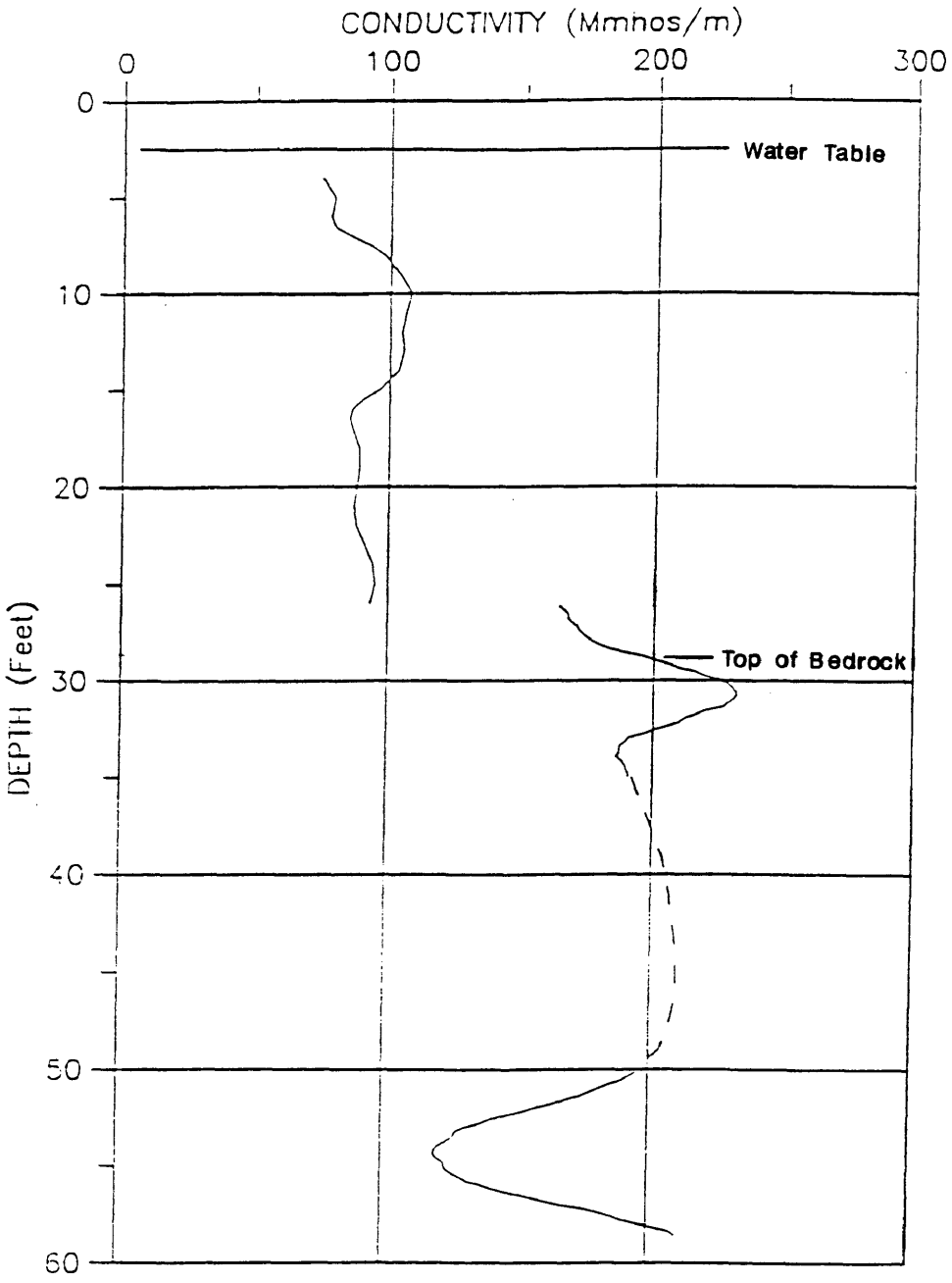

Figure A-1 Borehole Induction Log from Wells 37313 and 37317

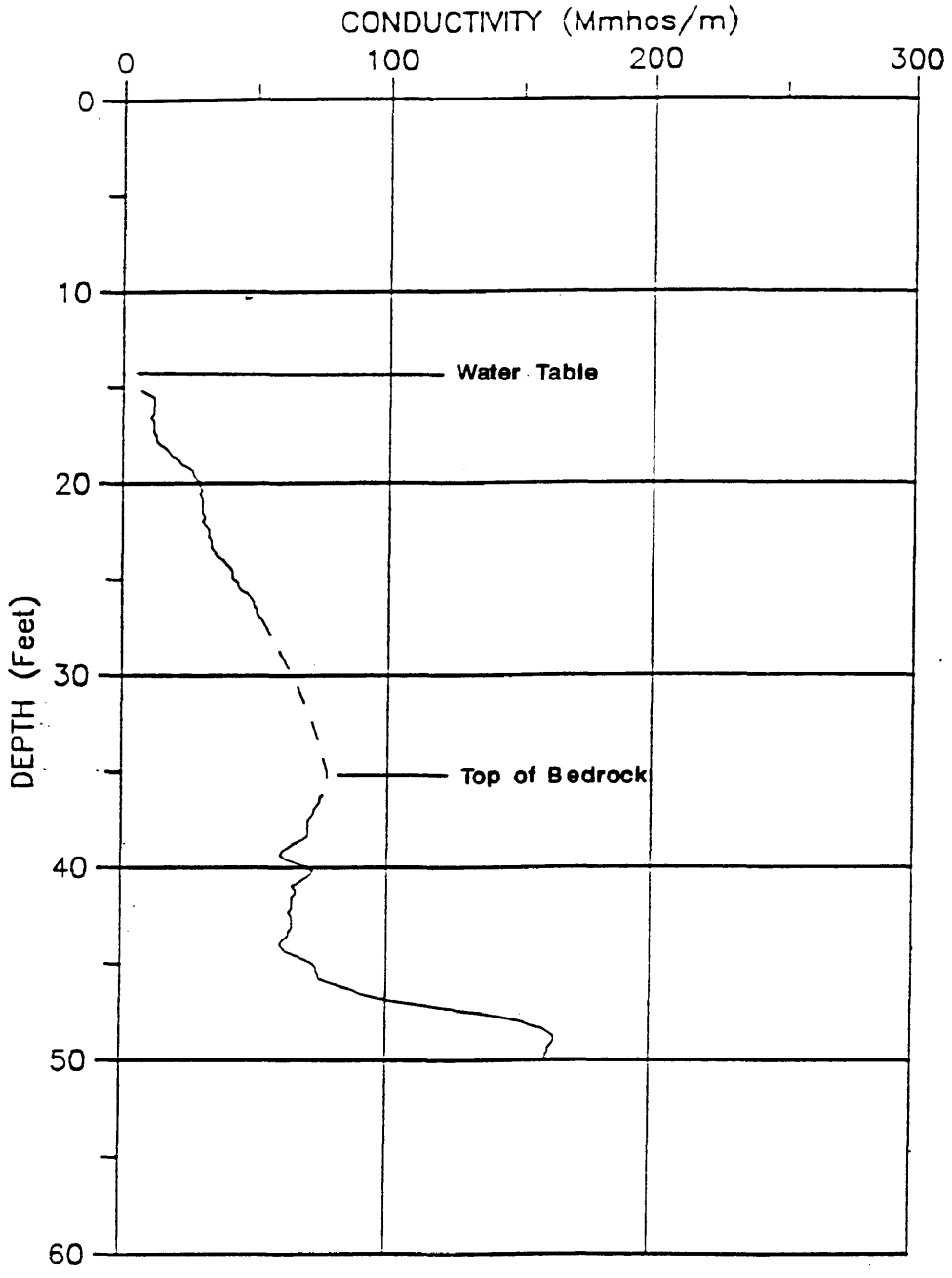

Figure A-2 Borehole Induction Log from Wells 37320 amd 37321

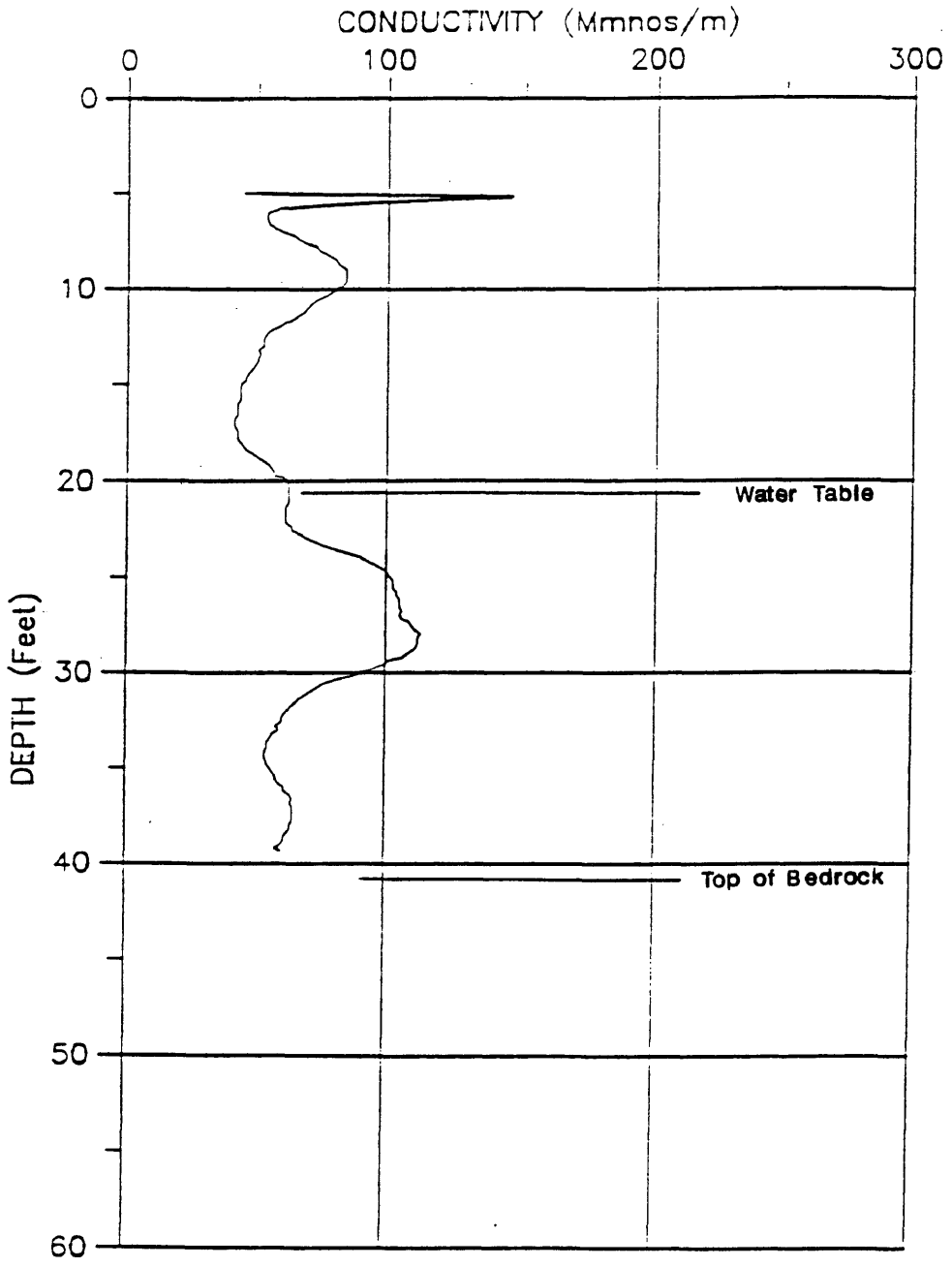

Figure A-3 Borehole Induction Log from Well 37344

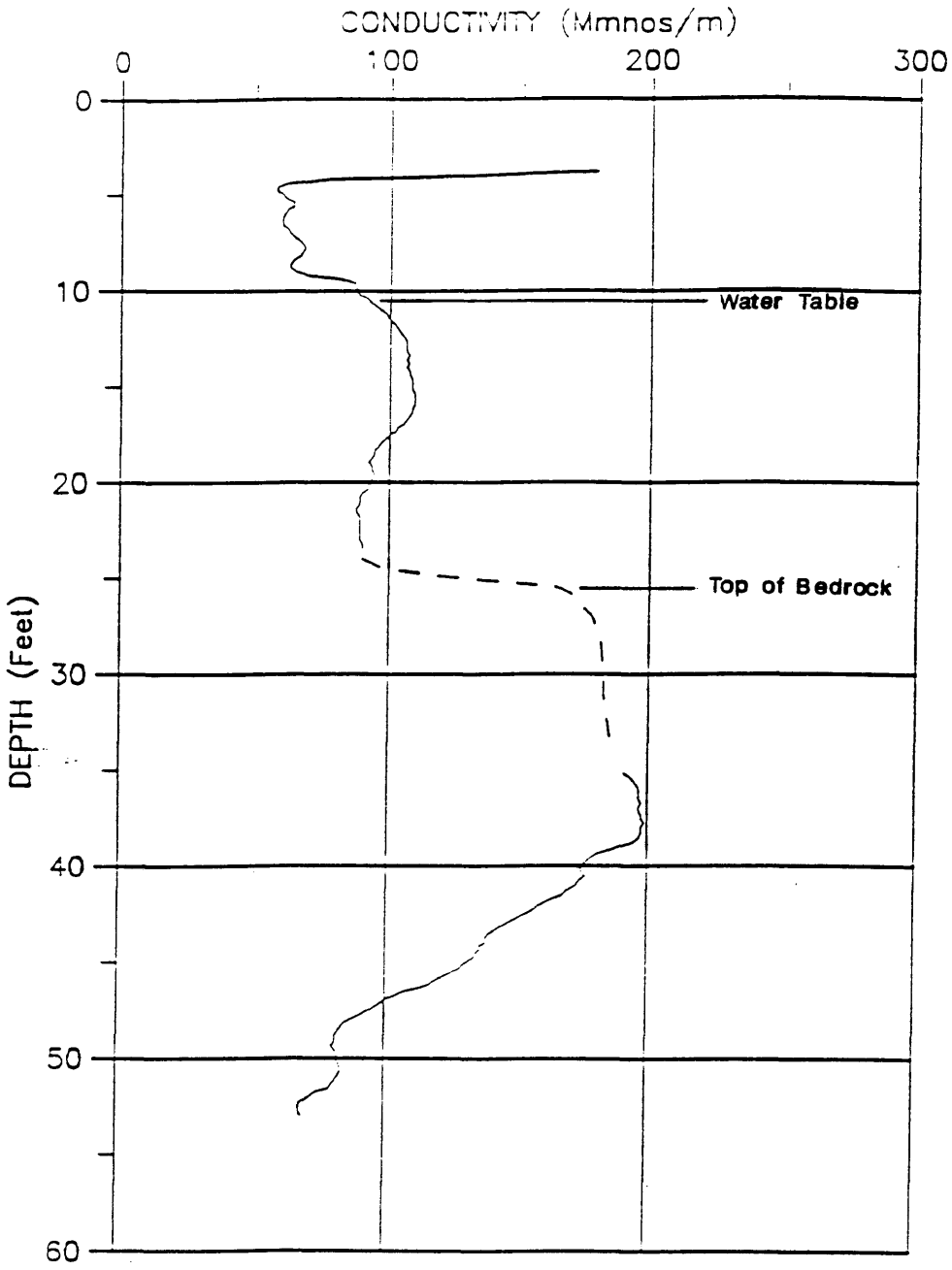

Figure A-4 Borehole Induction Log from Wells 37374 and 37379

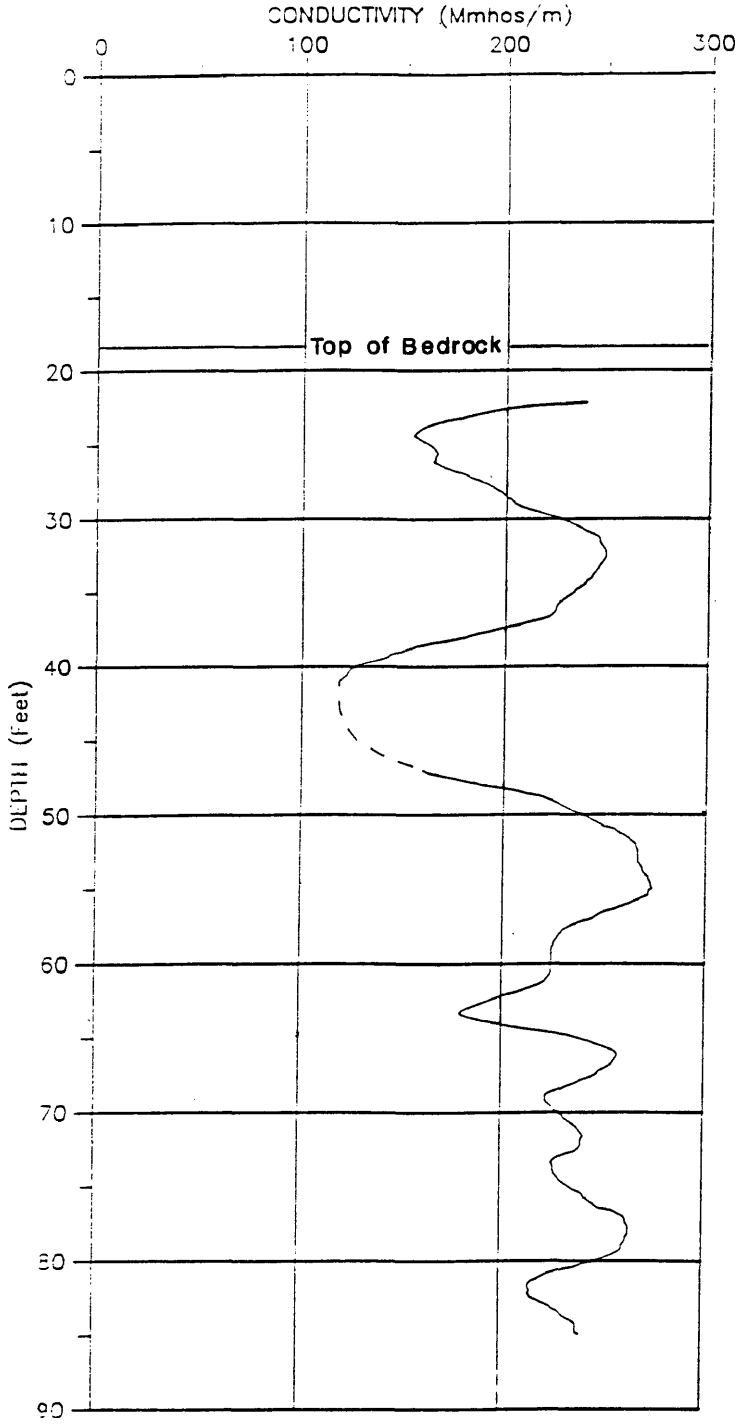

Figure A-5 Borehole Induction Log from Wells 37387 and 37388

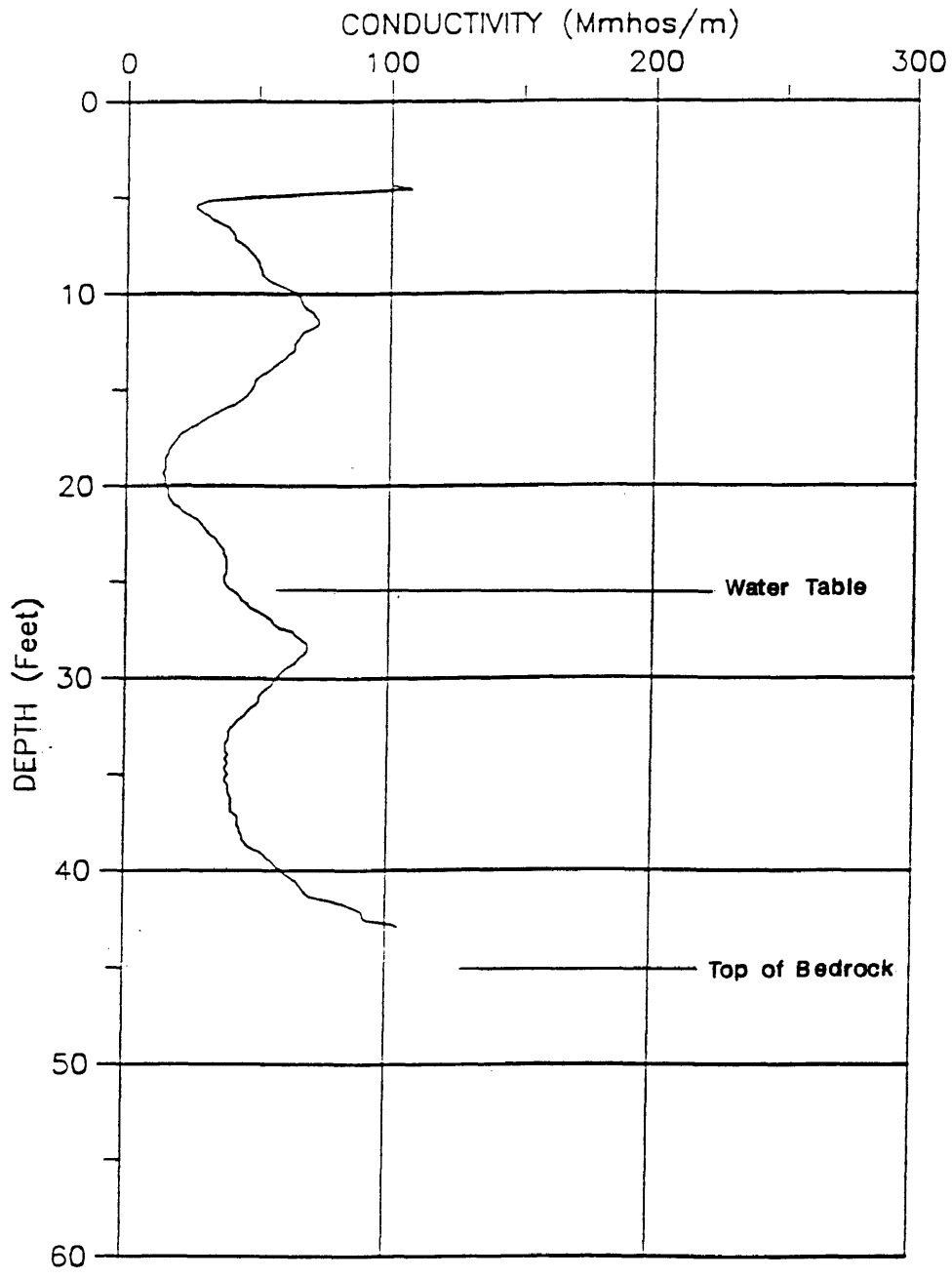

Figure A-6 Borehole Induction Log from Well 37395

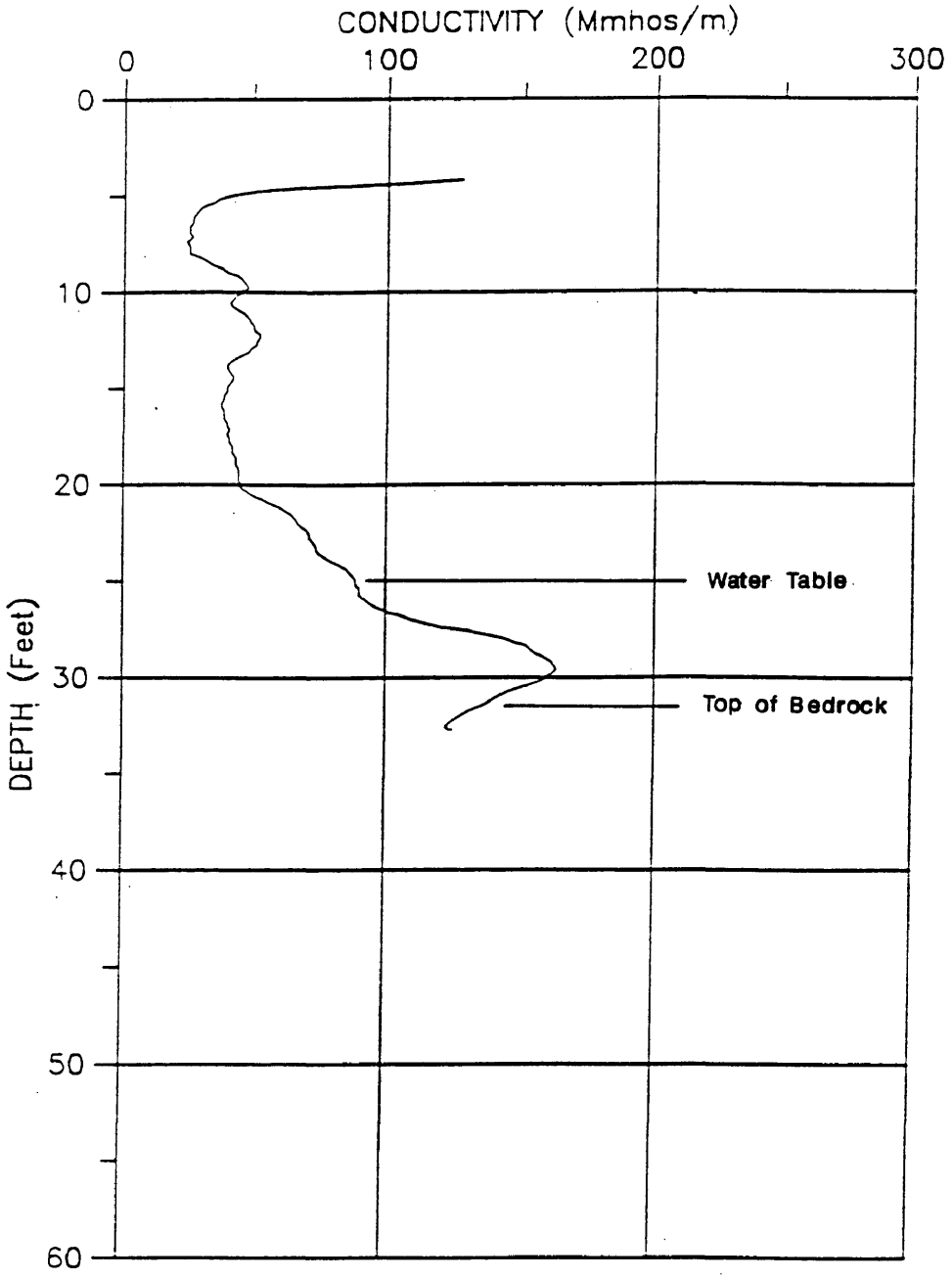

Figure A-7 Borehole Induction Log from Well 37397

APPENDIX B
DATA PLOTS

APPENDIX B - DATA PLOTS

Plots of data types important to this study are presented in this appendix.

Figures B-1 through B-10: Resistivity Sounding Data and Interpretations
Figures B-11 through B-31: Actual and Synthetic Apparent Conductivity Data
Figures B-32 through B-47: Residual Conductivity and Standardized Residuals for Apparent Conductivity Data

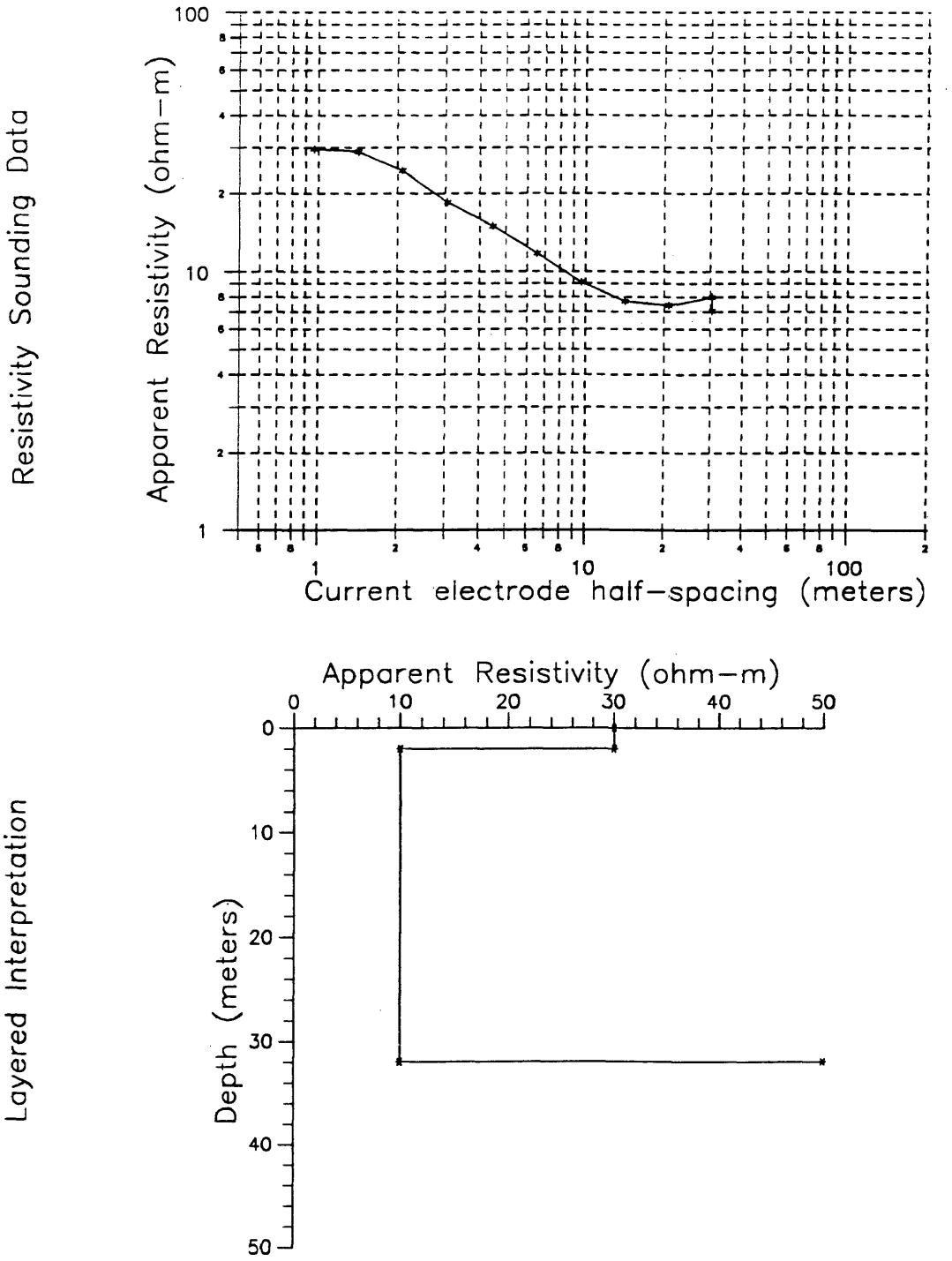

Figure B-1 Resistivity Sounding Data and Interpretation for VES-A

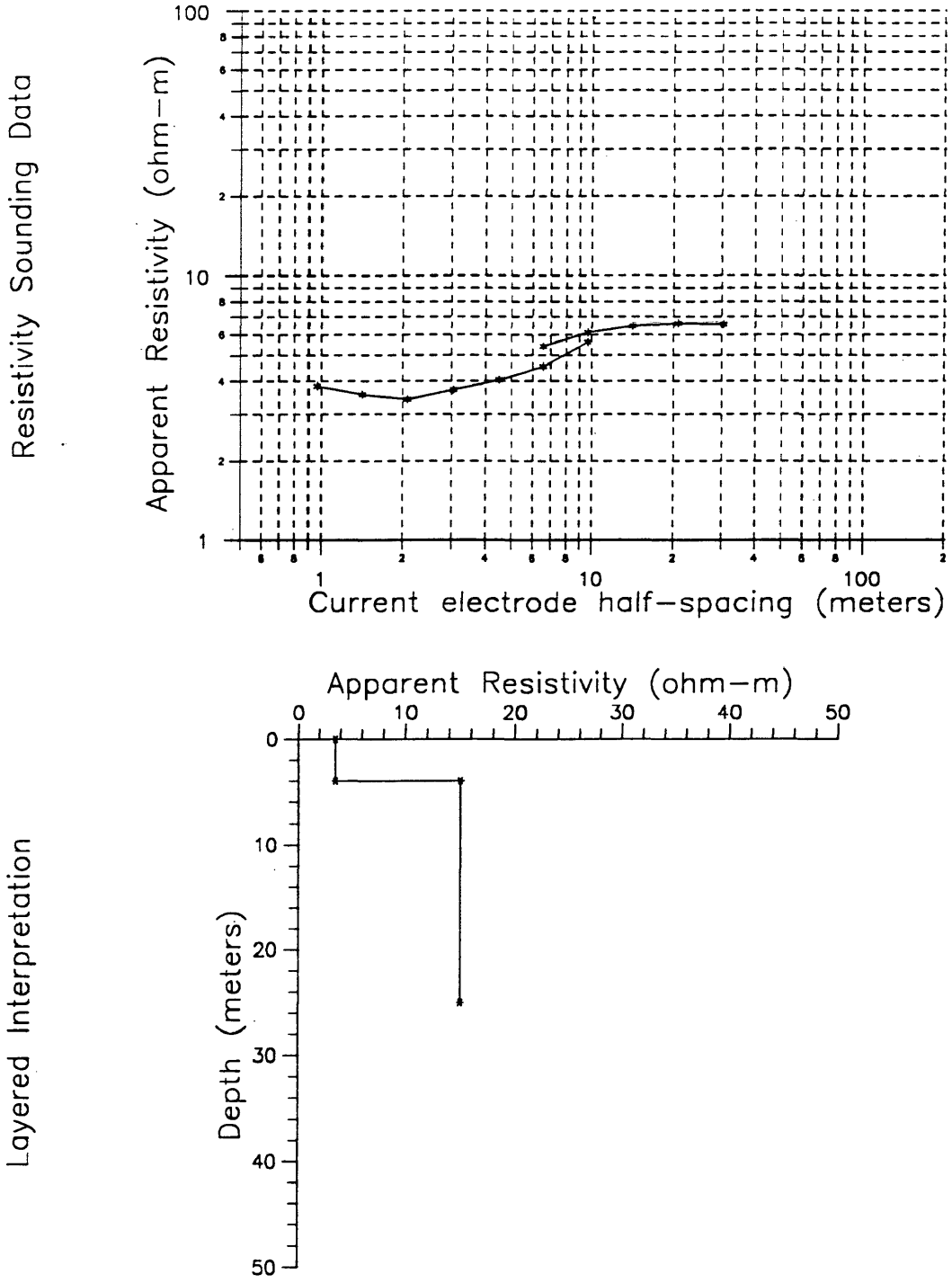

Figure B-2 Resistivity Sounding Data and Interpretation for VES-B

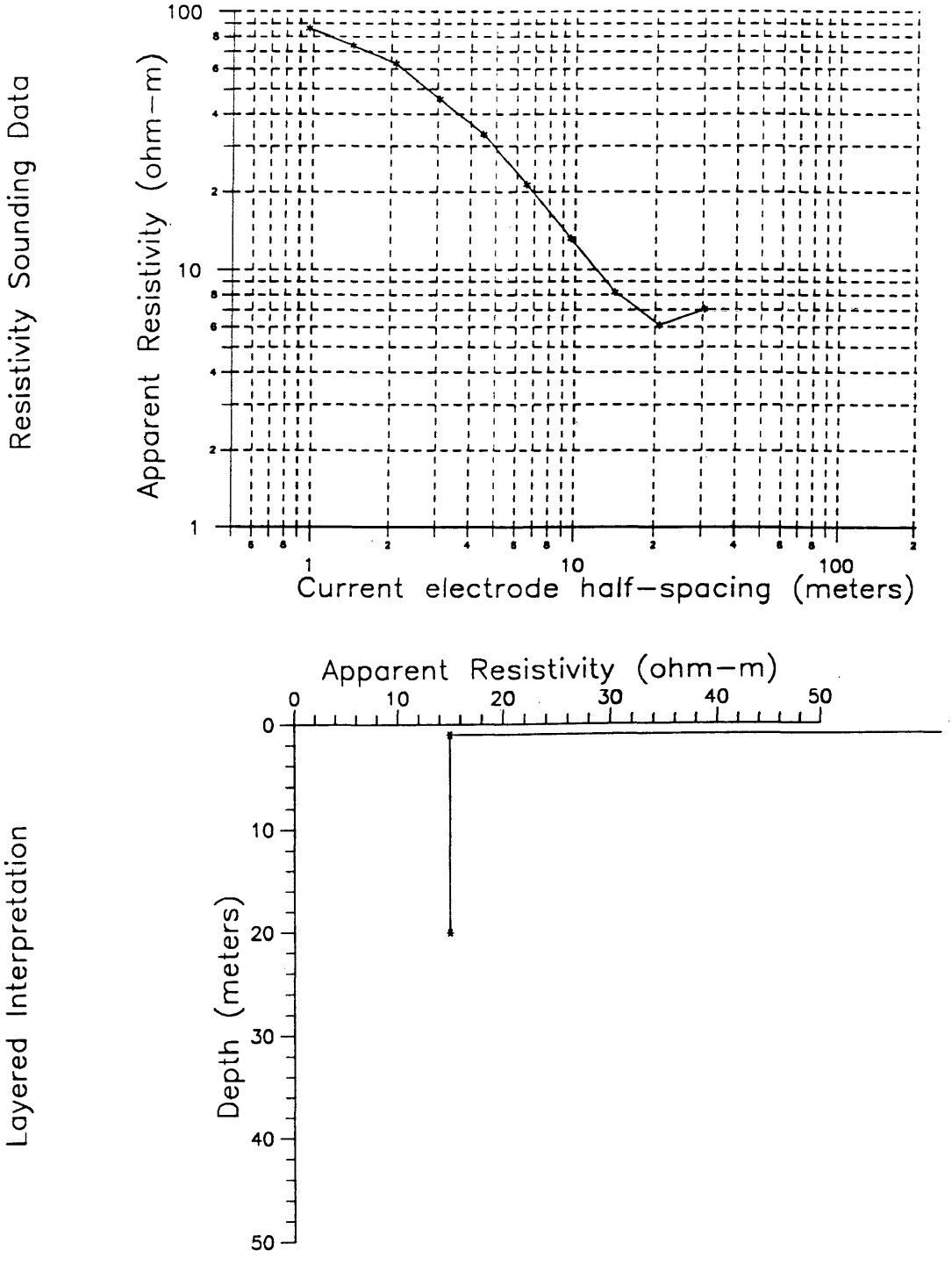

Figure B-3 Resistivity Sounding Data and Interpretation for VES-C

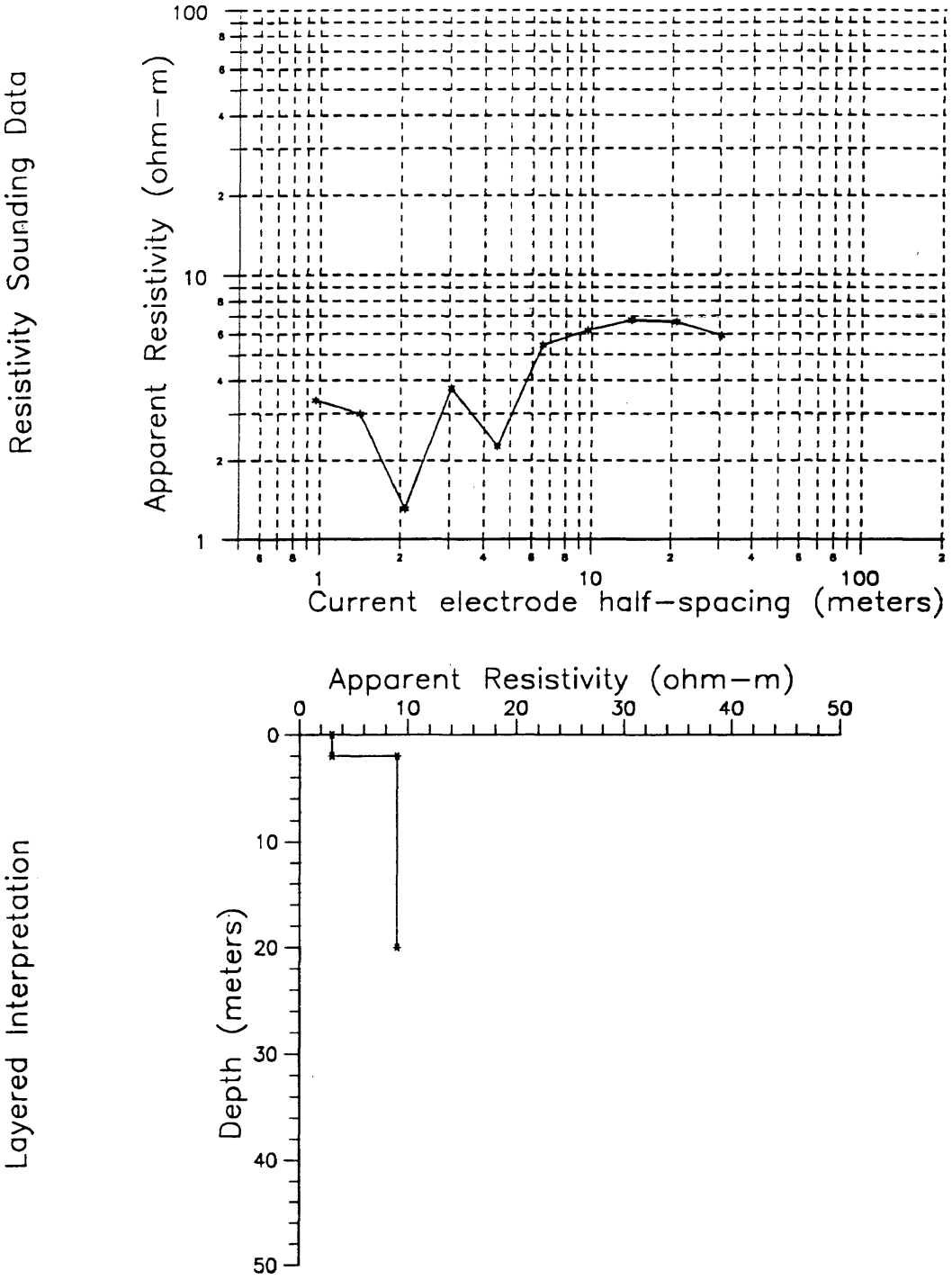

Figure B-4 Resistivity Sounding Data and Interpretation for VES-D

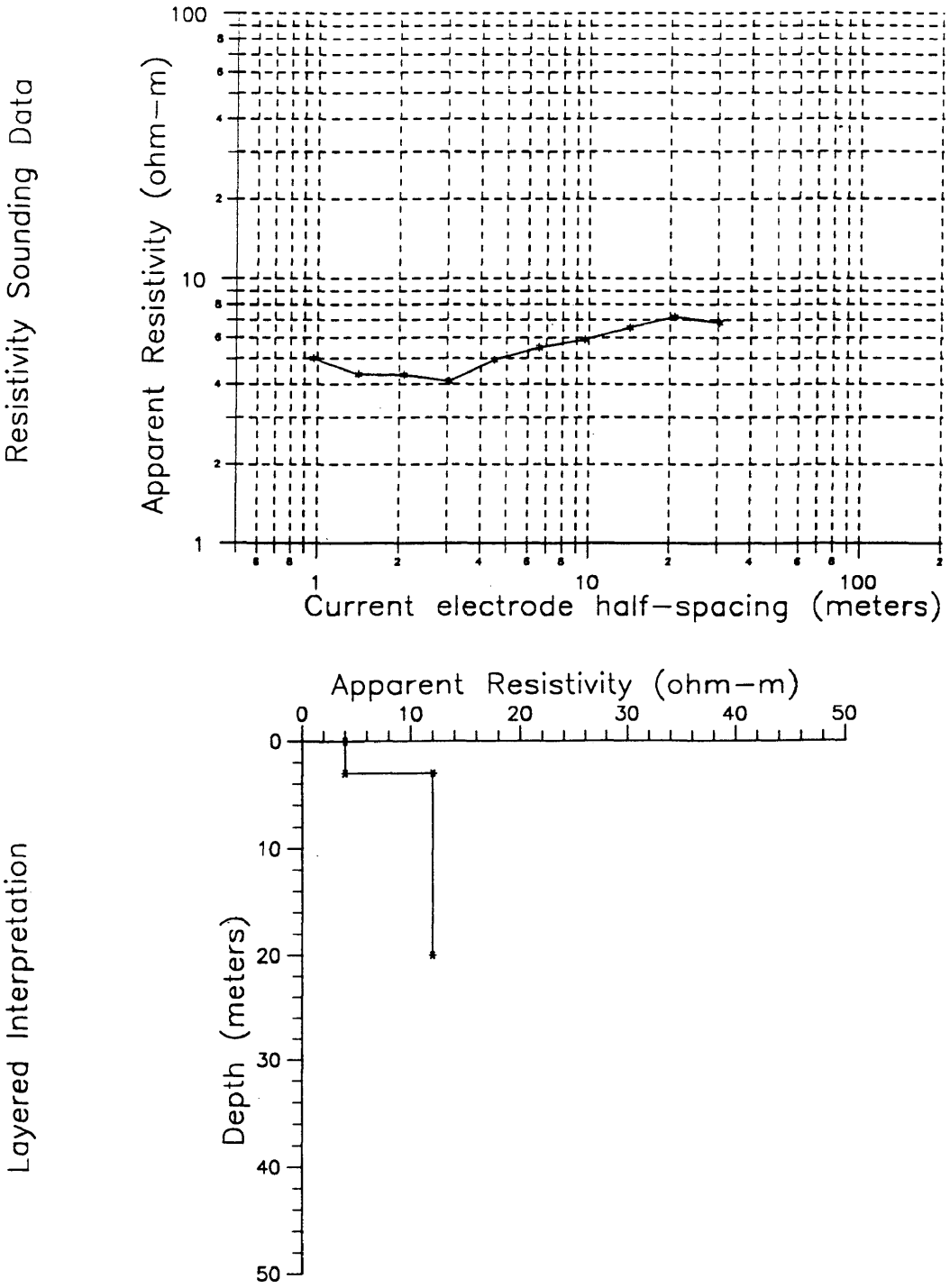

Figure B-5 Resistivity Sounding Data and Interpretation for VES-E

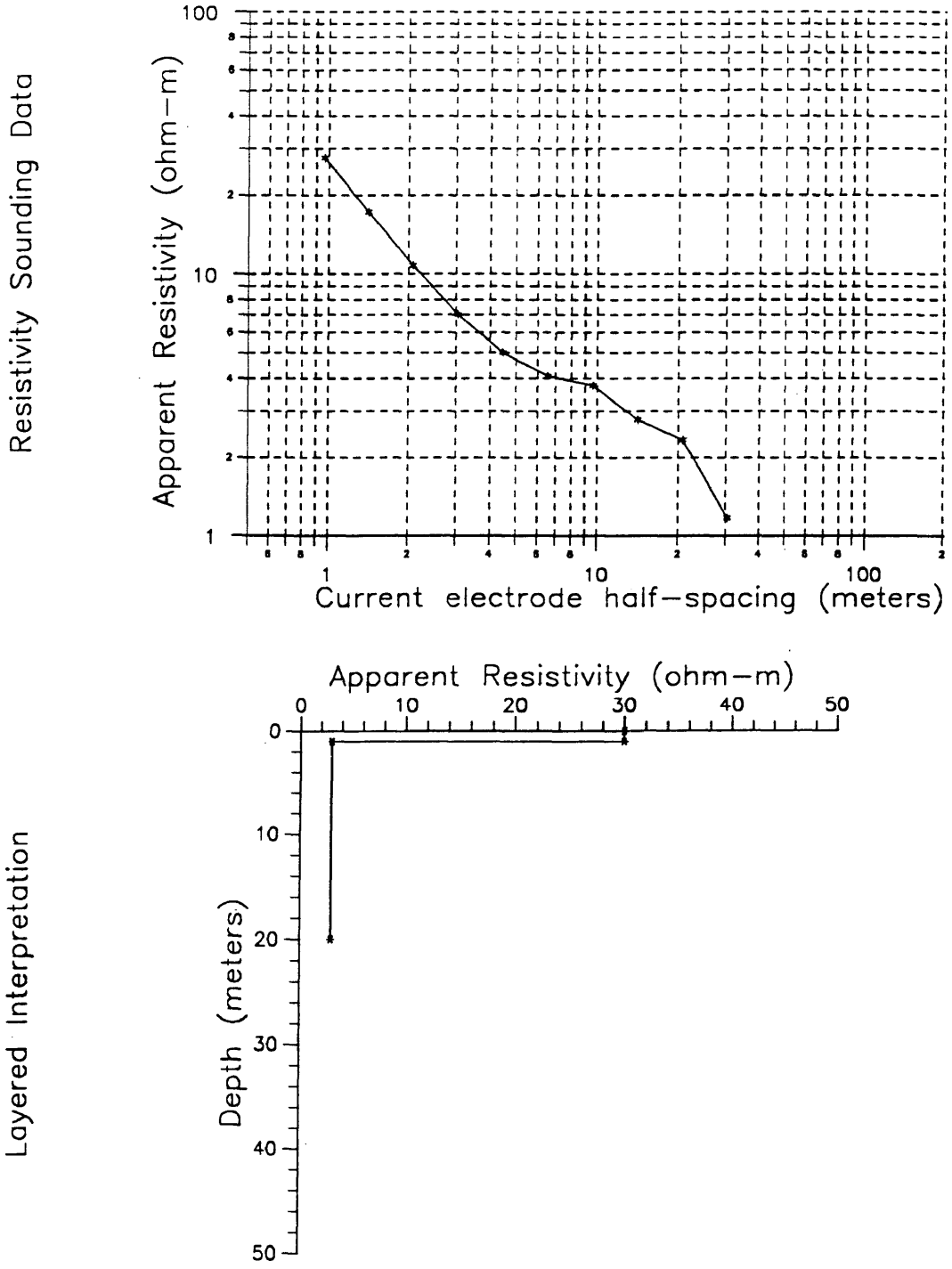

Figure B-6 Resistivity Sounding Data and Interpretation for VES-F

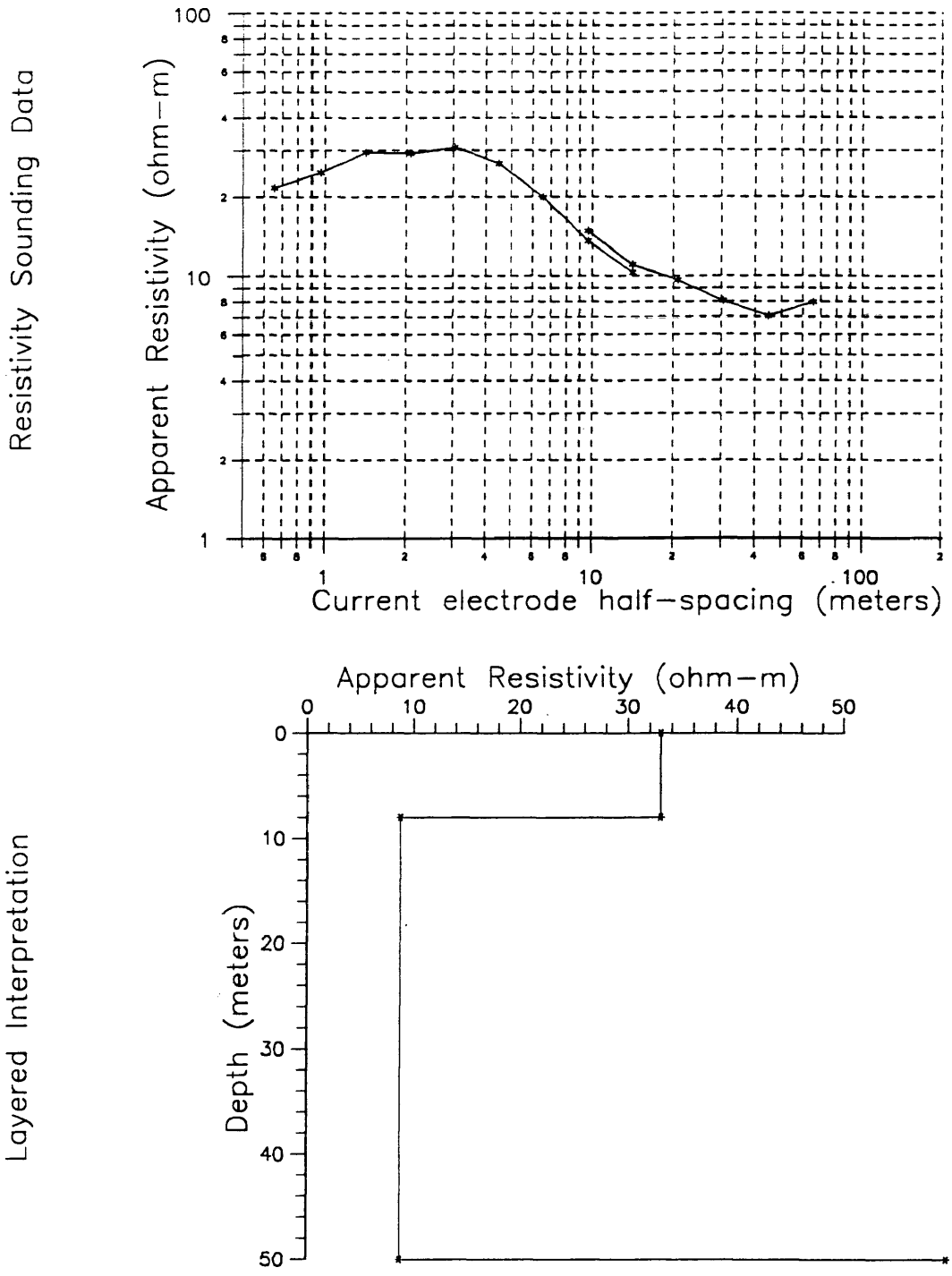

Figure B-7 Resistivity Sounding Data and Interpretation for VES-1

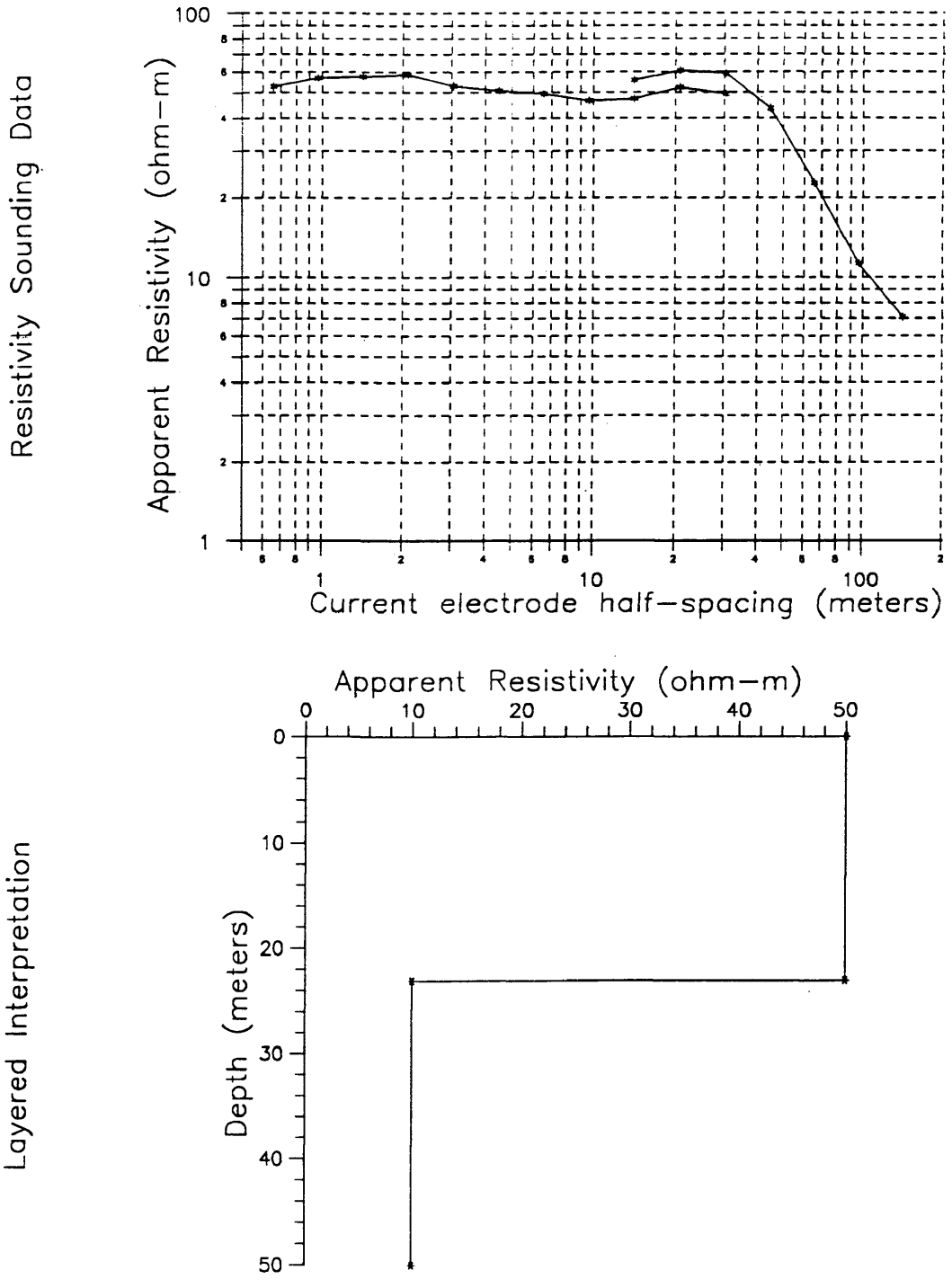

Figure B-8 Resistivity Sounding Data and Interpretation for VES-2

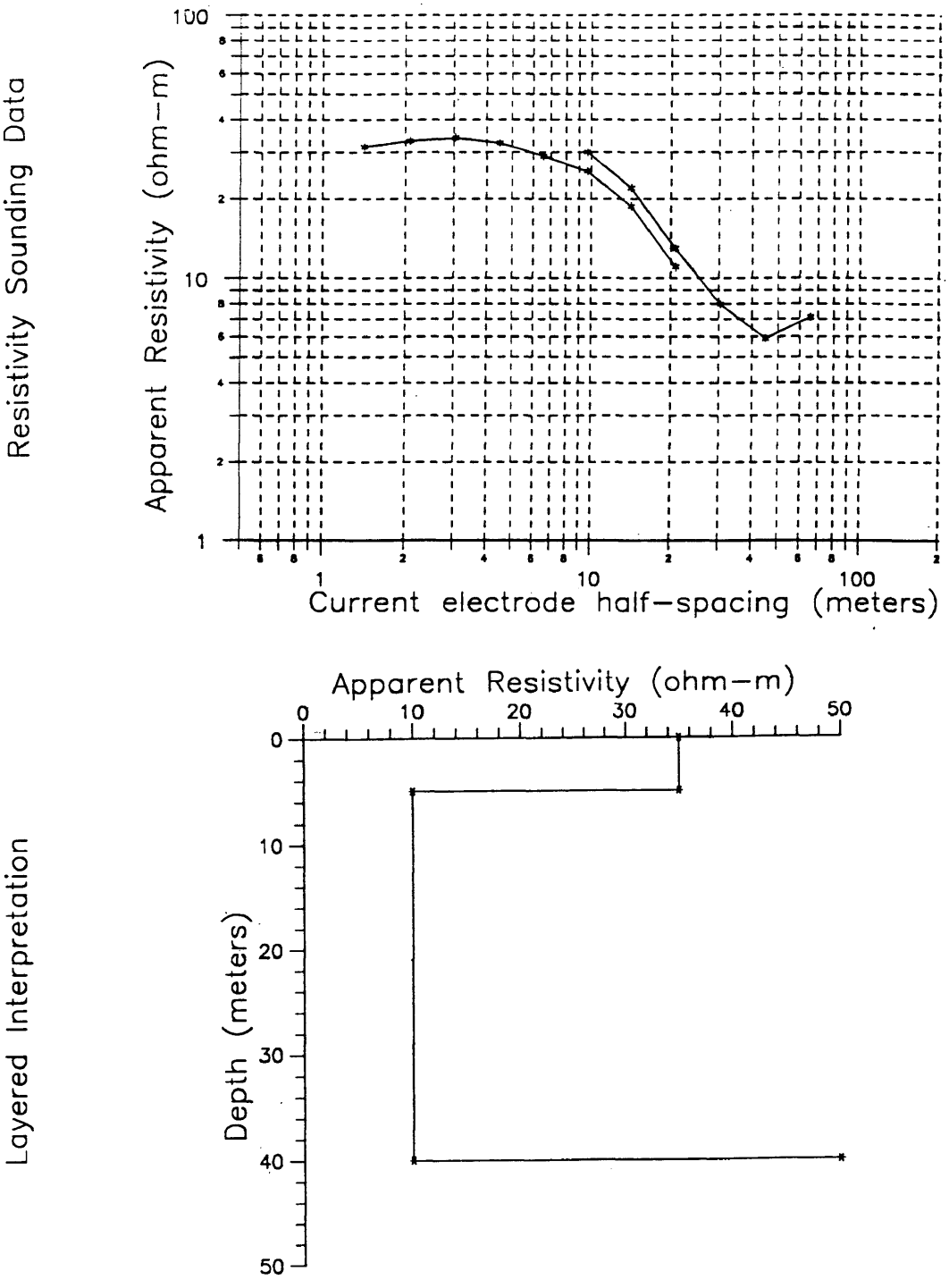

Figure B-9 Resistivity Sounding Data and Interpretation for VES-3

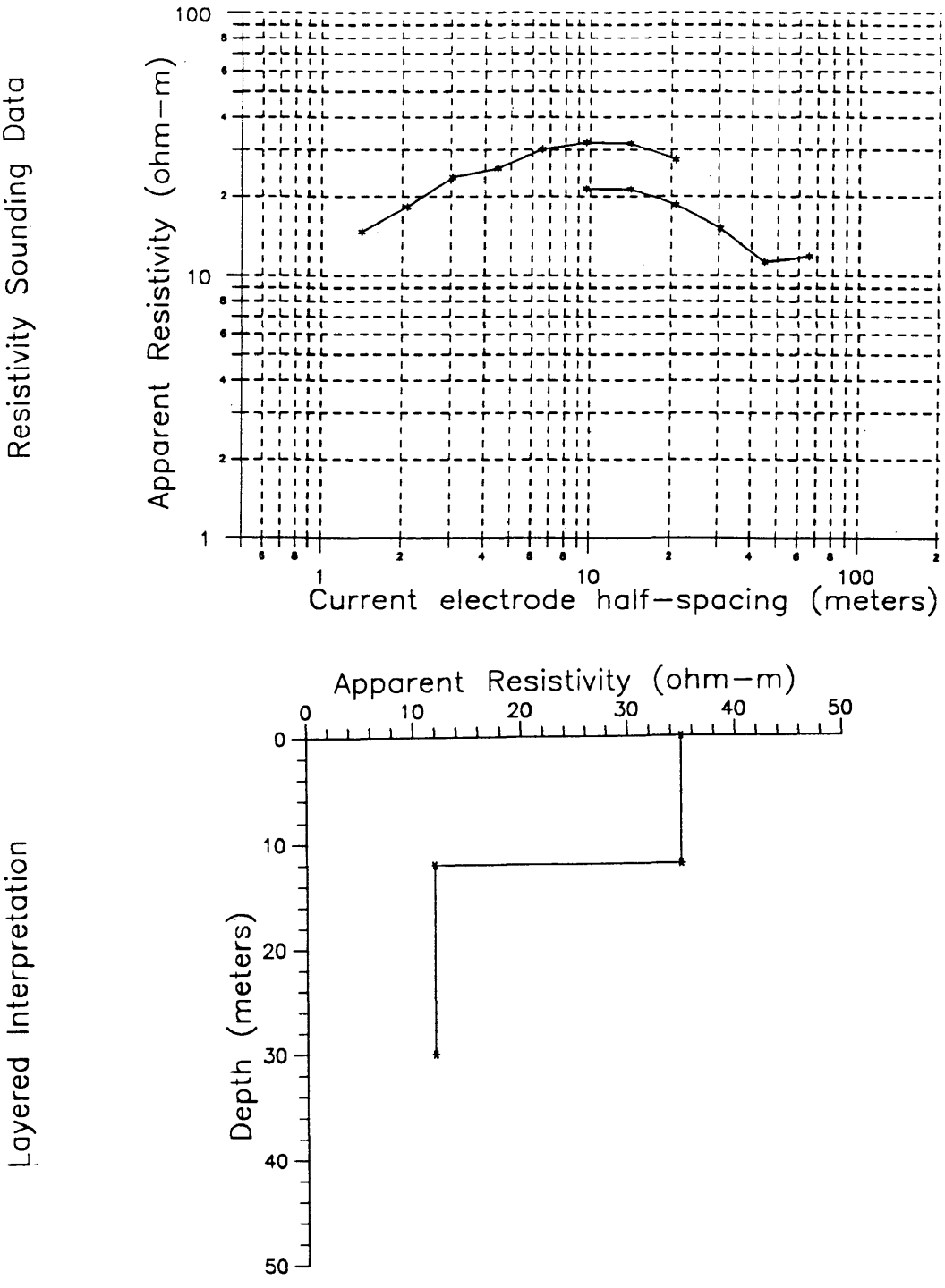

Figure B-10 Resistivity Sounding Data and Interpretation for VES-4

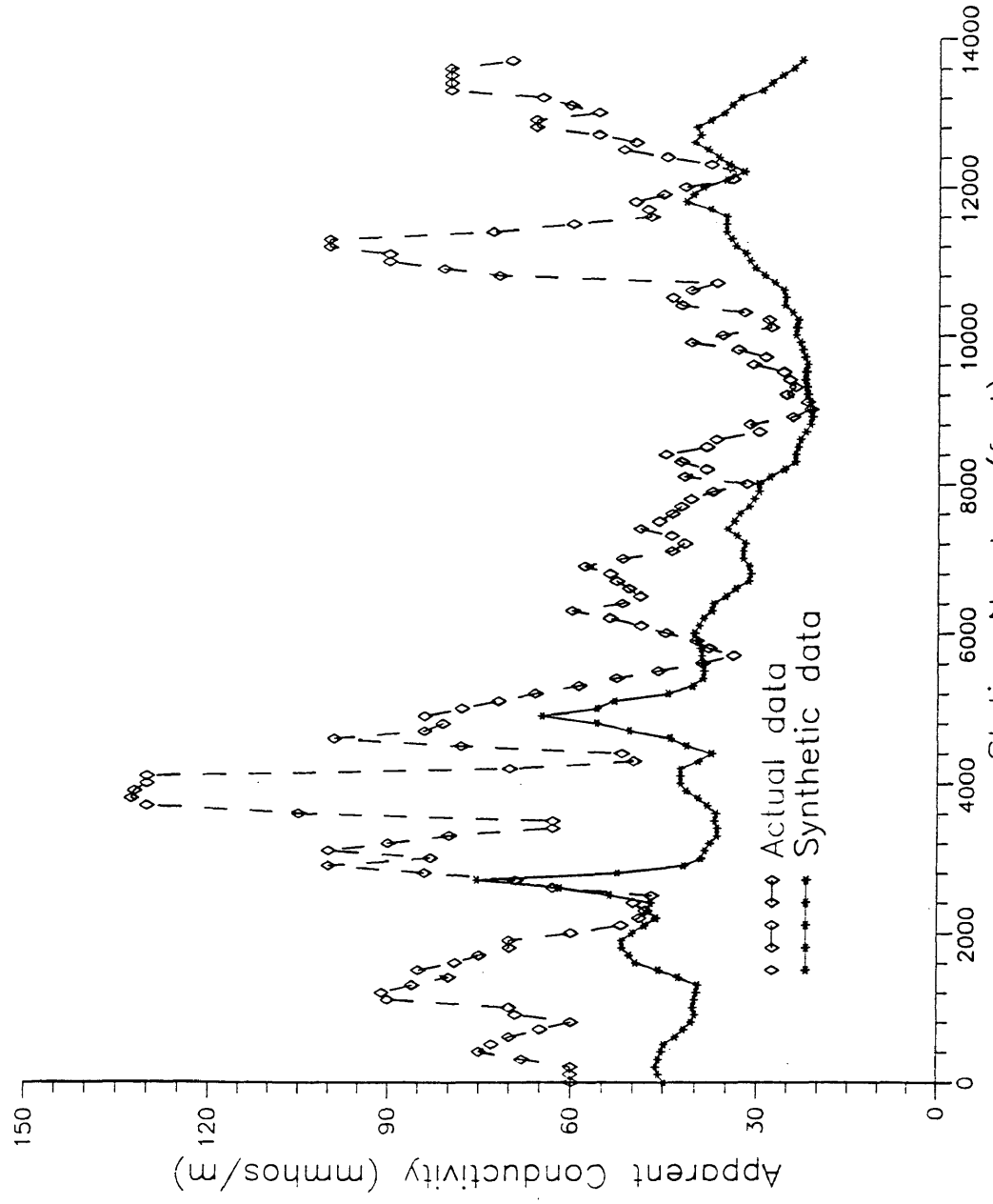

Figure B-11 Actual and Synthetic Apparent Conductivity Data for 10-Meter Coil Spacing for Line HL-1

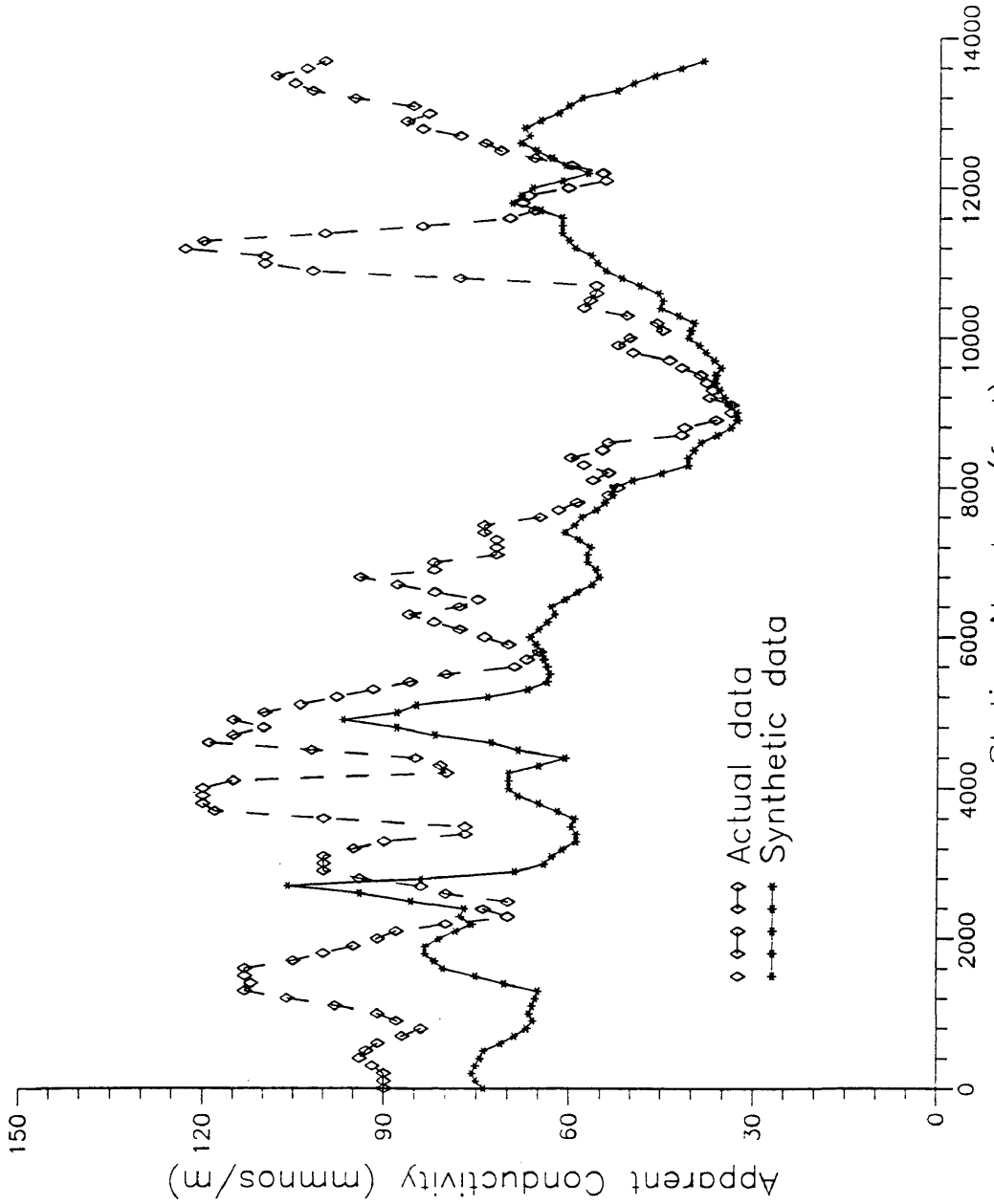

Figure B-12 Actual and Synthetic Apparent Conductivity Data for 20-Meter Coil Spacing for Line HL-1

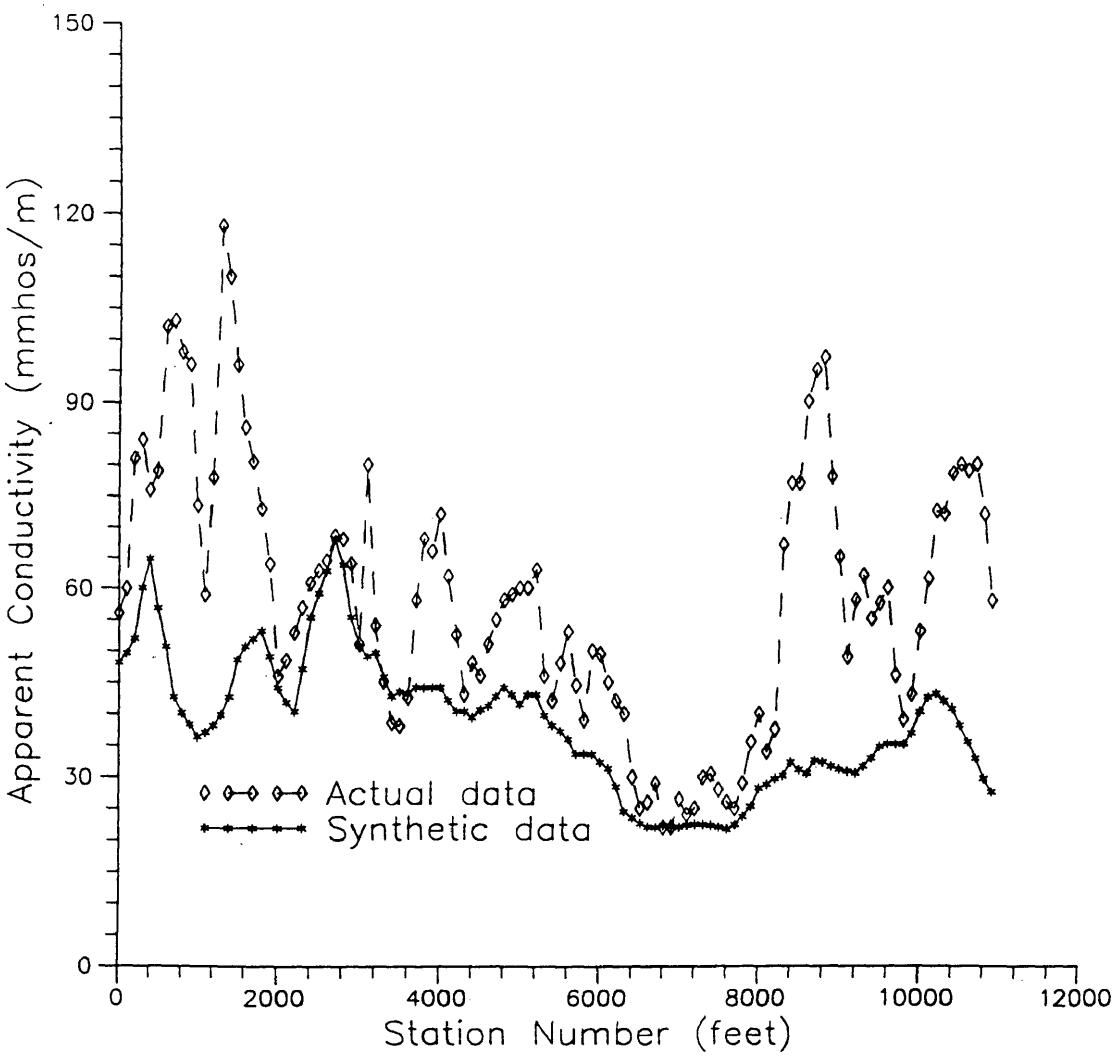

Figure B-13 Actual and Synthetic Apparent Conductivity Data for 10-Meter Coil Spacing for Line HL-3

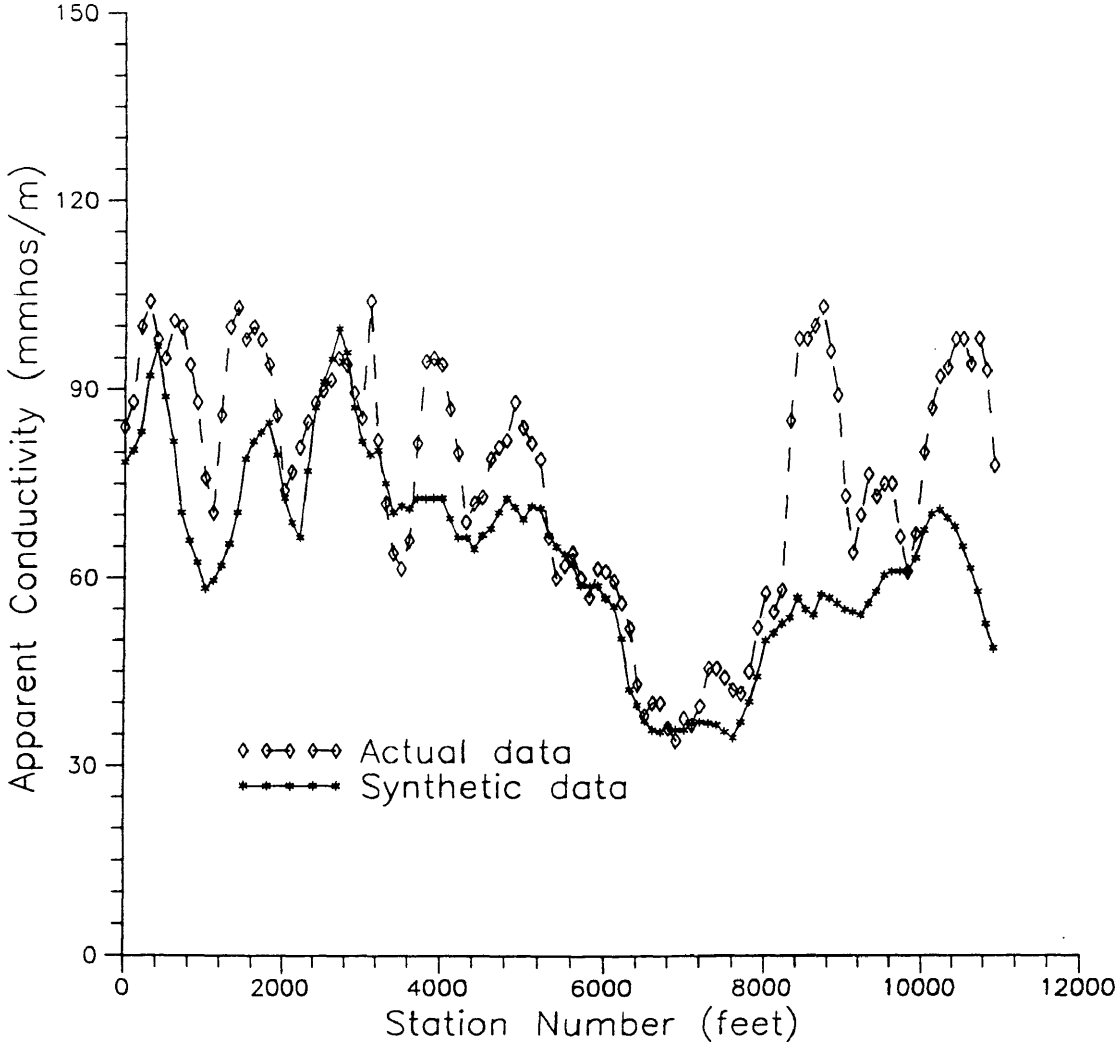

Figure B-14 Actual and Synthetic Apparent Conductivity Data for 20-Meter Coil Spacing for Line HL-3

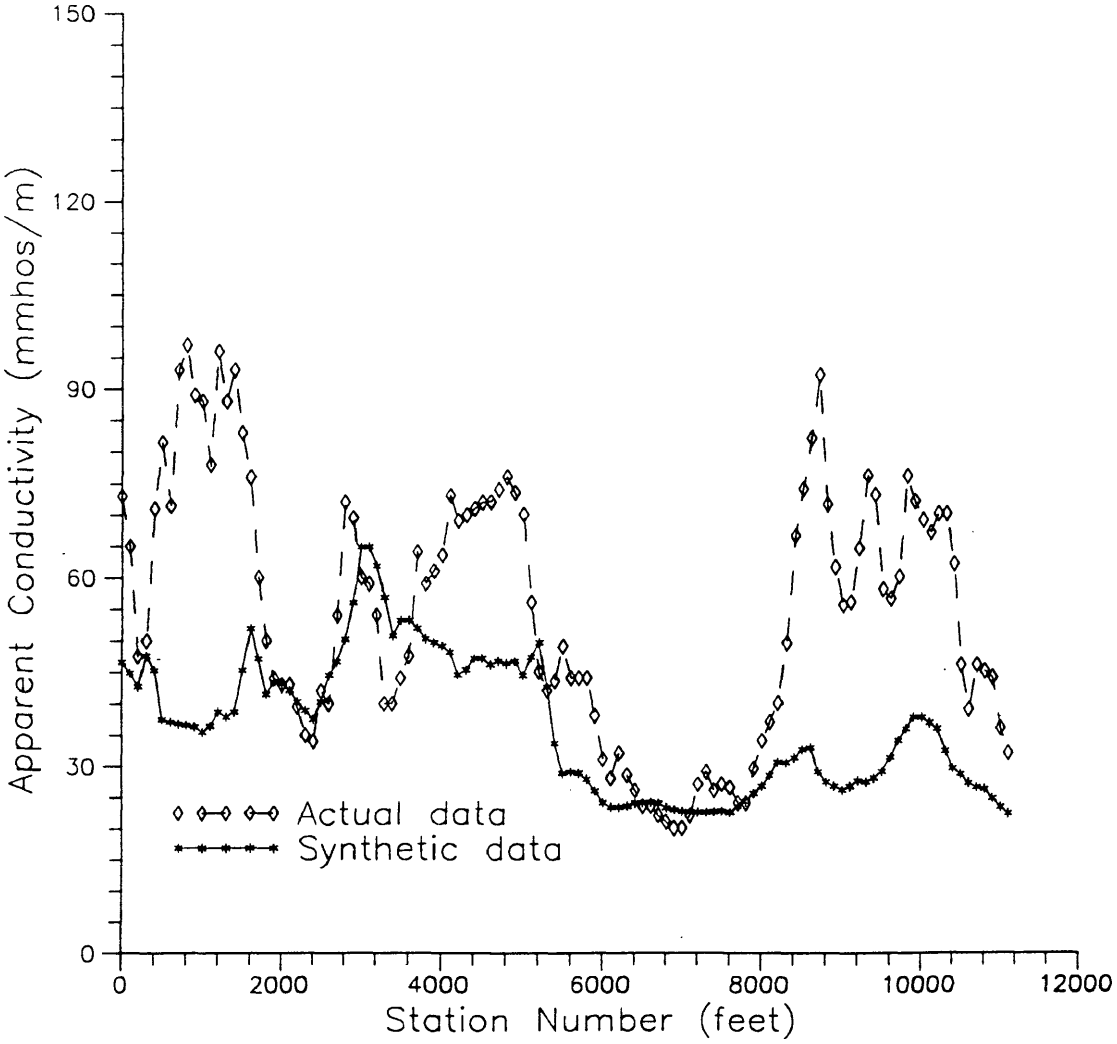

Figure B-15 Actual and Synthetic Apparent Conductivity Data for 10-Meter Coil Spacing for Line HL-4

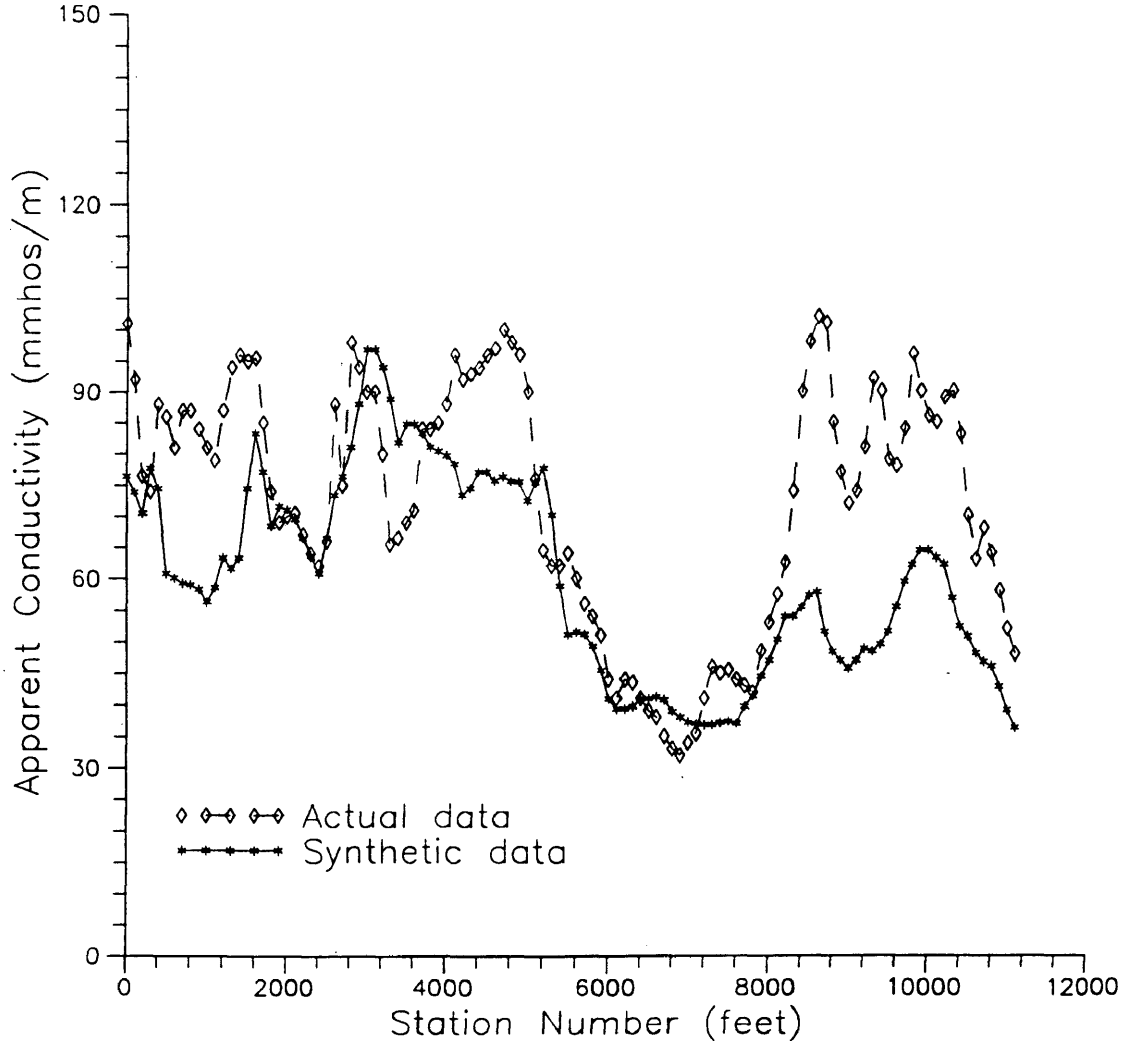

Figure B-16 Actual and Synthetic Apparent Conductivity Data for 20-Meter Coil Spacing for Line HL-4

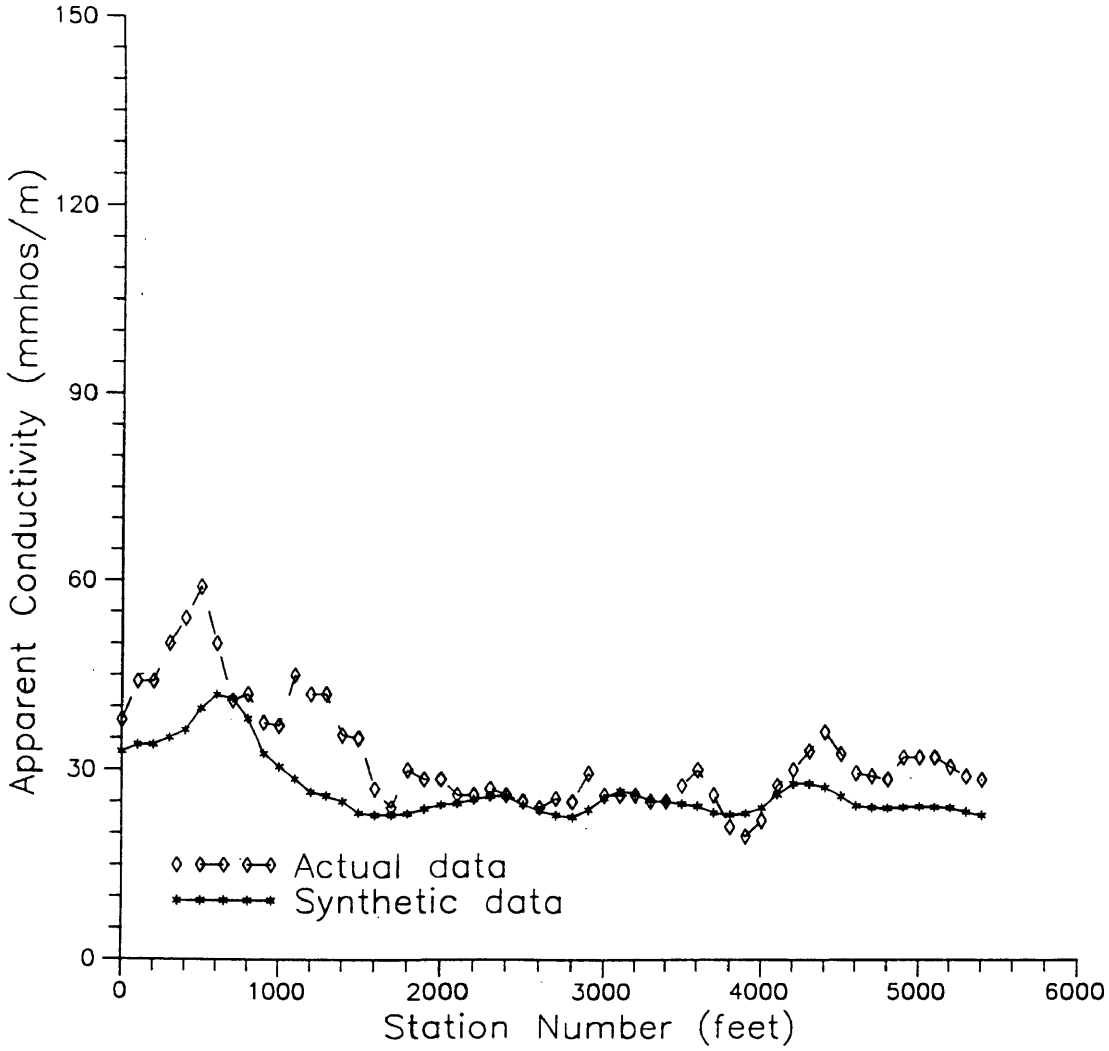

Figure B-17 Actual and Synthetic Apparent Conductivity Data for 10-Meter Coil Spacing for Line HL-5

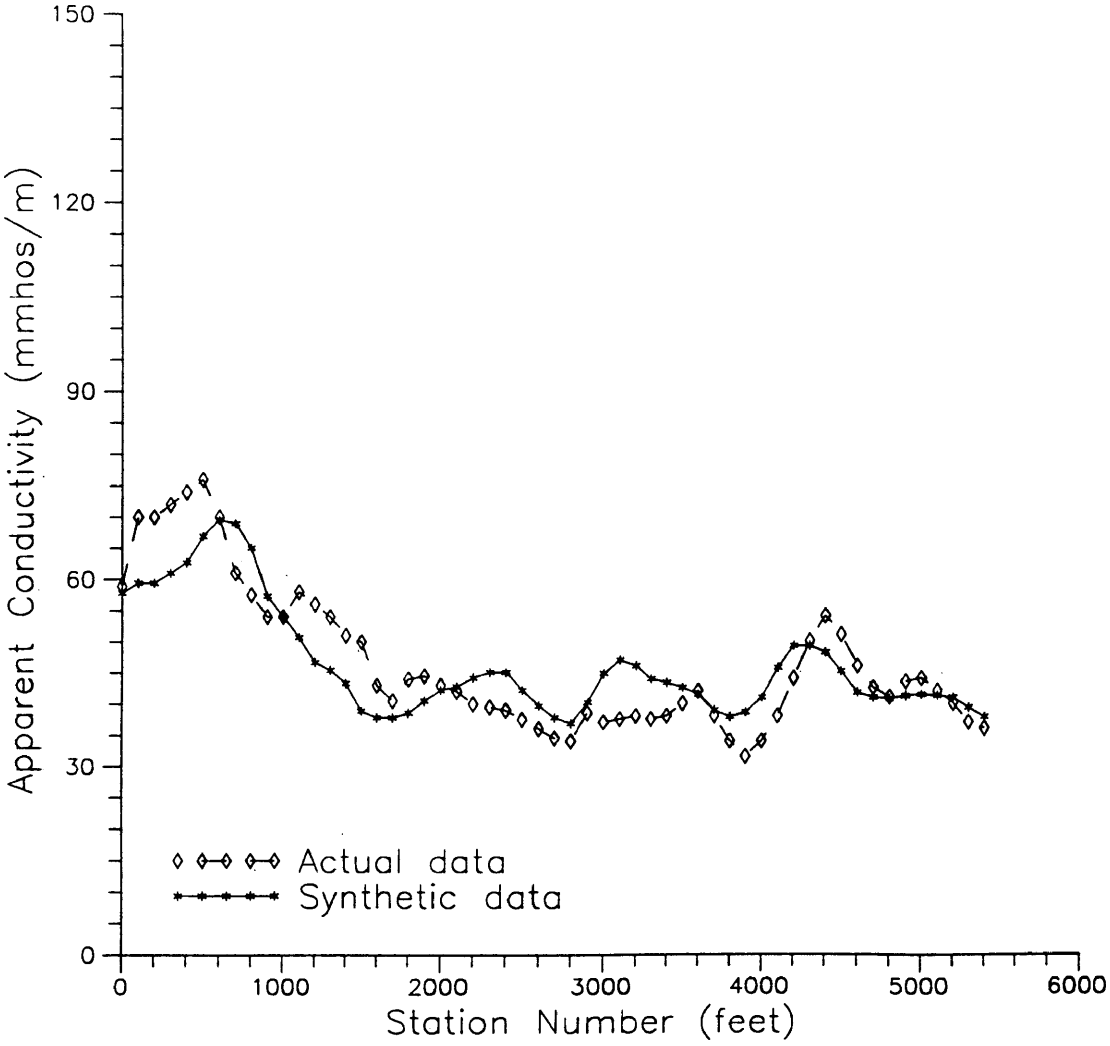

Figure B-18 Actual and Synthetic Apparent Conductivity Data for 20-Meter Coil Spacing for Line HL-5

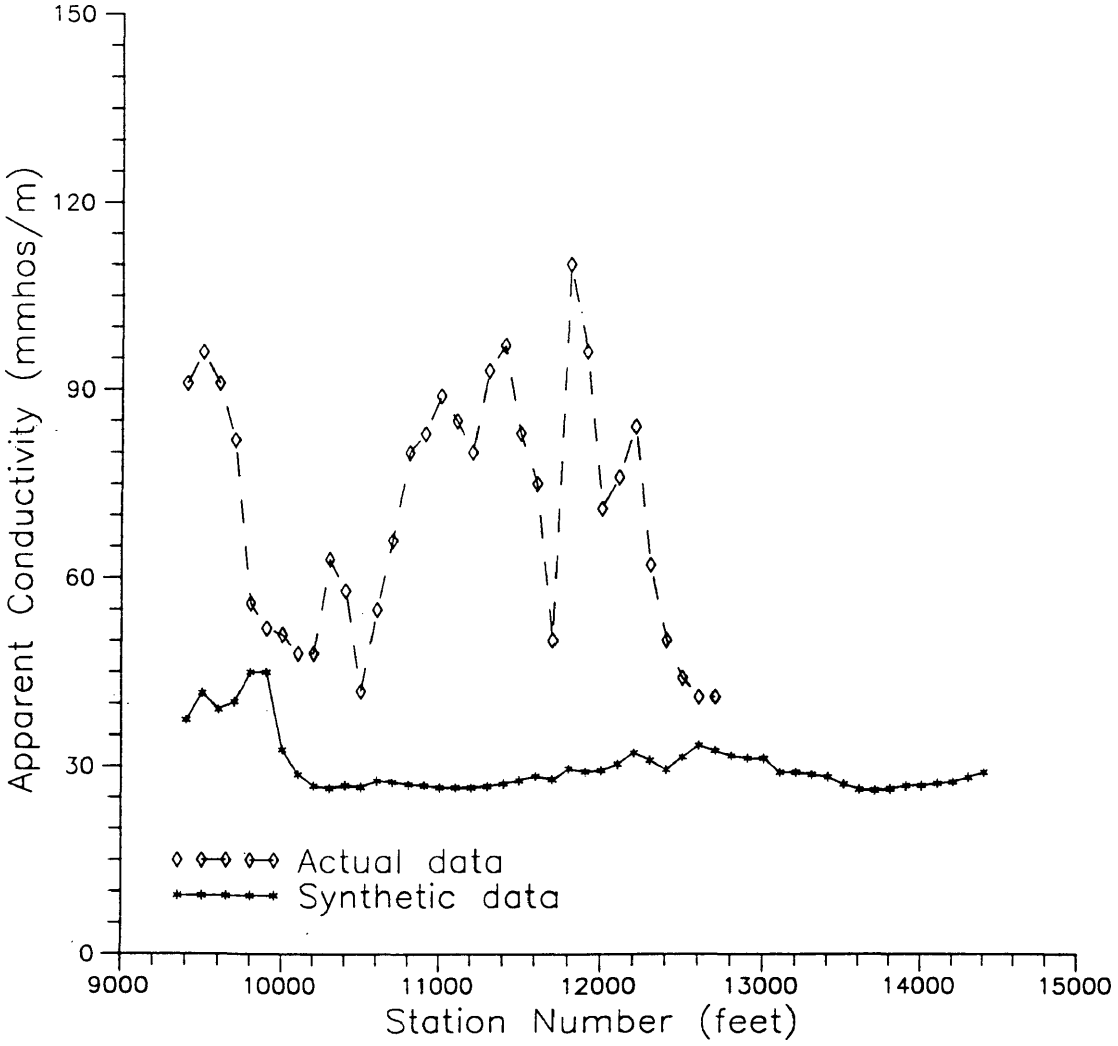

Figure B-19 Actual and Synthetic Apparent Conductivity Data for 3.67-Meter Coil Spacing for Line MWP-1

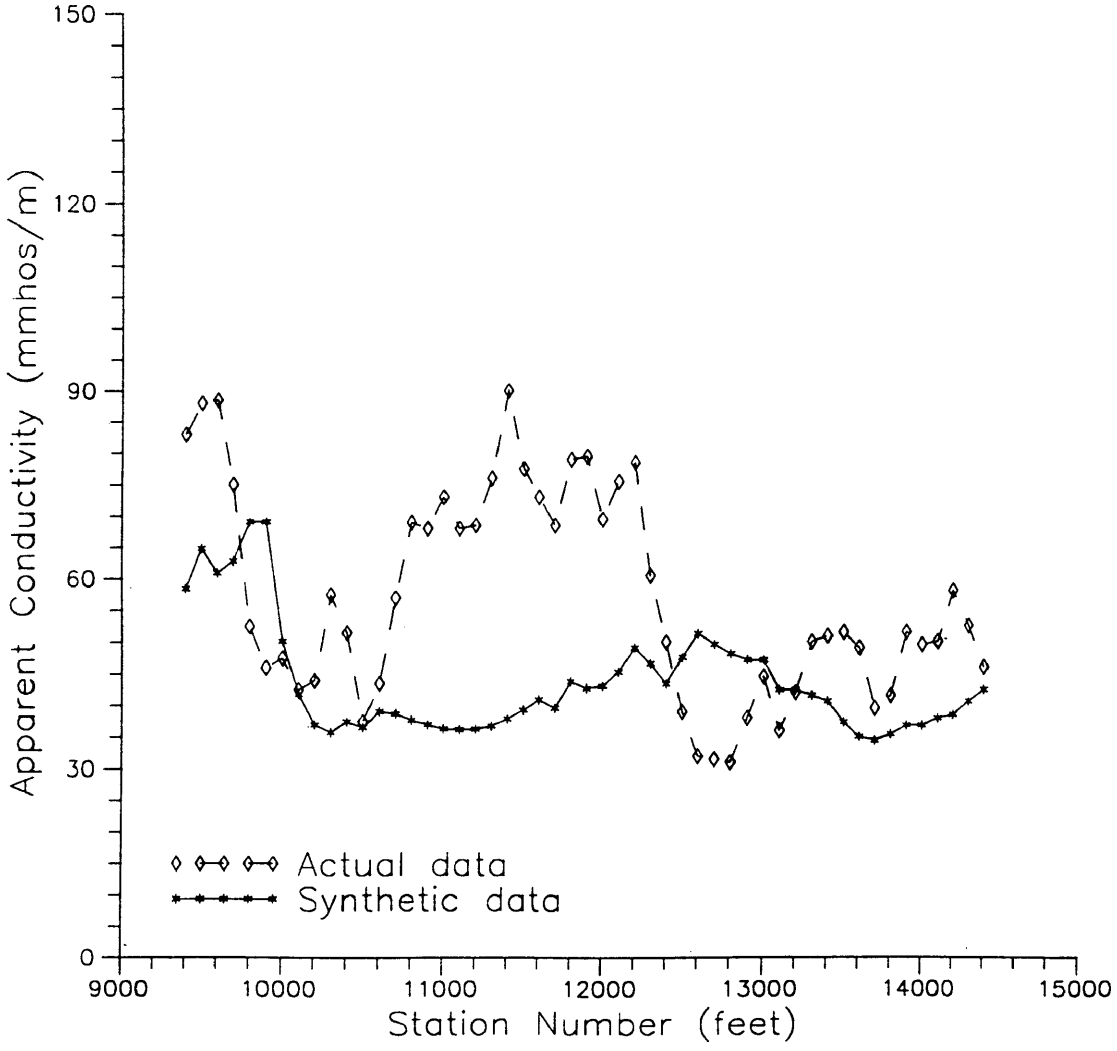

Figure B-20 Actual and Synthetic Apparent Conductivity Data for 10-Meter Coil Spacing for Line MWP-1

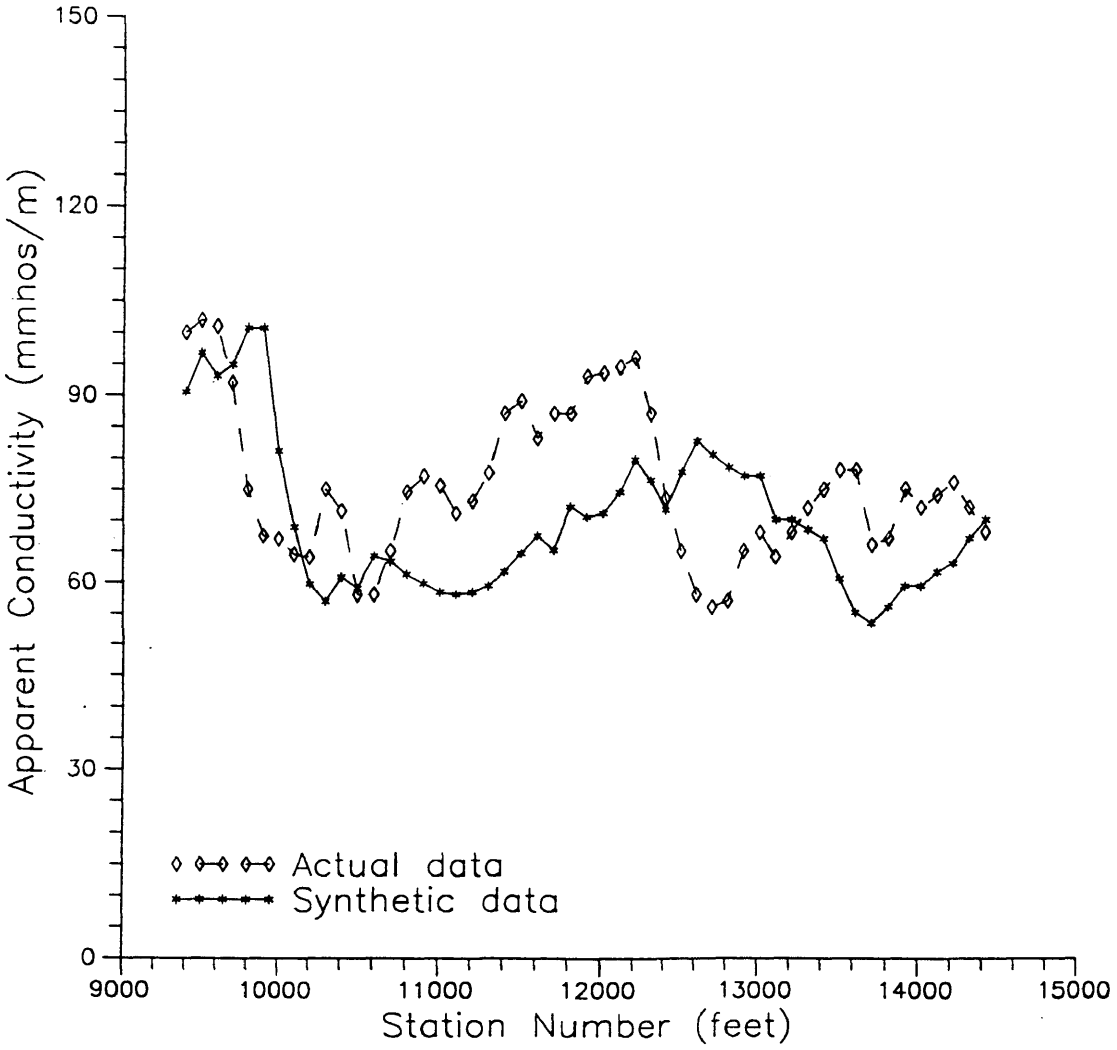

Figure B-21 Actual and Synthetic Apparent Conductivity Data for 20-Meter Coil Spacing for Line MWP-1

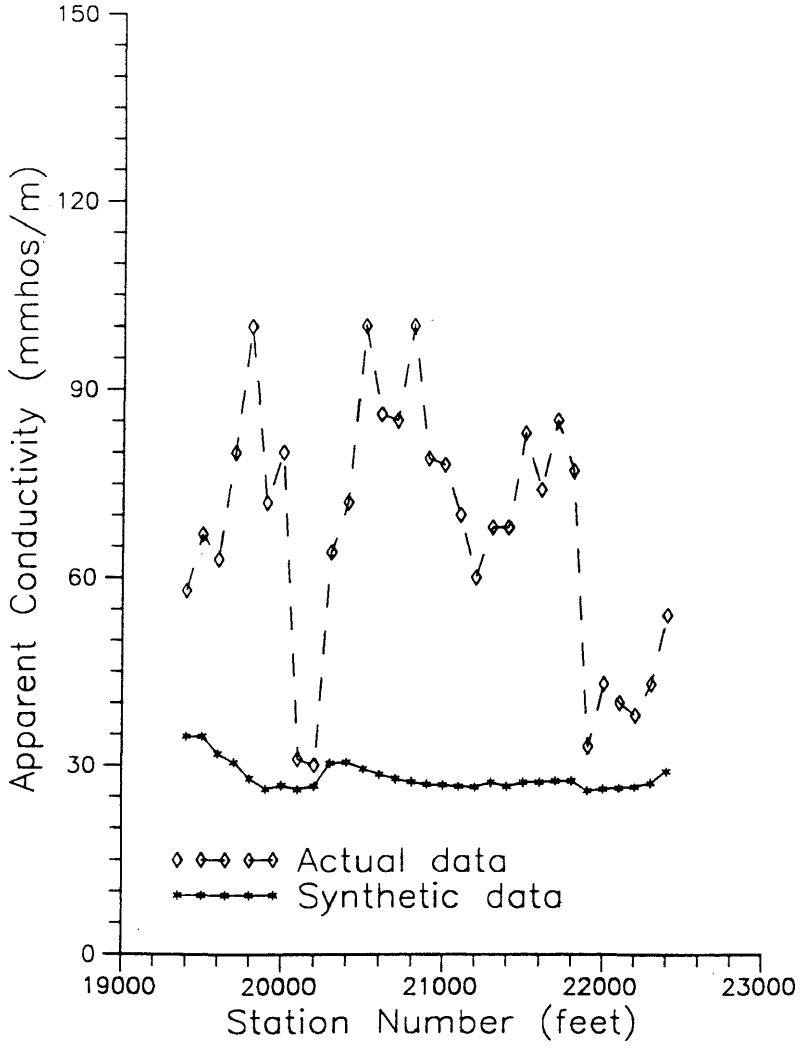

Figure B-22 Actual and Synthetic Apparent Conductivity Data for 3.67-Meter Coil Spacing for Line MWP-2

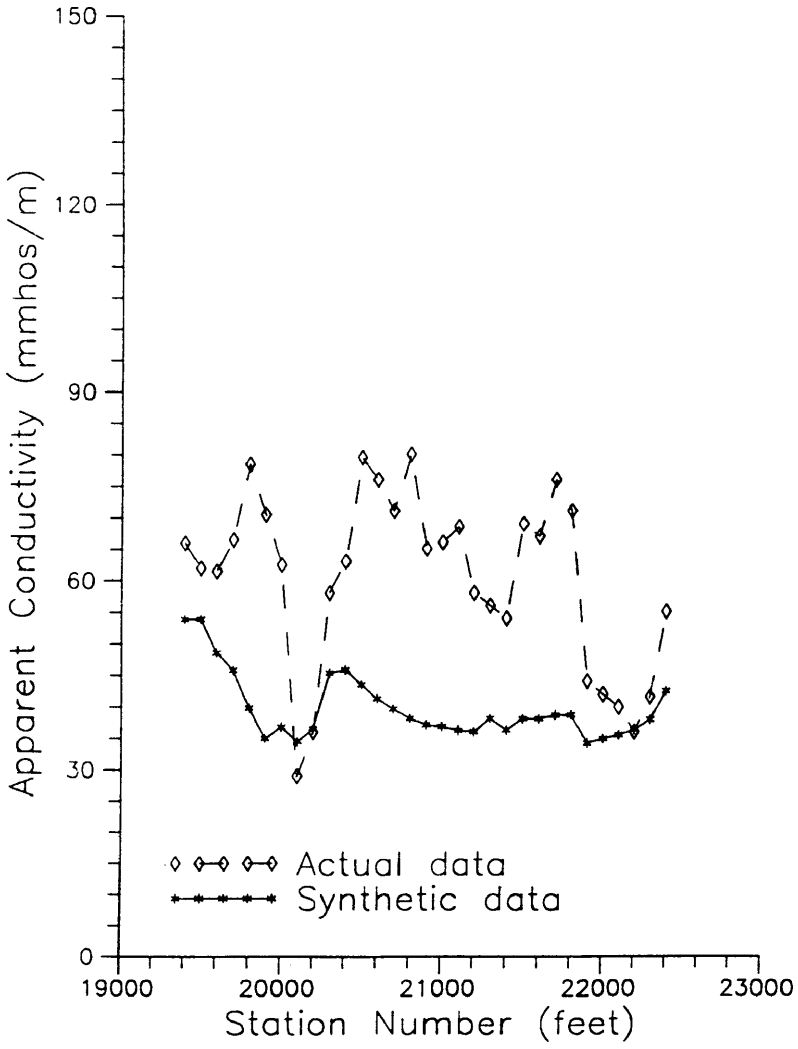

Figure B-23 Actual and Synthetic Apparent Conductivity Data for 10-Meter Coil Spacing for Line MWP-2

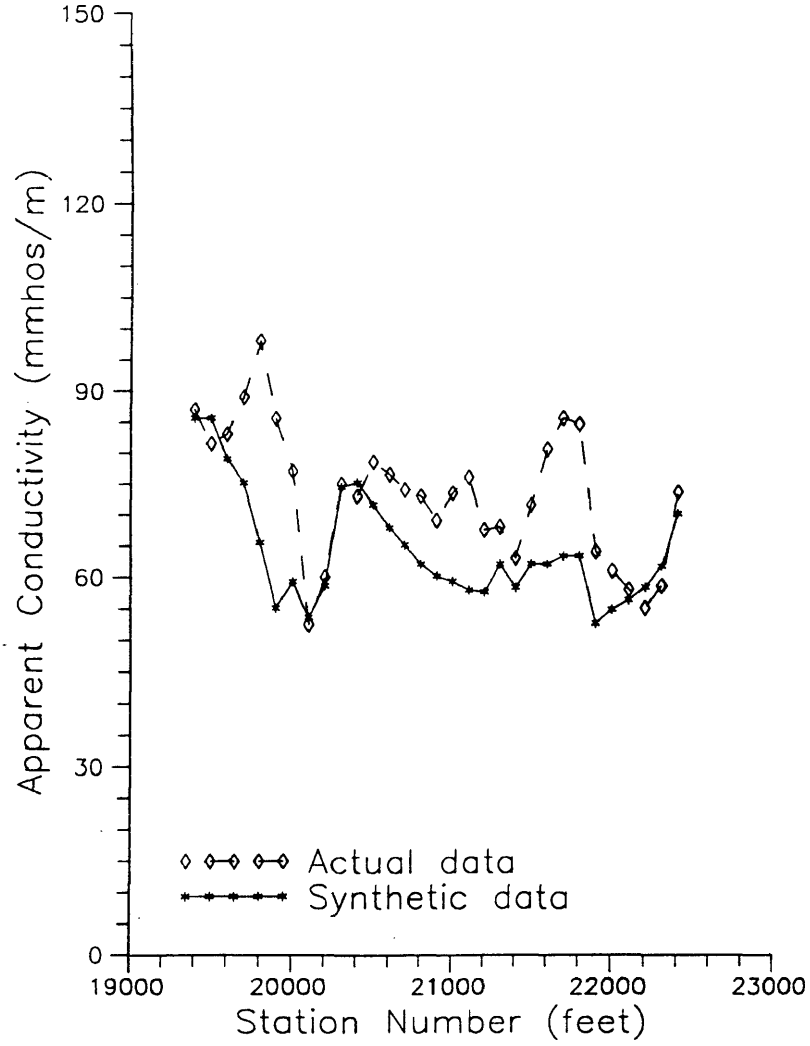

Figure B-24 Actual and Synthetic Apparent Conductivity Data for 20-Meter Coil Spacing for Line MWP-2

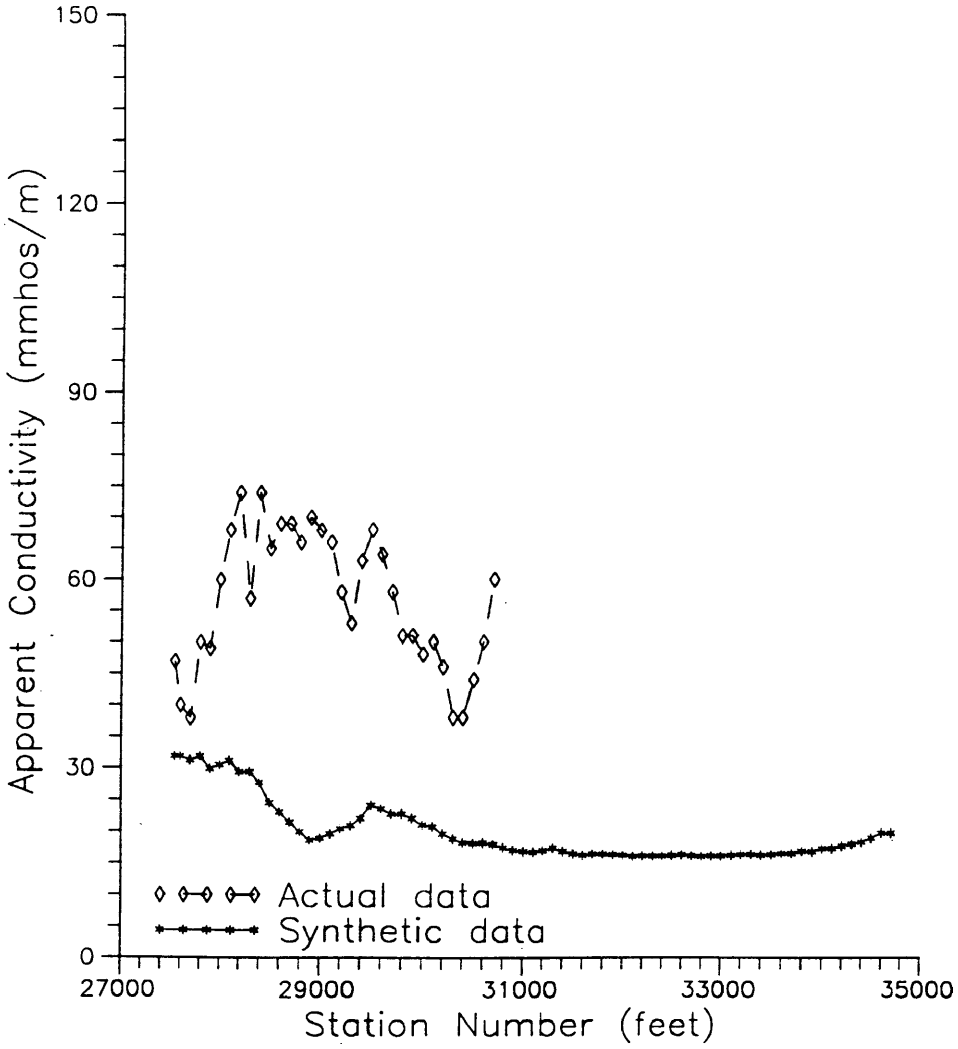

Figure B-25 Actual and Synthetic Apparent Conductivity Data for 3.67-Meter Coil Spacing for Line MWP-3

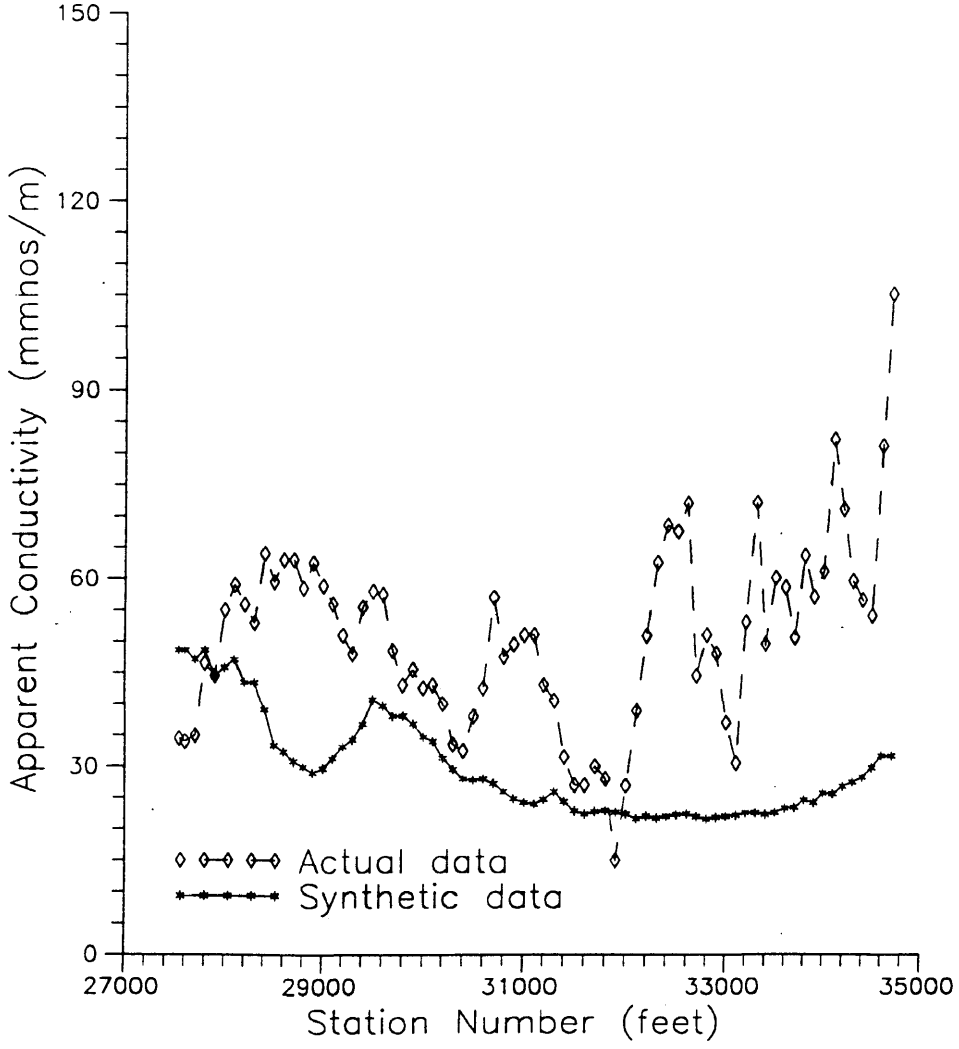

Figure B-26 Actual and Synthetic Apparent Conductivity Data for 10-Meter Coil Spacing for Line MWP-3

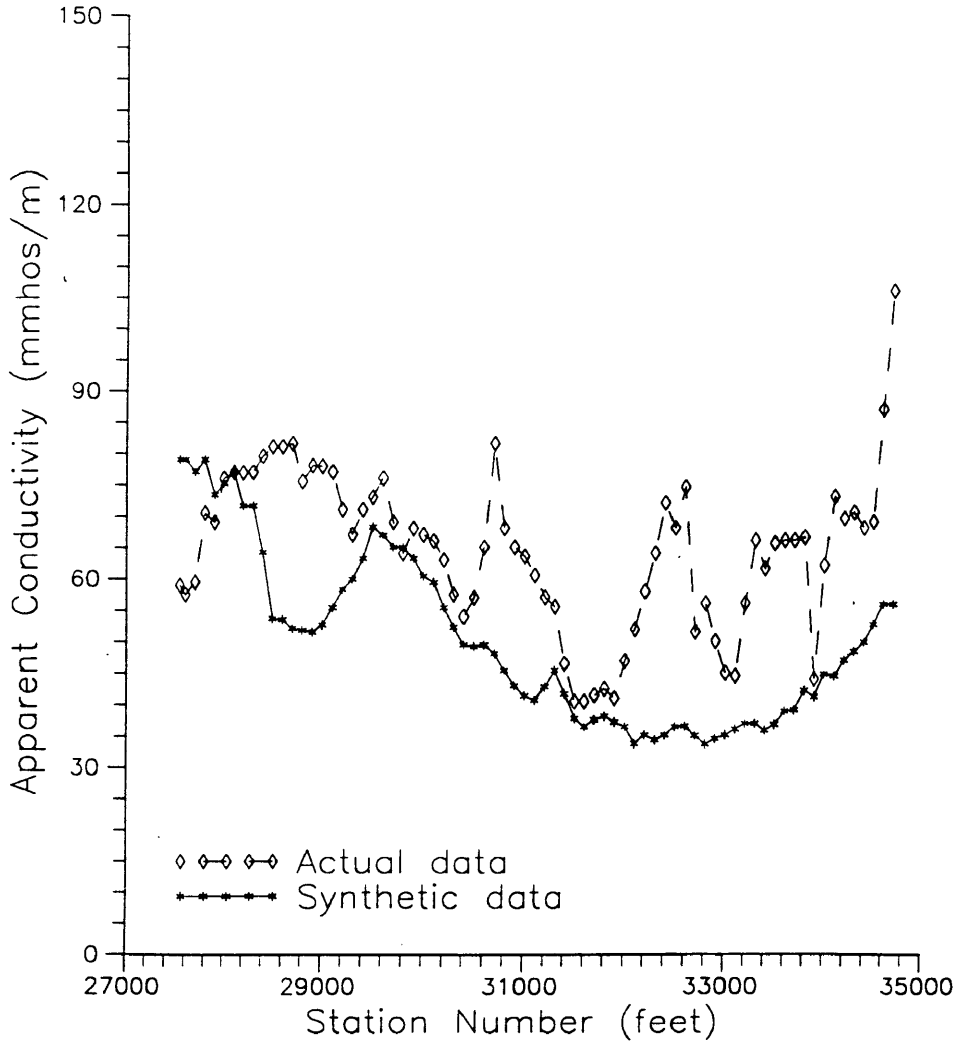

Figure B-27 Actual and Synthetic Apparent Conductivity Data for 20-Meter Coil Spacing for Line MWP-3

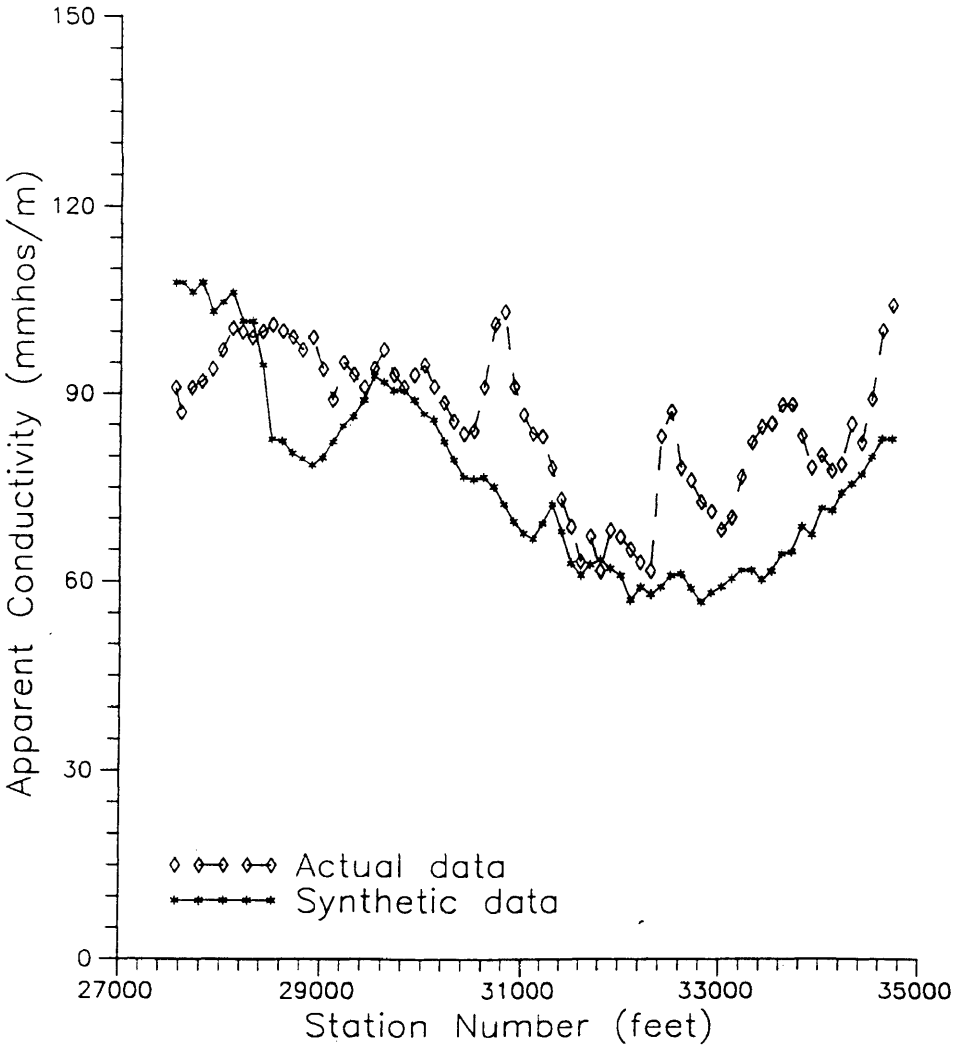

Figure B-28 Actual and Synthetic Apparent Conductivity Data for 40-Meter Coil Spacing for Line MWP-3

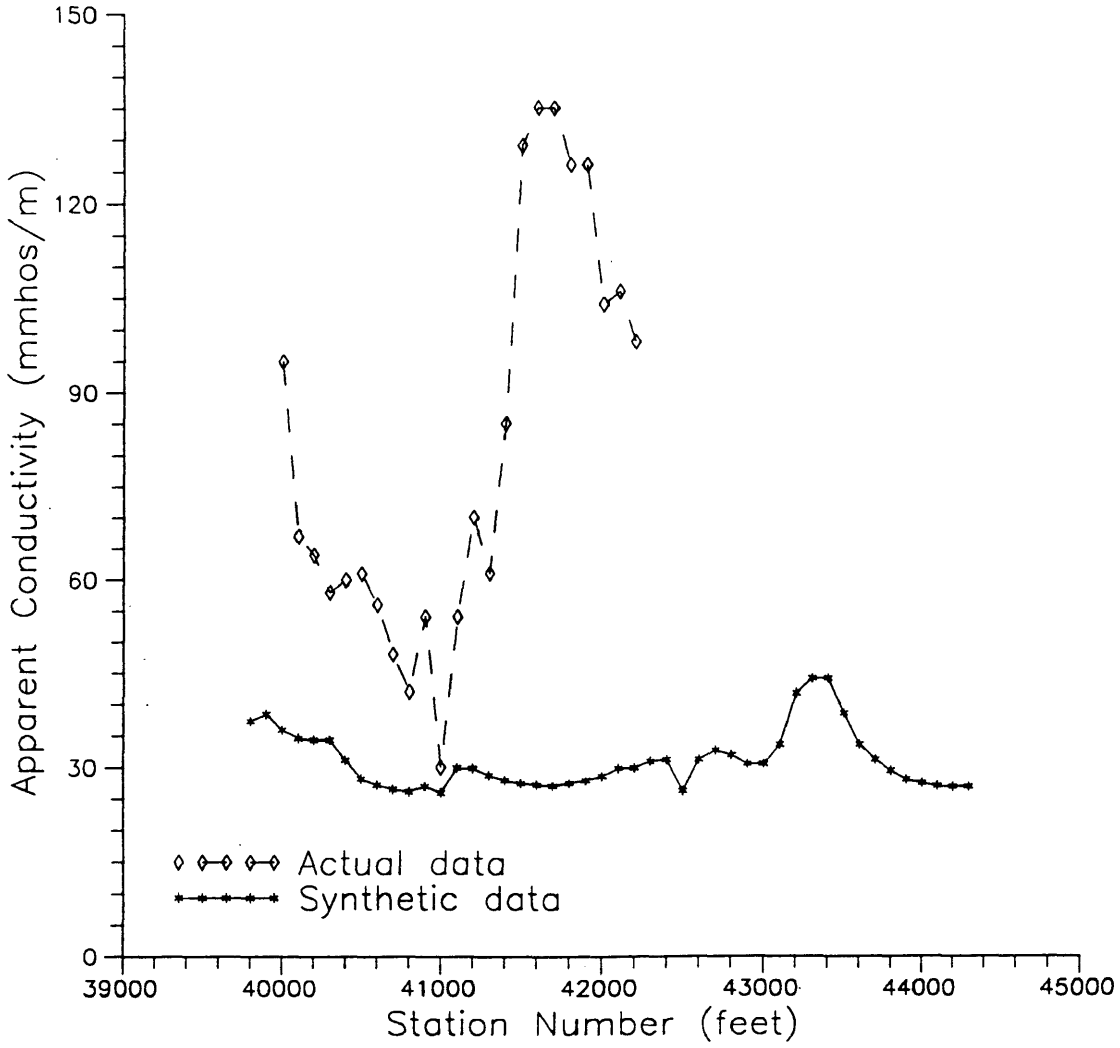

Figure B-29 Actual and Synthetic Apparent Conductivity Data for 3.67-Meter Coil Spacing for Line MWP-4

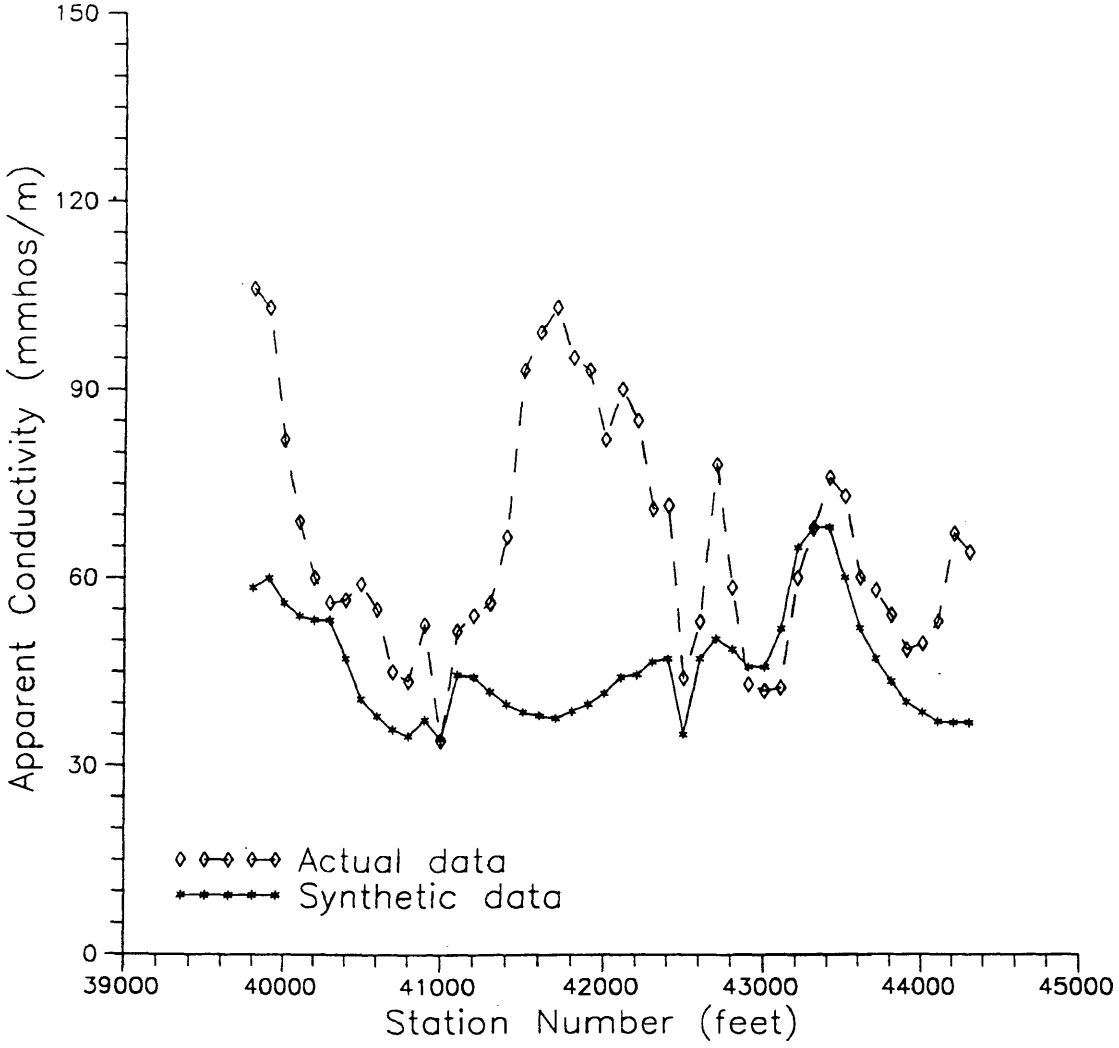

Figure B-30 Actual and Synthetic Apparent Conductivity Data for 10-Meter Coil Spacing for Line MWP-4

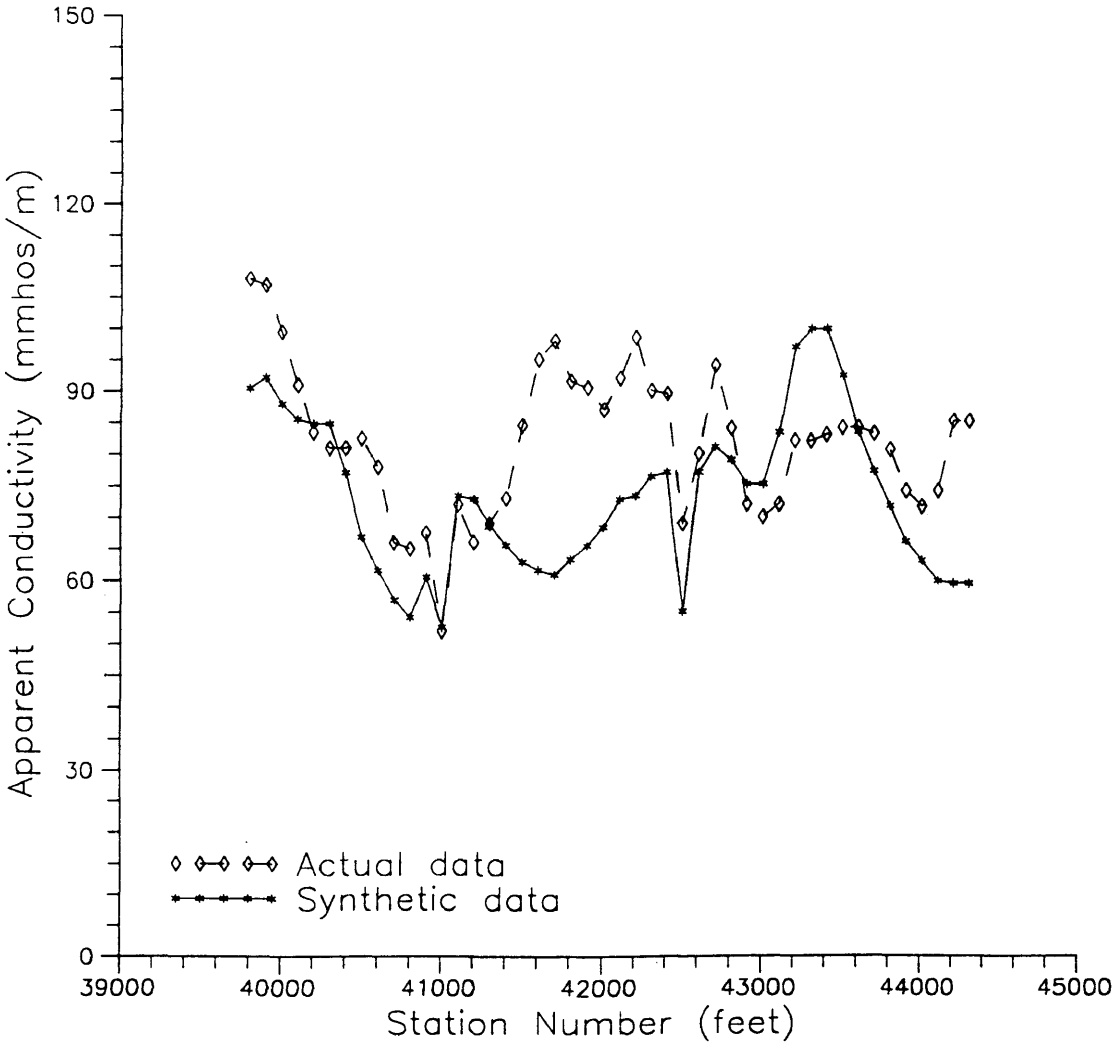

Figure B-31 Actual and Synthetic Apparent Conductivity Data for 20-Meter Coil Spacing for Line MWP-4

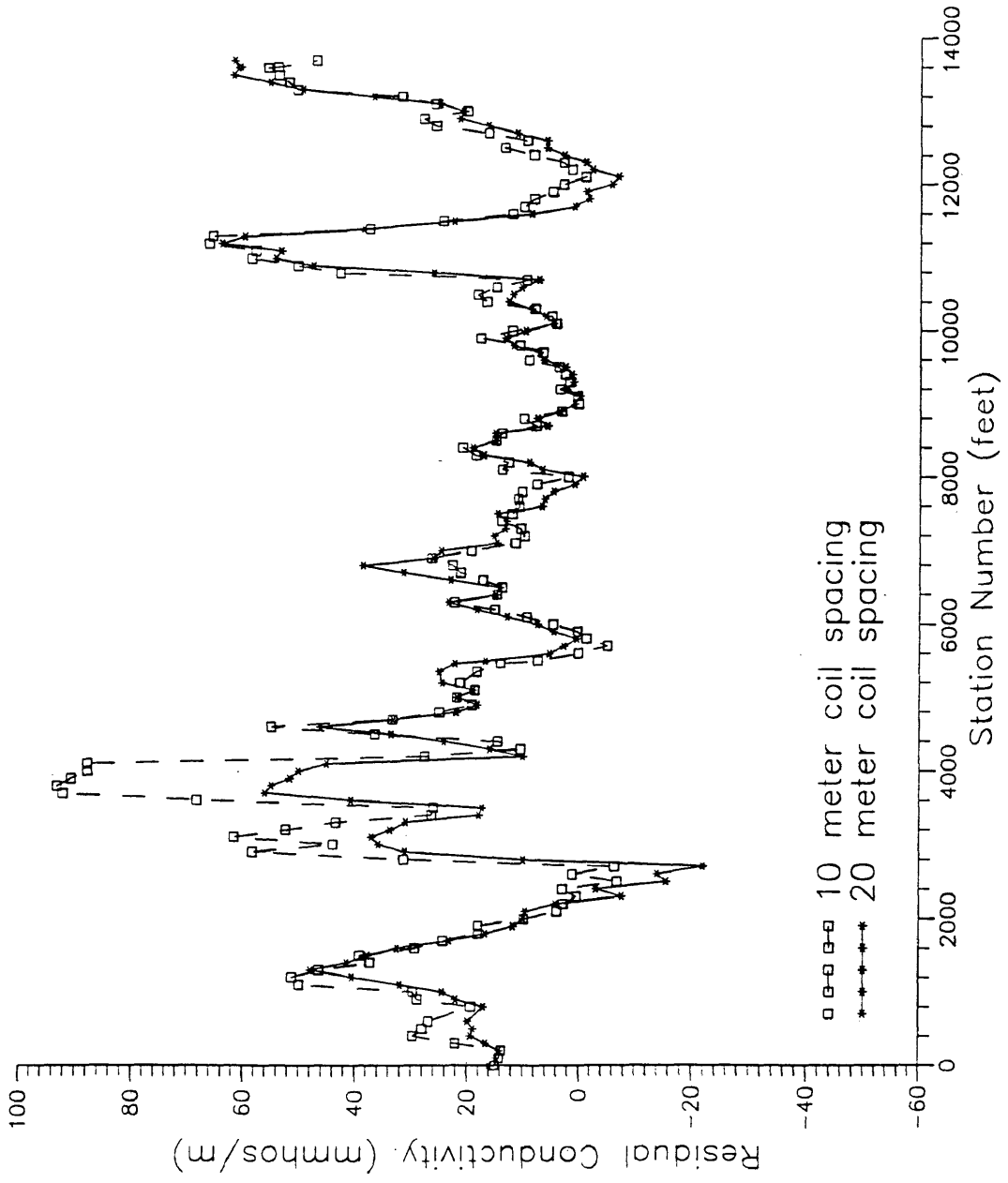

Figure B-32 Residual Apparent Conductivity Data for Line HL-1

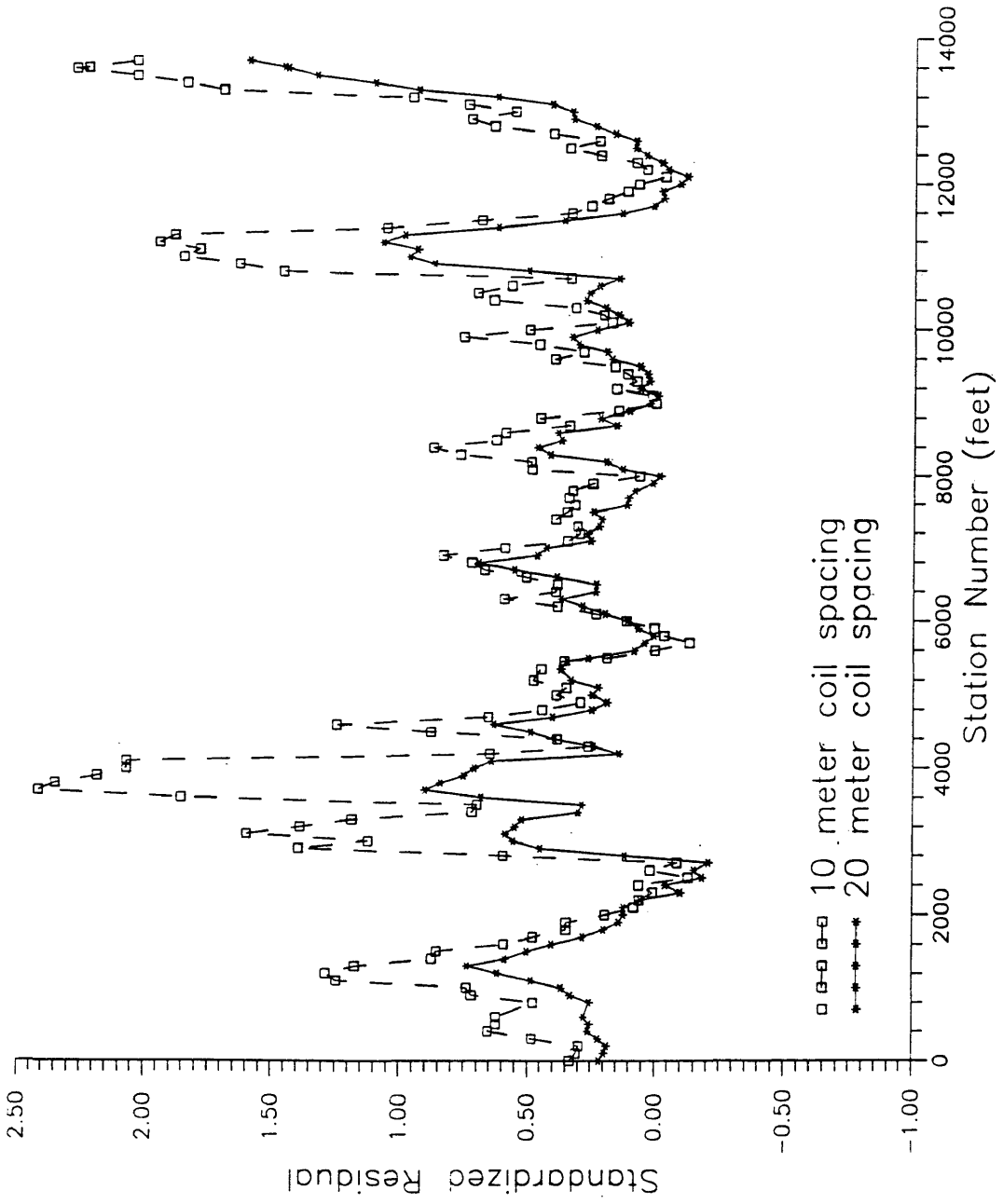

Figure B-33 Standardized Residuals for Line HL-1

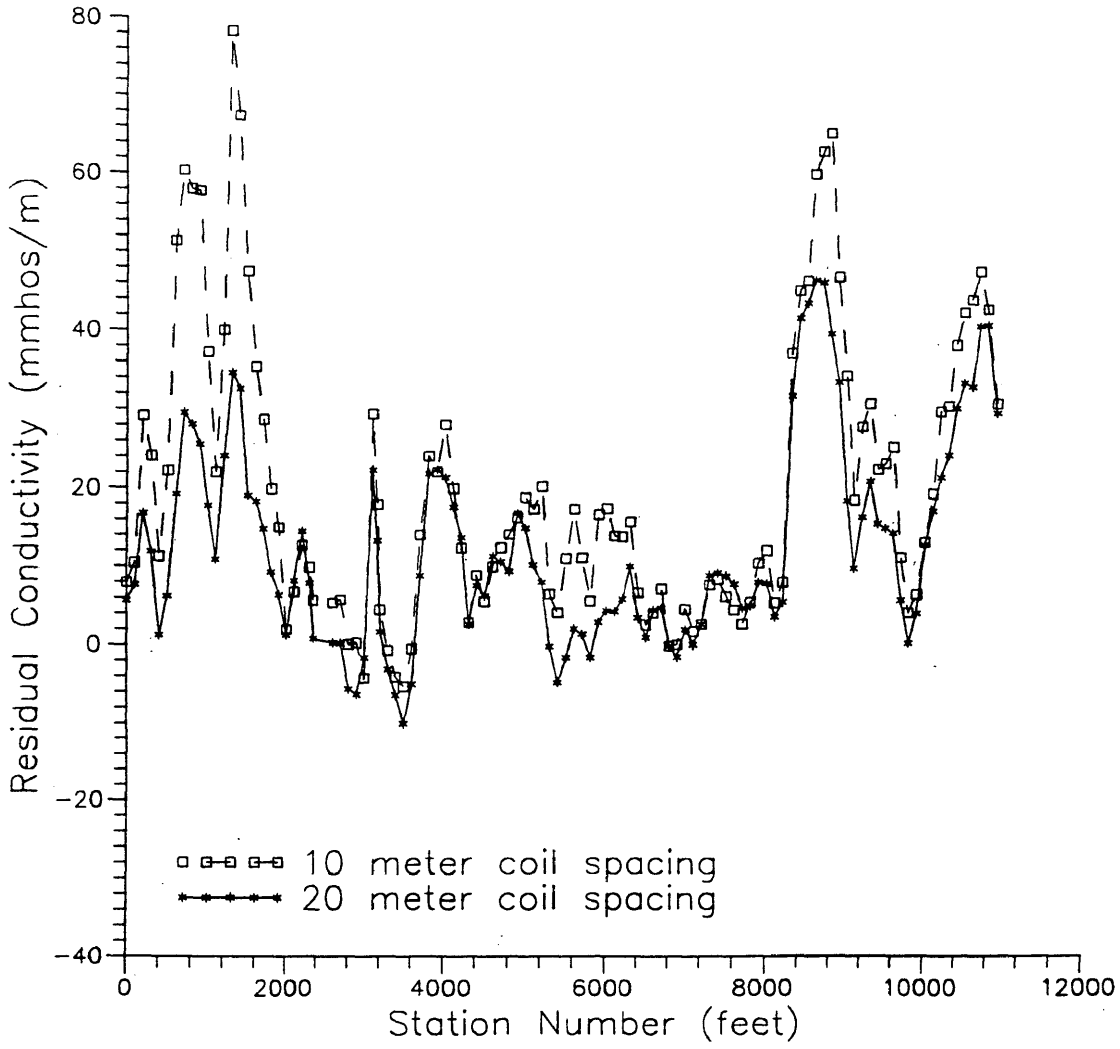

Figure B-34 Residual Apparent Conductivity Data for Line HL-3

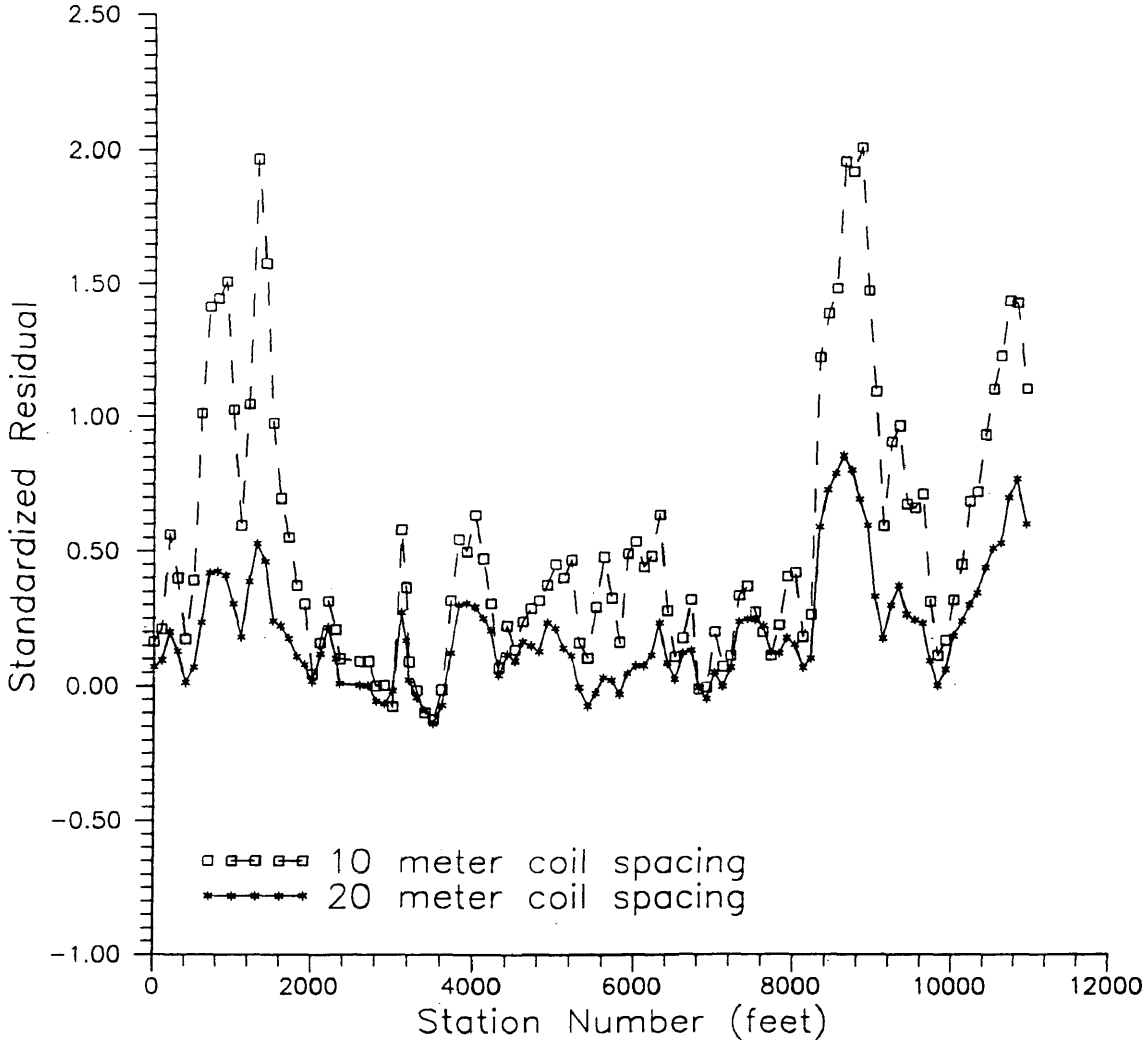

Figure B-35 Standardized Residuals for Line HL-3

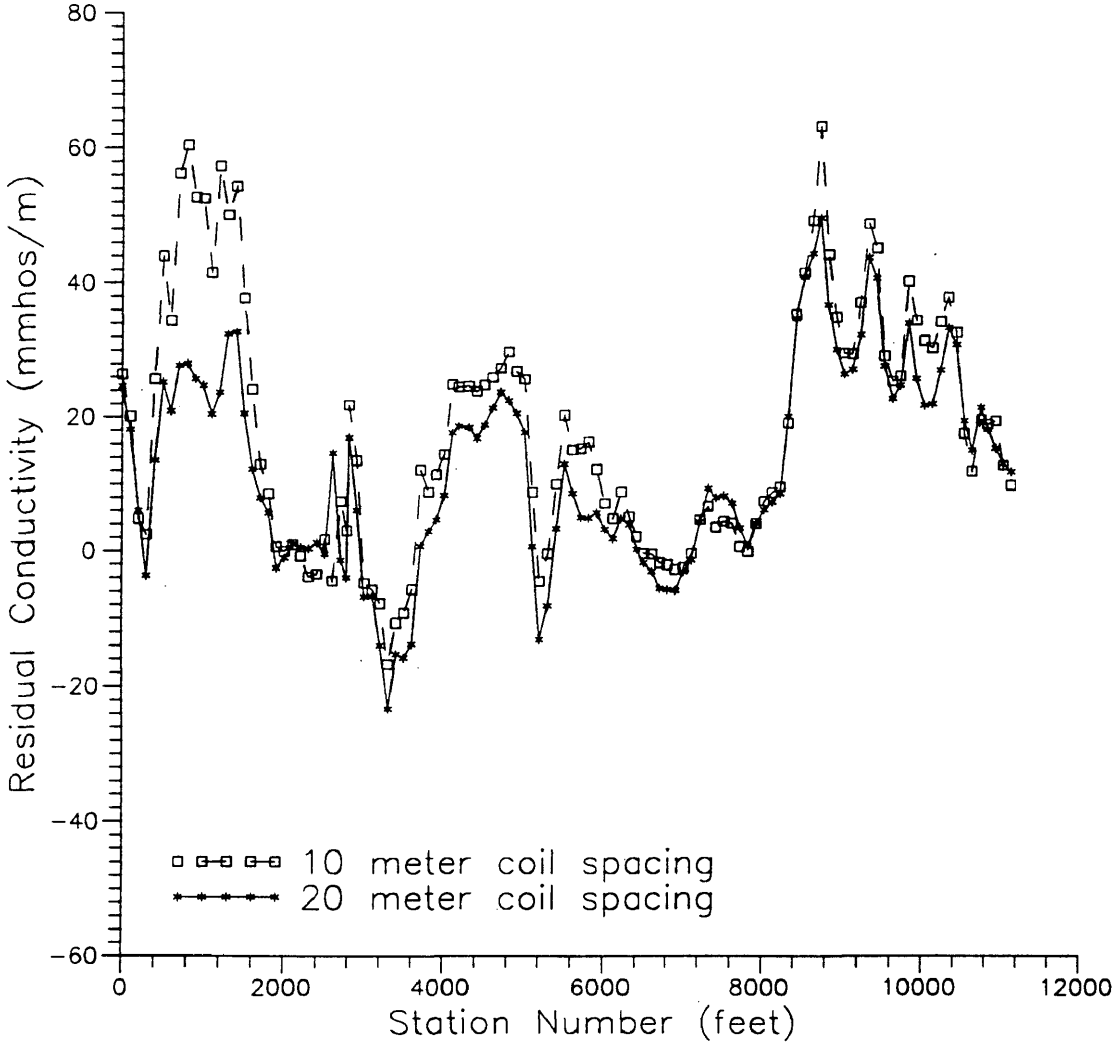

Figure B-36 Residual Apparent Conductivity Data for Line HL-4

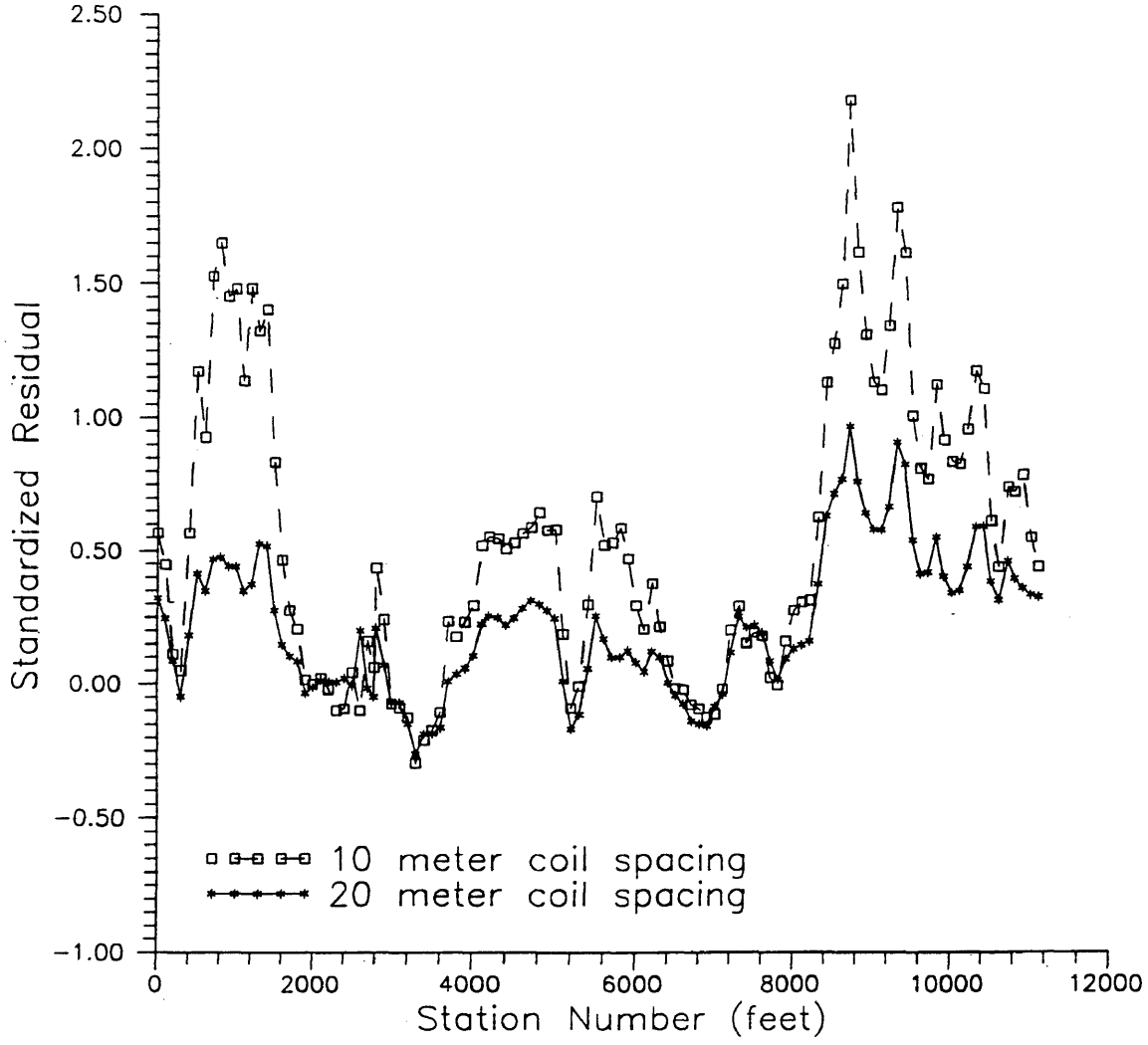

Figure B-37 Standardized Residuals for Line HL-4

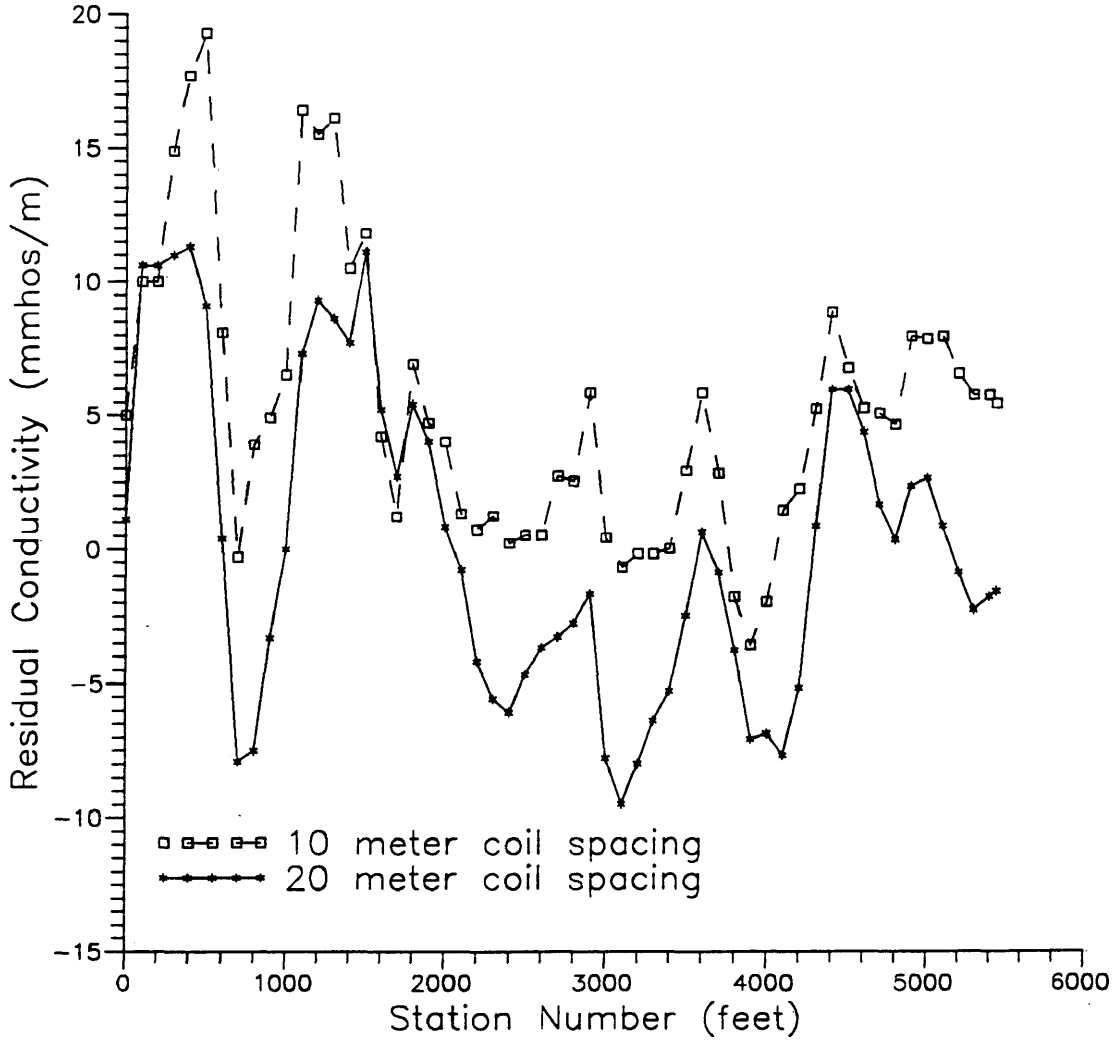

Figure B-38 Residual Apparent Conductivity Data for Line HL-5

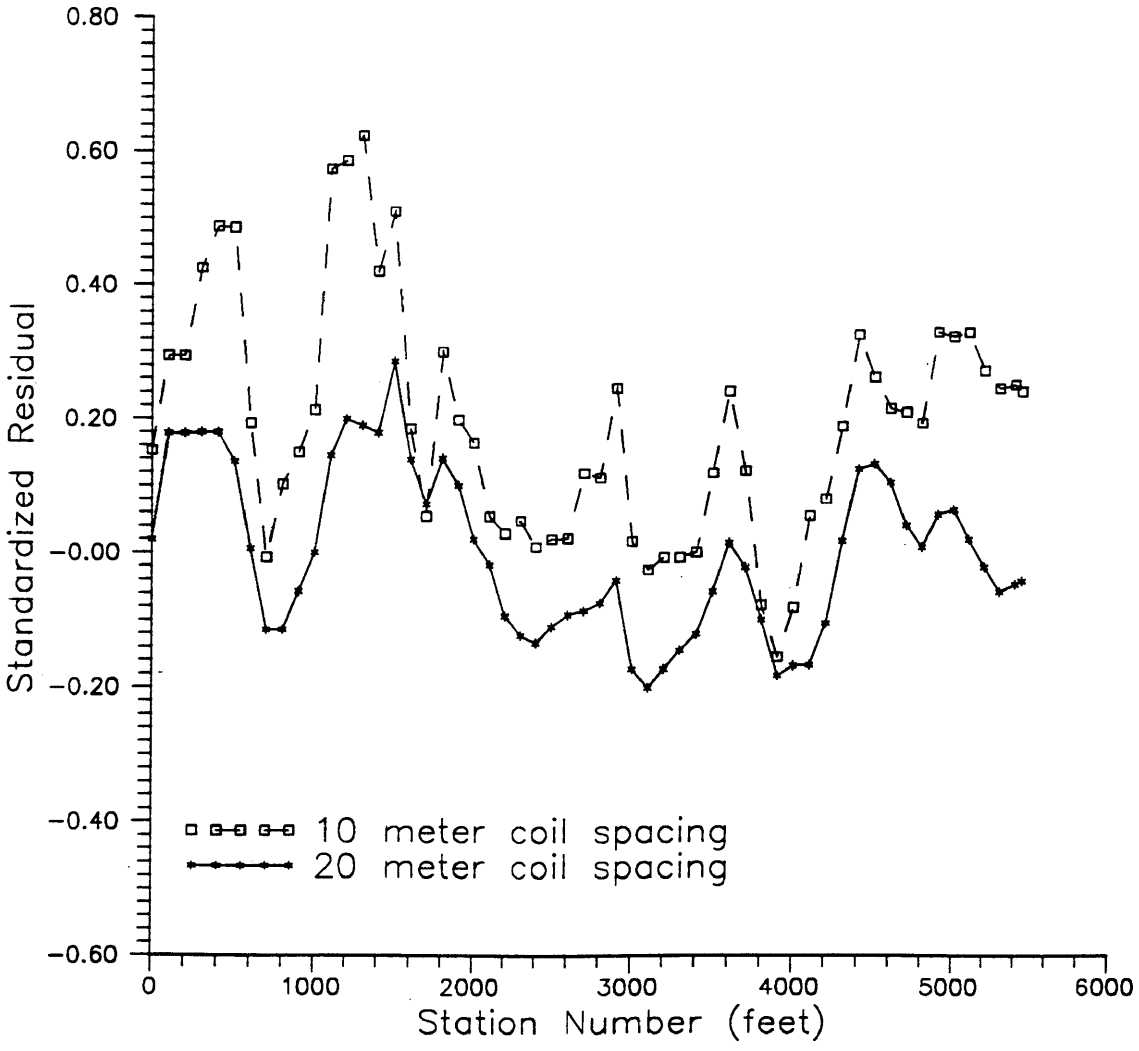

Figure B-39 Standardized Residuals for Line HL-5

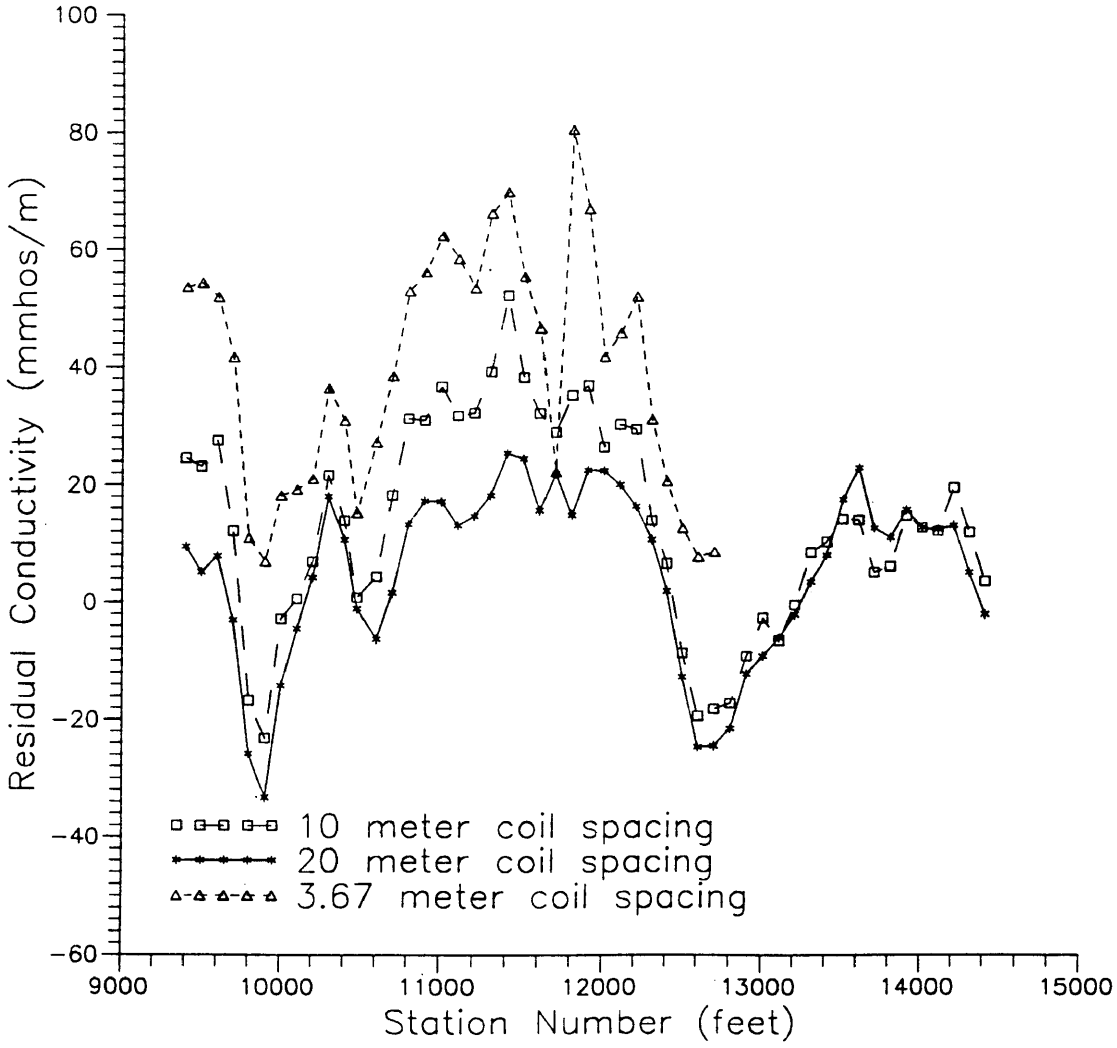

Figure B-40 Residual Apparent Conductivity Data for Line MWP-1

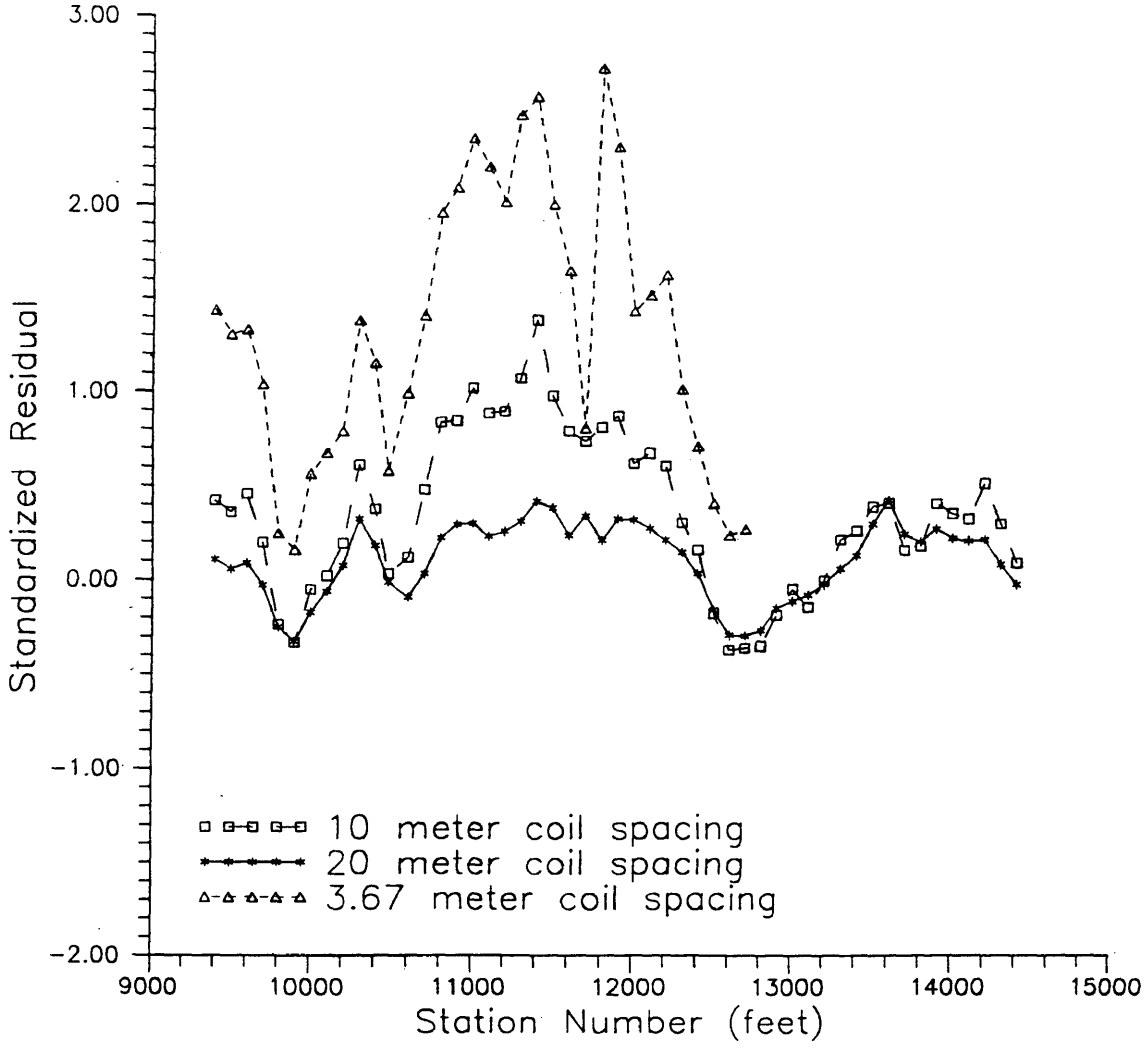

Figure B-41 Standardized Residuals for Line MWP-1

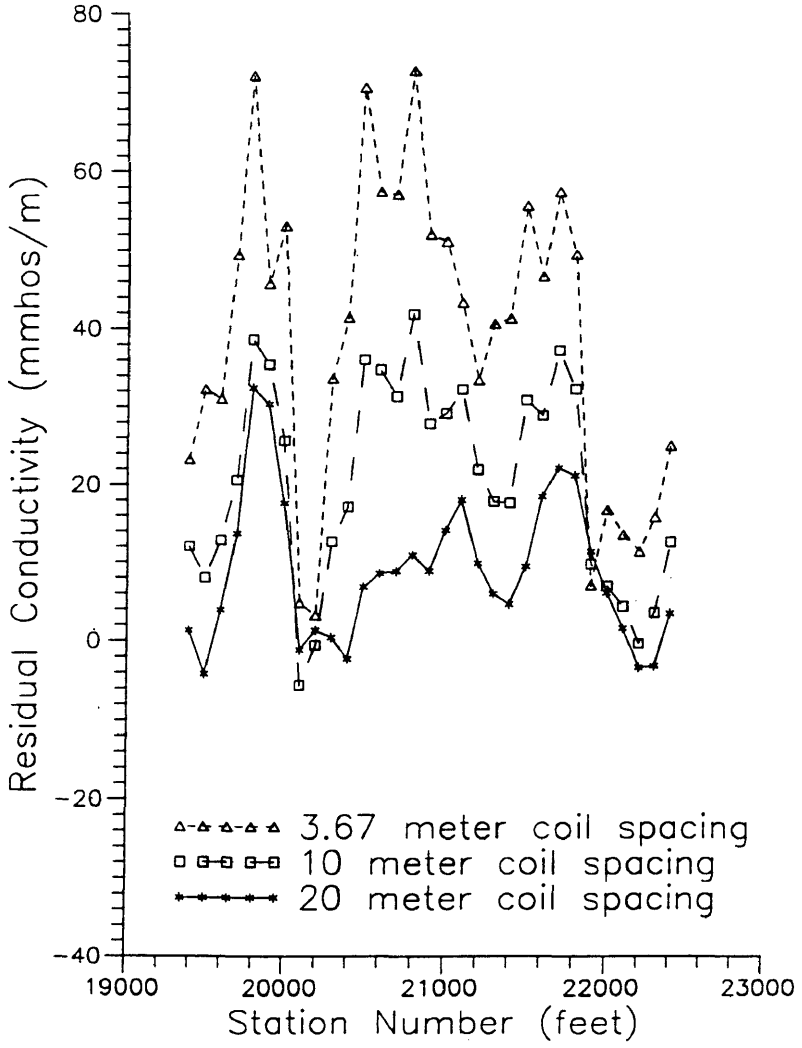

Figure B-42 Residual Apparent Conductivity Data for Line MWP-2

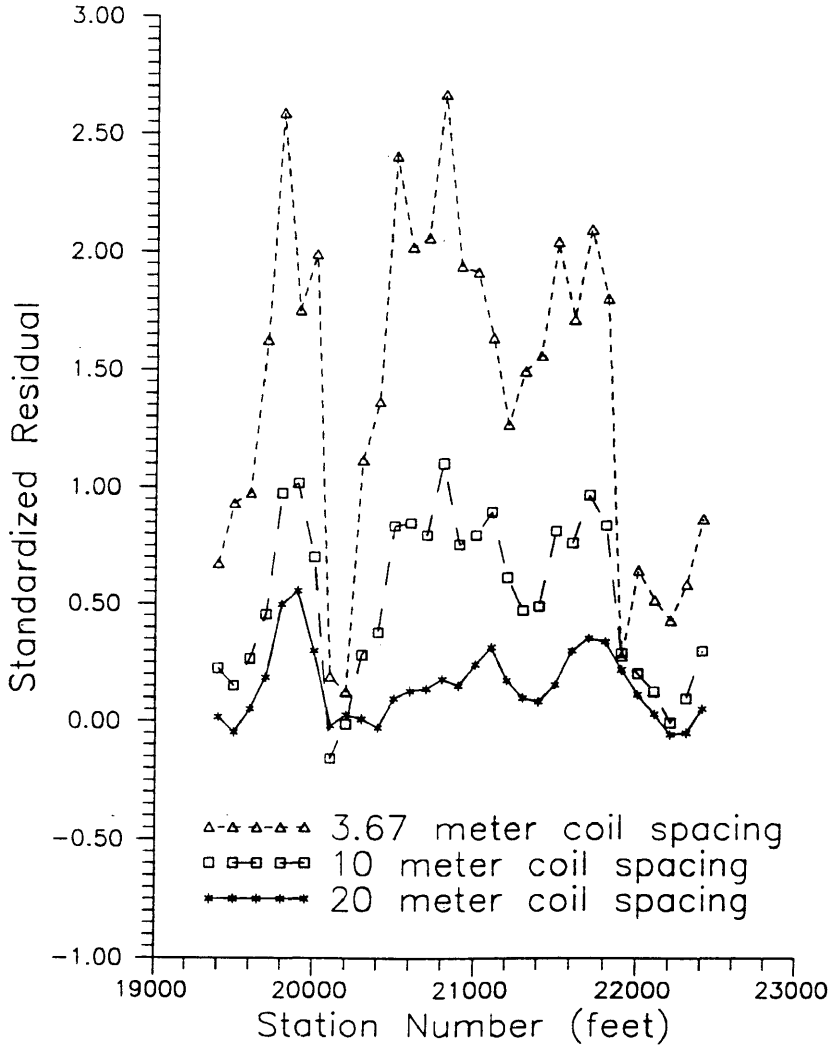

Figure B-43 Standardized Residuals for Line MWP-2

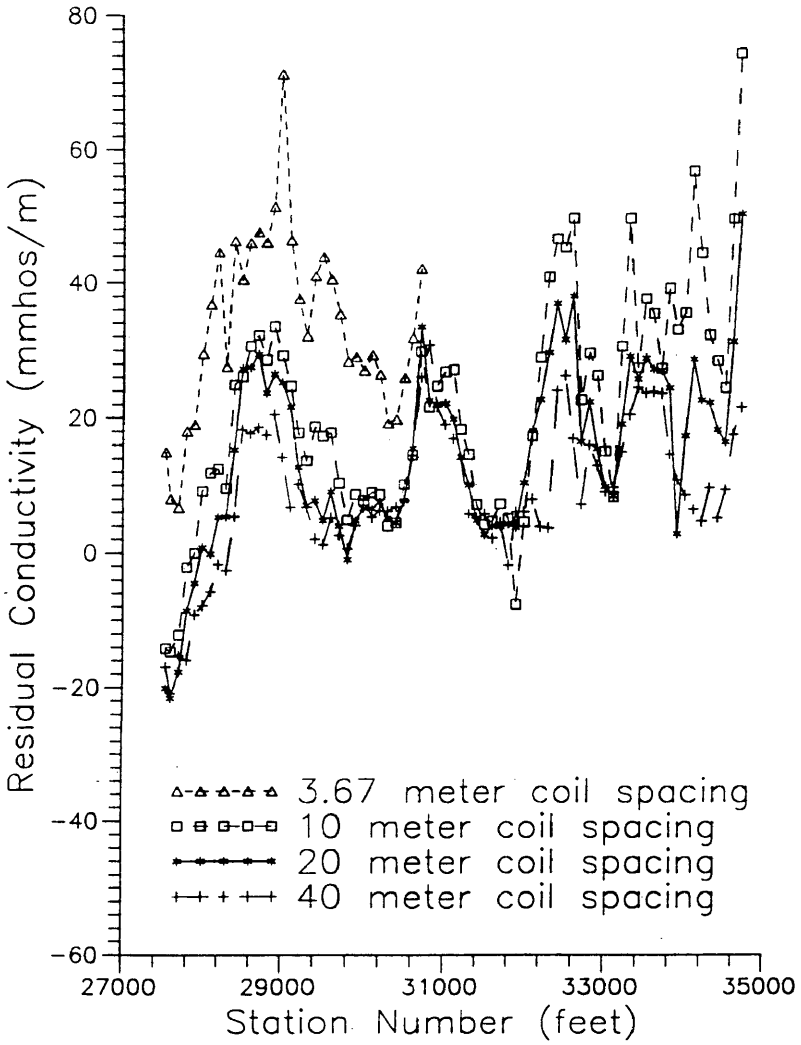

Figure B-44 Residual Apparent Conductivity Data for Line MWP-3

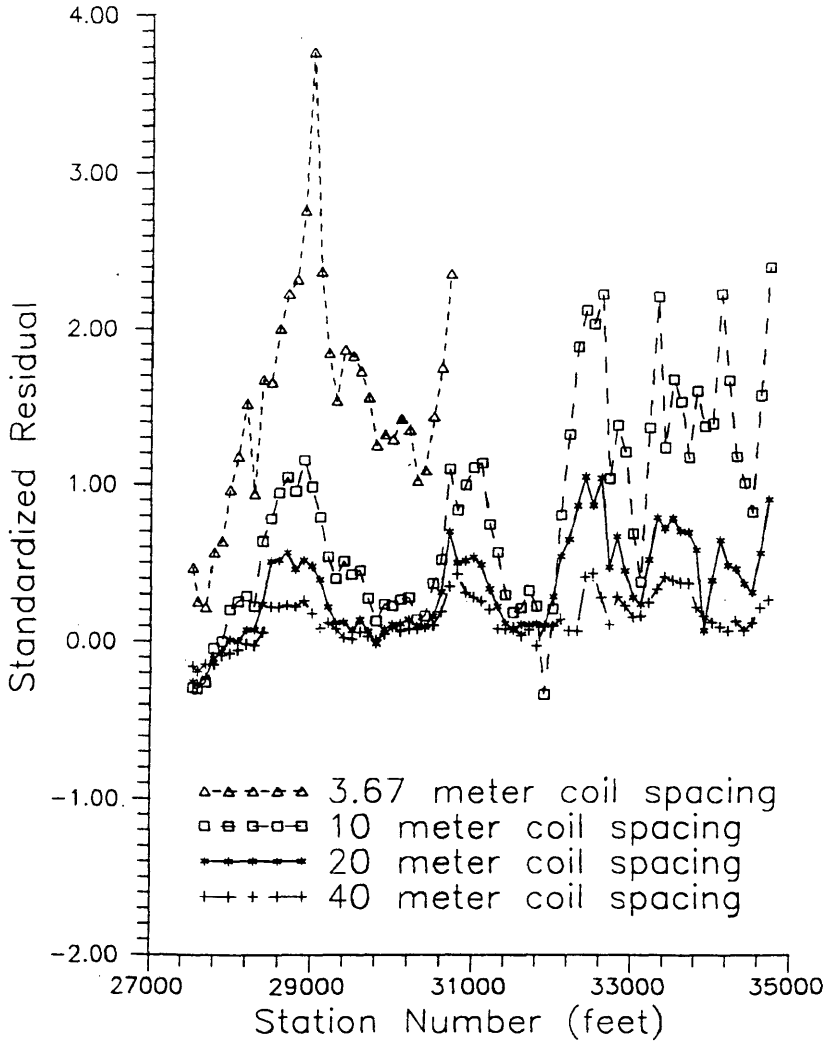

Figure B-45 Standardized Residuals for Line MWP-3

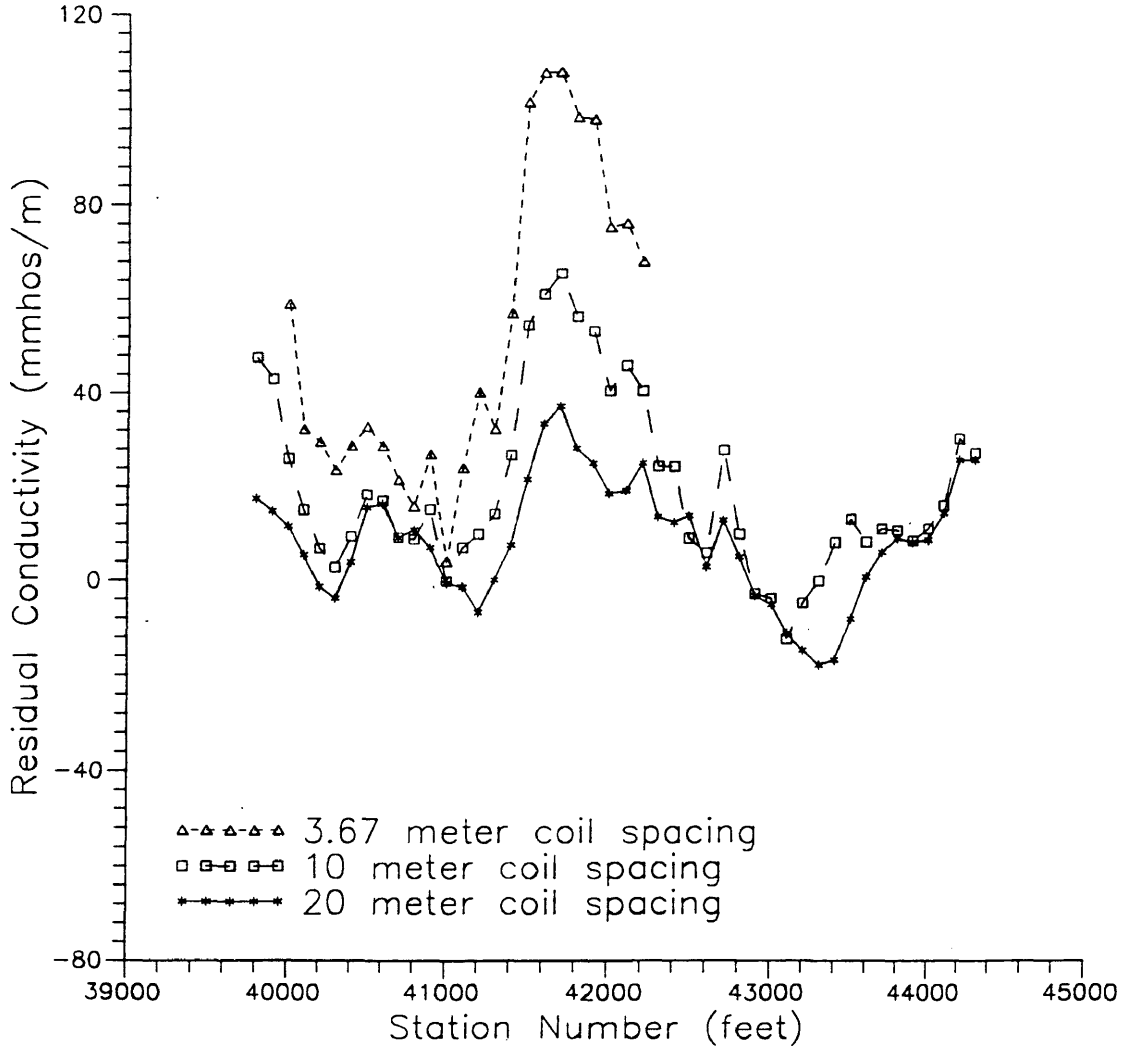

Figure B-46 Residual Apparent Conductivity Data for Line MWP-4

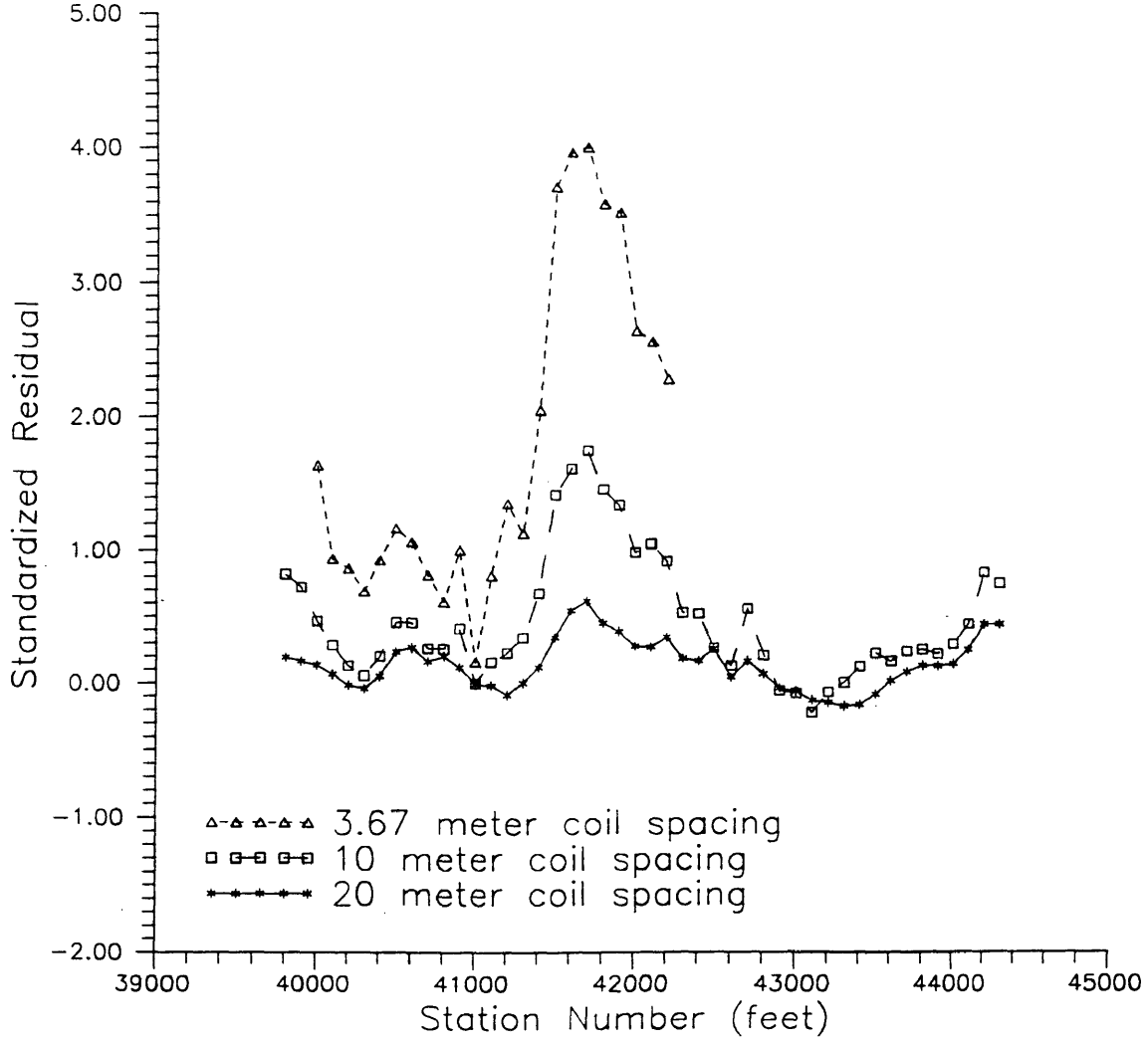

Figure B-47 Standardized Residuals for Line MWP-4

ER-4502

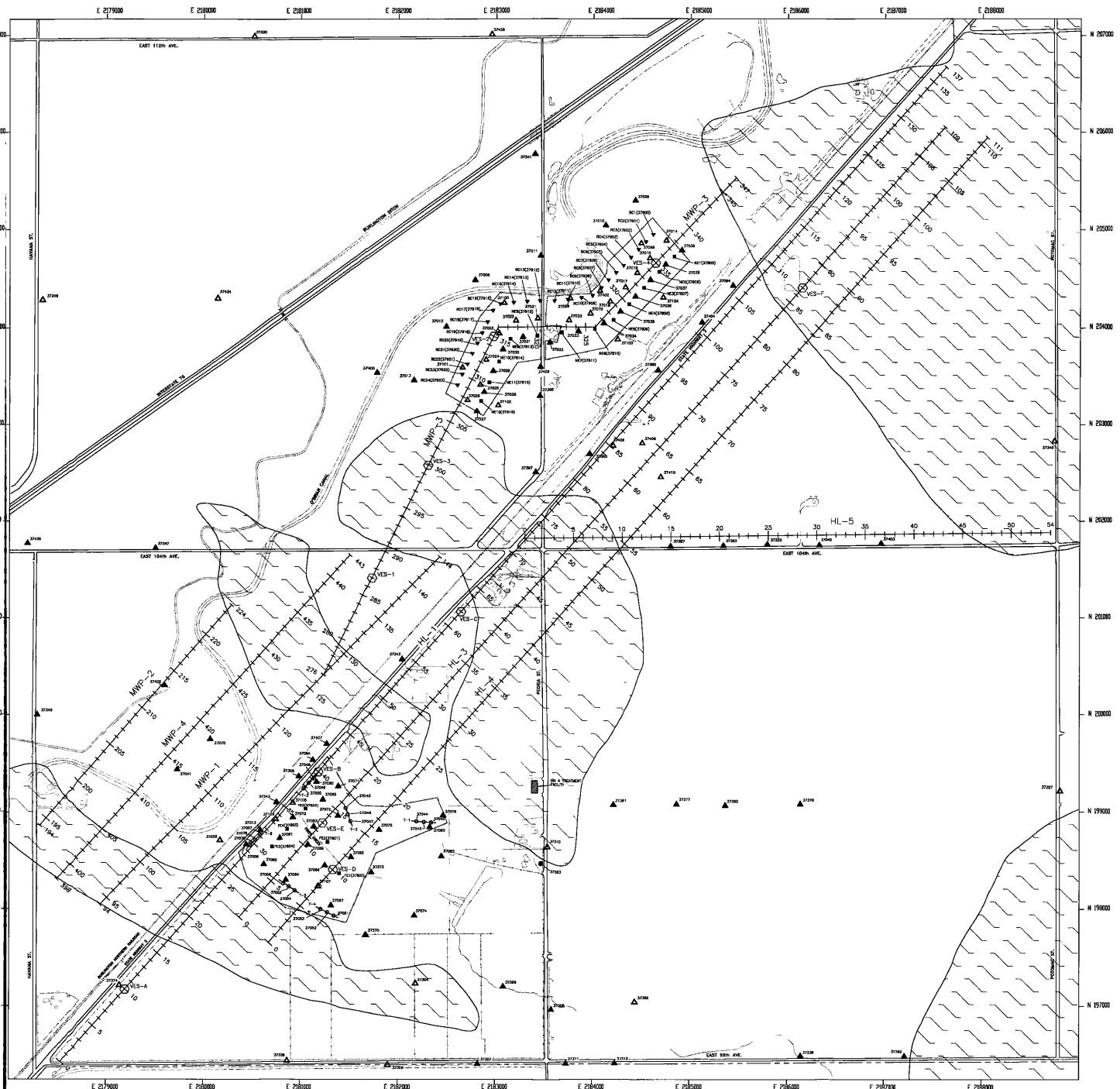

0 400 800

Scale in Feet

EXPLANATION

- ALLUVIAL MONITORING WELL MEASURED FOR WATER LEVEL AND SAMPLED FOR WATER QUALITY
- ALLUVIAL MONITORING WELL MEASURED FOR WATER LEVEL ONLY
- UNCONFINED DENVER FORMATION MONITORING WELL MEASURED FOR WATER LEVEL AND SAMPLED FOR WATER QUALITY
- RECHARGE TRENCH PIEZOMETER
- IRA A EXTRACTION WELL
- IRA A RECHARGE WELL
- IRA A RECHARGE TRENCH
- APPROXIMATE AREA OF UNSATURATED ALLUVIUM NOVEMBER 1992
- IRA A FENCE LINE
- ROCKY MOUNTAIN ARSENAL BOUNDARY
- VES-1 VERTICAL ELECTRICAL SOUNDING LOCATION
- MWP-1 ELECTROMAGNETIC PROFILE LOCATION AND STATIONS

NOTE: PROFILES MWP-1 THROUGH MWP-4 AND VES-1 THROUGH VES-4 WERE SURVEYED IN 1992; PROFILES HL-1 THROUGH HL-5 AND VES-A THROUGH VES-F WERE SURVEYED IN 1989 (PROFILE HL-2 WAS NOT SURVEYED). THE 1989 DATA ARE DISCUSSED IN THE IRA A PILOT TEST REPORT (H.L.A. JUNE 1990–DRAFT FINAL)

ARTHUR LAKES LIBRARY
COLORADO SCHOOL OF MINES
GOLDEN, CO 80401

Source: Harding Lawson Associates; used by permission of Program Manager for Rocky Mountain Arsenal

Plate 1

Locations of Electromagnetic Profiles and Vertical Electrical Soundings

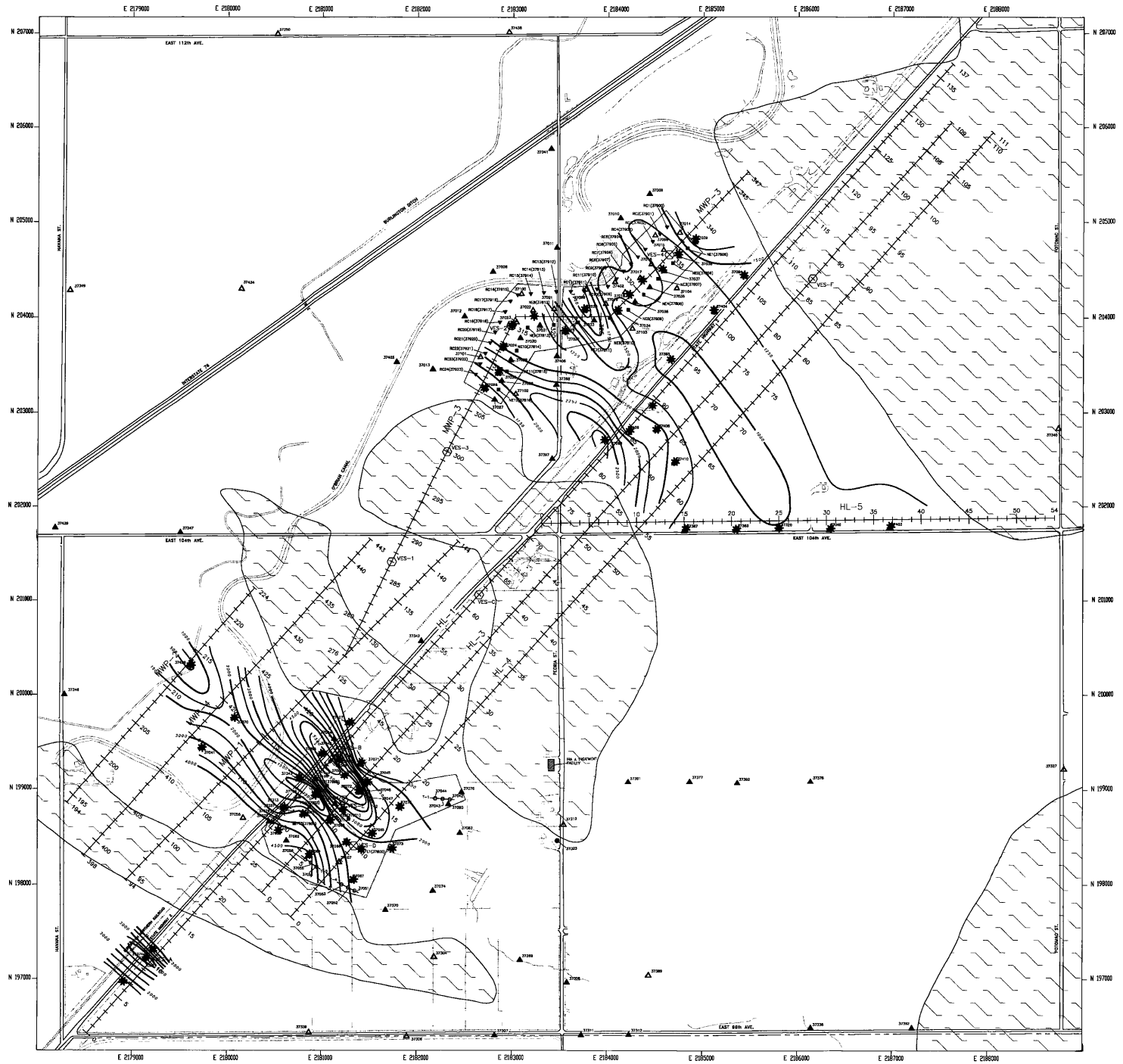

ER-4502

EXPLANATION

- ALLUVIAL MONITORING WELL MEASURED FOR WATER LEVEL AND SAMPLED FOR WATER QUALITY
- ALLUVIAL MONITORING WELL MEASURED FOR WATER LEVEL ONLY
- UNCONFINED DENVER FORMATION MONITORING WELL MEASURED FOR WATER LEVEL AND SAMPLED FOR WATER QUALITY
- RECHARGE TRENCH PIEZOMETER
- IRA A EXTRACTION WELL
- IRA A RECHARGE WELL
- IRA A RECHARGE TRENCH
- APPROXIMATE AREA OF UNSATURATED ALLUVIUM NOVEMBER 1992
- IRA A FENCE LINE
- ROCKY MOUNTAIN ARSENAL BOUNDARY
- VERTICAL ELECTRICAL SOUNDING LOCATION
- ELECTROMAGNETIC PROFILE LOCATION AND STATIONS

NOTE: PROFILES MWP-1 THROUGH MWP-4 AND VES-1 THROUGH VES-4 WERE SURVEYED IN 1992; PROFILES HL-1 THROUGH HL-5 AND VES-A THROUGH VES-F WERE SURVEYED IN 1989 (PROFILE HL-2 WAS NOT SURVEYED) THE 1989 DATA ARE DISCUSSED IN THE IRA A PILOT TEST REPORT (HLA JUNE 1990-DRAFT FINAL)

- INTERPRETED TOTAL DISSOLVED SOLIDS CONCENTRATION CONTOUR LINE (parts per million)

Contour Interval:
250 ppm in northern paleochannel,
500 ppm in First Creek paleochannel

- DATA POINT

Source: Harding Lawson Associates;
used by permission of
Program Manager for
Rocky Mountain Arsenal

Plate 2

Concentration of Total Dissolved Solids in Ground Water

ER-4502

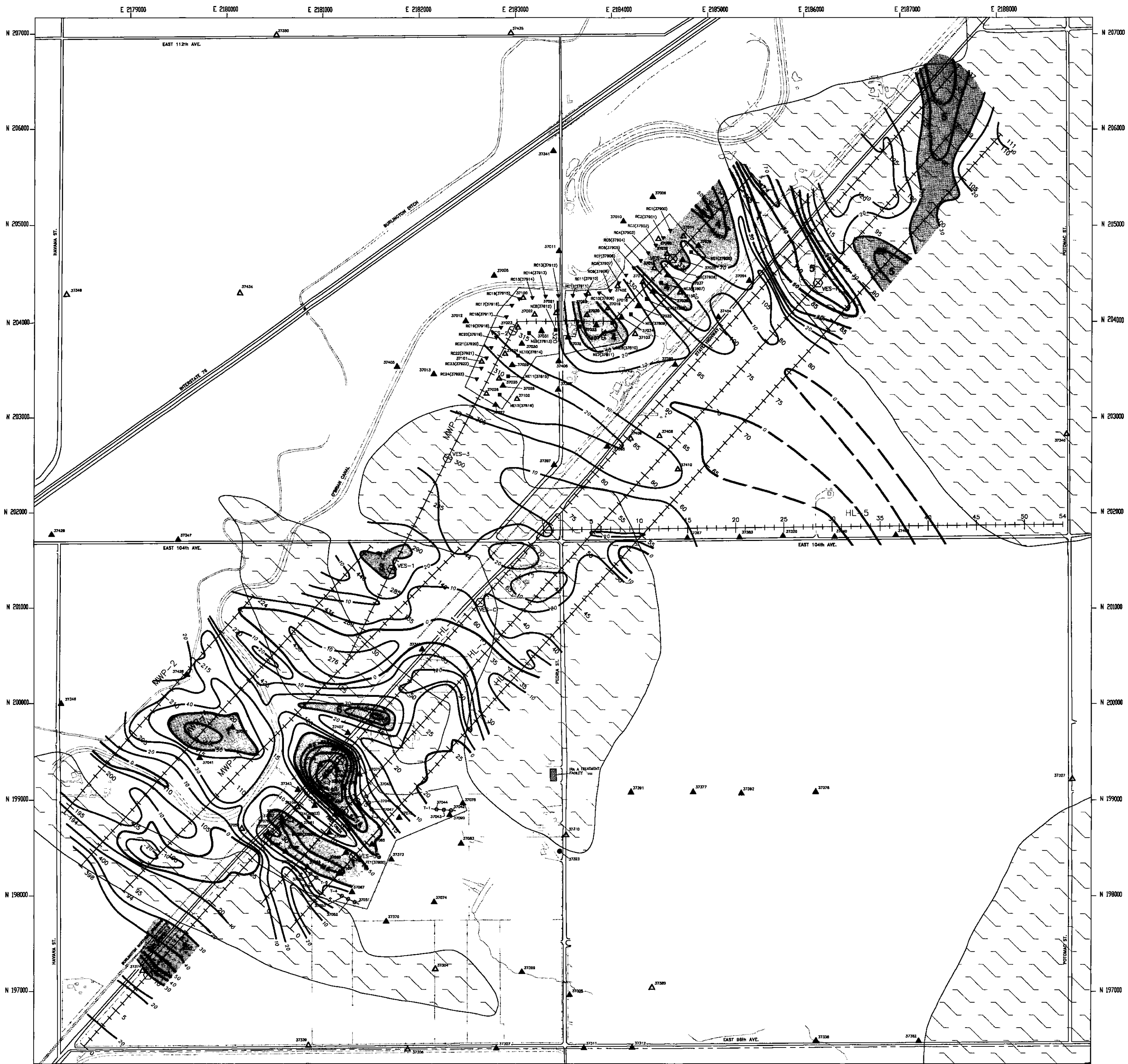

N

0 400 800
Scale in Feet

EXPLANATION

- 37056 — ALLUVIAL MONITORING WELL MEASURED FOR WATER LEVEL AND SAMPLED FOR WATER QUALITY
- 37410 — ALLUVIAL MONITORING WELL MEASURED FOR WATER LEVEL ONLY
- 37380 — UNCONFINED DENVER FORMATION MONITORING WELL MEASURED FOR WATER LEVEL AND SAMPLED FOR WATER QUALITY
- 37044 — RECHARGE TRENCH PIEZOMETER
- FE-3(37800) — IRA A EXTRACTION WELL
- RC-1(37900) — IRA A RECHARGE WELL
- T-1 — IRA A RECHARGE TRENCH
- APPROXIMATE AREA OF UNSATURATED ALLUVIUM NOVEMBER 1992
- IRA A FENCE LINE
- ROCKY MOUNTAIN ARSENAL BOUNDARY
- VES-1 — VERTICAL ELECTRICAL SOUNDING LOCATION
- MWP-1 (0–4) — ELECTROMAGNETIC PROFILE LOCATION AND STATIONS

NOTE: PROFILES MWP-1 THROUGH MWP-4 AND VES-1 THROUGH VES-4 WERE SURVEYED IN 1992; PROFILES HL-1 THROUGH HL-5 AND VES-A THROUGH VES-F WERE SURVEYED IN 1989 (PROFILE HL-2 WAS NOT SURVEYED) THE 1989 DATA ARE DISCUSSED IN THE IRA A PILOT TEST REPORT (HLA, JUNE 1990-DRAFT FINAL)

- 60 — INTERPRETED RESIDUAL CONDUCTIVITY CONTOUR LINE (mmhos/m)

Contour interval: 10 mmhos/m

- ANOMALOUS AREA AND DESIGNATION (See Table 4.6)

Source: Harding Lawson Associates; used by permission of Program Manager for Rocky Mountain Arsenal

Plate 3

Residual Apparent Conductivity for 10-Meter Coil Spacing, Based on Two-Layer Geophysical Modeling